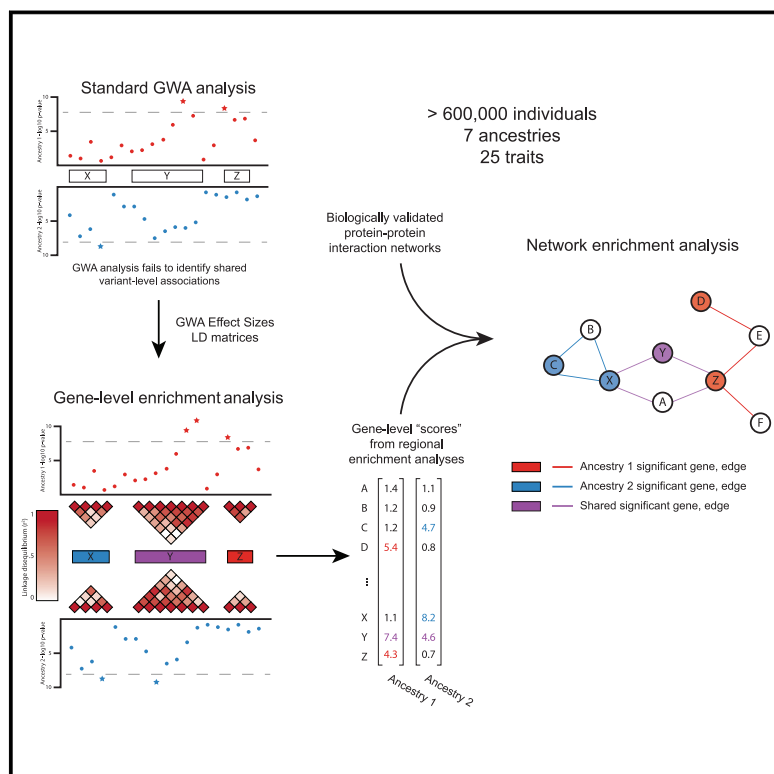


Enrichment analyses identify shared associations for 25 quantitative traits in over 600,000 individuals from seven diverse ancestries

Graphical abstract



Authors

Samuel Pattillo Smith,
Sahar Shahamatdar, Wei Cheng, ...,
Genevieve Wojcik, Lorin Crawford,
Sohini Ramachandran

Correspondence

sramachandran@brown.edu



Enrichment analyses identify shared associations for 25 quantitative traits in over 600,000 individuals from seven diverse ancestries

Samuel Pattillo Smith,^{1,2} Sahar Shahamatdar,^{1,2} Wei Cheng,^{1,2} Selena Zhang,¹ Joseph Paik,¹ Misa Graff,³ Christopher Haiman,⁴ T.C. Matise,⁵ Kari E. North,³ Ulrike Peters,⁶ Eimear Kenny,^{7,8,9,10} Chris Gignoux,¹¹ Genevieve Wojcik,¹² Lorin Crawford,^{1,13,14,16} and Sohini Ramachandran^{1,2,15,16,*}

Summary

Since 2005, genome-wide association (GWA) datasets have been largely biased toward sampling European ancestry individuals, and recent studies have shown that GWA results estimated from self-identified European individuals are not transferable to non-European individuals because of various confounding challenges. Here, we demonstrate that enrichment analyses that aggregate SNP-level association statistics at multiple genomic scales—from genes to genomic regions and pathways—have been underutilized in the GWA era and can generate biologically interpretable hypotheses regarding the genetic basis of complex trait architecture. We illustrate examples of the robust associations generated by enrichment analyses while studying 25 continuous traits assayed in 566,786 individuals from seven diverse self-identified human ancestries in the UK Biobank and the Biobank Japan as well as 44,348 admixed individuals from the PAGE consortium including cohorts of African American, Hispanic and Latin American, Native Hawaiian, and American Indian/Alaska Native individuals. We identify 1,000 gene-level associations that are genome-wide significant in at least two ancestry cohorts across these 25 traits as well as highly conserved pathway associations with triglyceride levels in European, East Asian, and Native Hawaiian cohorts.

Introduction

Over the past two decades, funding agencies and biobanks around the world have made enormous investments to generate large-scale datasets of genotypes, exomes, and whole-genome sequences from diverse human ancestries that are merged with medical records and quantitative trait measurements.^{1–8} However, analyses of such datasets are usually limited to the application of standard genome-wide association (GWA) SNP-level association analyses in which SNPs are tested one-by-one for significant association with a phenotype^{9–11} (Table 1). Yet, even in the largest available multi-ancestry biobanks, GWA analyses fail to offer a comprehensive view of genetic trait architecture among human ancestries.

SNP-level GWA results are difficult to interpret across multiple human ancestries because of a litany of confounding variables, including (1) ascertainment bias in genotyping,^{2,5} (2) varying linkage disequilibrium (LD) patterns,^{18,19} (3) variation in allele frequencies due to different selective pressures and unique population his-

stories,^{19–23} and (4) the effect of environmental factors on phenotypic variation.^{24–27} These confounders and the observed low transferability of GWA results across ancestries^{2,28,29} have generated an important call for increasing GWA efforts focused on populations of diverse, non-European ancestry individuals.

We also note, as other studies have,^{6,30} that the GWA SNP-level test of association is rarely applied to non-European ancestry individuals.³¹ There are two likely explanations for leaving non-European ancestry individuals out of analyses: (1) researchers are electing to not analyze diverse cohorts because of a lack of statistical power and concerns over other confounding variables (recently covered in Ben-Eghan et al.³⁰) or (2) the analyses of non-European cohorts yield no genome-wide significant SNP-level associations. In either case, valuable information is being ignored in GWA studies or going unreported in resulting publications.^{30–32} Even when diverse ancestries are analyzed, GWA studies usually condition on GWA results identified with European ancestry cohorts to detect and give validity to other SNP-level associations.⁶ While

¹Center for Computational Molecular Biology, Brown University, Providence, RI 02912, USA; ²Department of Ecology, Evolution, and Organismal Biology, Brown University, Providence, RI 02912, USA; ³Department of Epidemiology, University of North Carolina, Chapel Hill, Chapel Hill, NC 27599, USA; ⁴Department of Preventative Medicine, University of Southern California, Los Angeles, CA 90089, USA; ⁵Department of Genetics, Rutgers University, Piscataway, NJ 08854, USA; ⁶Public Health Sciences Division, Fred Hutchinson Cancer Research Center, Seattle, WA 98109, USA; ⁷The Center for Genomic Health, Icahn School of Medicine at Mount Sinai, New York City, NY 10029, USA; ⁸The Charles Bronfman Institute for Personalized Medicine, Icahn School of Medicine at Mount Sinai, New York City, NY 10029, USA; ⁹Department of Medicine, Icahn School of Medicine at Mount Sinai, New York City, NY 10029, USA; ¹⁰Department of Genetics and Genomic Sciences, Icahn School of Medicine at Mount Sinai, New York City, NY 10029, USA; ¹¹Division of Biomedical Informatics and Personalized Medicine, University of Colorado, Denver, CO 80204, USA; ¹²Department of Epidemiology, Johns Hopkins University, Baltimore, MD 21287, USA; ¹³Department of Biostatistics, Brown University, Providence, RI 02906, USA; ¹⁴Microsoft Research New England, Cambridge, MA 02142, USA; ¹⁵Data Science Initiative, Brown University, Providence, RI 02912, USA

¹⁶These authors contributed equally

*Correspondence: sramachandran@brown.edu

<https://doi.org/10.1016/j.ajhg.2022.03.005>

© 2022 The Author(s). This is an open access article under the CC BY-NC-ND license (<http://creativecommons.org/licenses/by-nc-nd/4.0/>).



Table 1. The three genomic scales and corresponding association tests used in this study

Genomic scale	Association test	Model of genetic trait architecture	Relevant example
SNPs	standard univariate genome-wide association (GWA) test	the true mutation-level trait architecture is the same for all individuals	many inflammatory bowel disease mutations replicate across ancestries ¹²
SNP-sets/genes	gene-level association tests (e.g., gene-e, ¹³ SKAT ¹⁴)	core genes are the same across all ancestries, with potentially varying causal SNPs	late-onset Alzheimer disease risk from <i>ApoE4</i> allele is lower in African ancestry individuals ¹⁵
Pathways/networks	pathway enrichment and network propagation (e.g., Hierarchical HotNet, ¹⁶ RSS ¹⁷)	core genes differ across ancestries but are all in the same annotated pathway	skin pigmentation architecture in the same pathway differs between African and European ancestry individuals ²

The models of genetic trait architecture corresponding to each genomic scale and statistical method that have been previously invoked in the literature (including relevant examples cited in the last column). These nested genomic scales should routinely be leveraged in multi-ancestry GWA studies to generate biologically interpretable hypotheses of trait architecture across ancestries.

this study design can also identify shared SNP-level associations in non-European ancestry cohorts that are underpowered for applications of the standard GWA framework, it will not identify ancestry-specific associations in non-European ancestry cohorts. In our own analysis of abstracts of publications between 2012 and 2020 with UK Biobank data, we found that only 33 out of 166 studies (19.87%) reported genome-wide significant associations in any non-European ancestry cohort (Figures S1 and S2). Focusing energy and resources on increasing GWA sample sizes without intentional focus on sampling of non-European populations will thus likely perpetuate an already troubling history of leaving non-European ancestry samples out of GWA analyses of large-scale biobanks such as the UK Biobank.³⁰ However, we note that non-European ancestry GWA studies have—and will continue to have—smaller sample sizes than existing and emerging European-ancestry GWA cohorts, limiting the precision of effect size estimates in these studies. What has received less attention than the need to improve GWA study design is the potential of enrichment analyses to characterize genetic trait architecture in multi-ancestry datasets while accounting for variable statistical power to detect, estimate, and replicate genetic associations among cohorts.

In this analysis, we illustrate that focusing solely on *p* values from the standard GWA framework is insufficient to capture the genetic architecture of complex traits. Specifically, we propose that expansion of association analyses to the genomic scale of genes and pathways generates robust and interpretable hypotheses about trait architecture in multi-ancestry cohorts. We define enrichment analyses as testing whether a user-specified set of SNPs, such as SNPs in a given gene or pathway, is enriched for trait associations beyond what is expected by chance based on the number of SNPs in the set and the LD structure among SNPs in the set.^{13,17,33} These enrichment analyses can increase the power to detect associated genes through the aggregation of SNPs of small effect (which explain the majority of the heritability of most traits^{34,35}). Mathieson³⁶ recently highlighted the pattern of homogeneity of direction of effect in multi-ancestry studies even when individual SNPs are not categorized as genome-wide significant in multiple ancestries. Gene-level and pathway-level

enrichment analyses can prioritize biological regions where there is homogeneity in the direction of SNP-level signals of association, generating biologically interpretable hypotheses for the genetic architecture of complex traits in multiple ancestry cohorts. Gene and pathway enrichment analyses expand the existing opportunity for the characterization of conserved genetic architecture across multiple ancestries, or other partitions of samples in biobank datasets (e.g., by biological sex or age), through the identification of biologically interpretable associations.

In this study of 25 quantitative traits and more than 600,000 diverse individuals from the UK Biobank (UKB), BioBank Japan (BBJ), and the PAGE study data (Tables S1–S10), we detail biological insights gained from the application of gene and pathway level enrichment analyses to seven diverse ancestry cohorts. We perform genetic association tests for SNPs, genes, and pathways across multiple ancestry groups with a trait of interest. We test for significantly mutated subnetworks of genes by using known protein-protein interaction networks and the Hierarchical HotNet software.¹⁶ Enrichment analyses do not require generating additional information beyond standard GWA inputs (or outputs for methods that take in GWA summary statistics). We demonstrate that moving beyond SNP-level associations allows for a biologically comprehensive prioritization of shared and ancestry-specific mechanisms underlying genetic trait architecture.

Material and methods

Data overview

We performed statistical tests of association at the SNP, gene, and pathway level for 25 quantitative traits. These analyses were performed on data from seven ancestry cohorts drawn from the UK Biobank, BioBank Japan (BBJ), and PAGE consortia (Table S3). The number of samples included in each ancestry cohort ranged from 574 (American Indian/Alaska Native in the PAGE study data) to 349,411 (European in UK Biobank). The number of SNPs tested in each ancestry ranged from 578,320 (African in the UK Biobank) to more than 12 million (African American in the PAGE dataset). Full enumeration of the samples studied, including sample size, and number of SNPs for each ancestry cohort are given in Tables S1 and S5–S10. For an extensive

description of each cohort from the three biobanks that we analyze in this study, see the [supplemental information](#).

SNP-level GWA analyses

In the European, African, and South Asian ancestry cohorts from the UK Biobank, we performed GWA studies for each ancestry-trait pair in order to test whether the same SNP or SNPs are associated with a given quantitative trait in different ancestries. SNP-level GWA effect sizes were calculated with `plink` and the `-glm` flag.³⁷ Age, sex, and the first twenty principal components were included as covariates for all traits analyzed.⁷ Principal-component analysis was performed with `flashpca 2.0`³⁸ on a set of independent markers derived separately for each ancestry cohort with the `plink` command `-indep-pairwise 100 10 0.1`. Using these parameters, `-indep-pairwise` removes all SNPs that have a pairwise correlation above 0.1 within a 100 SNP window and then slides forward in increments of ten SNPs genome wide. In the implementation of `gene-ε`, we assume pruning highly correlated SNPs still accurately captures the association signals identified in the standard GWA framework.^{14,39} Summary statistics for the 25 quantitative traits in the Biobank Japan, as well as available ancestry-trait pairs in the PAGE study data, were then compared with the results from the association analyses in the UK Biobank cohorts (same traits as listed in [Table S5](#)). In each analysis of an ancestry-trait pair, a separate Bonferroni-corrected significance threshold was calculated with the number of SNPs tested in that particular ancestry-trait pair. We elected to use a Bonferroni-corrected significance threshold to be conservative (compared to, say, an often-used GWA significance threshold of 5×10^{-8} ; see [Figure 1](#)). We label a given SNP association as replicating among cohorts if the estimated effect size of that SNP surpasses the Bonferroni-corrected significance threshold in more than two ancestry cohorts analyzed here ([Figure 1](#) and [Table S11](#)). We believe that the use of a conservative significance threshold, such as the Bonferroni correction, helps to illustrate the statistical challenges faced by multi-ancestry GWA studies due to very imbalanced sample sizes.

To further analyze our ability to accurately estimate GWA SNP-level effect sizes in each ancestry cohort given the imbalanced sample sizes of the datasets we studied, we performed theoretical power calculations across a range of values for both effect sizes and minor allele frequencies as described in Sham and Purcell.⁹ In this framework, we selected absolute value of effect sizes to be equal to 0.1, 0.5, and 1. We then performed power calculations for each of these when paired with a minor allele frequency of 0.01, 0.1, 0.25, and 0.5. In [Figure S3](#), we plot the power of the standard GWA framework to detect SNP-level associations between a genotype and a quantitative trait of interest for sample sizes for up to 30,000 individuals by using a standard GWA significance threshold of 5×10^{-8} .

Because multiple cohorts we analyzed (in particular the American Indian/Alaska Native and Native Hawaiian ancestry cohorts) lack power to estimate effect sizes accurately under the theoretical model described in Sham and Purcell,⁹ we also implemented two-stage GWA studies with a less stringent test of replication for SNP-level association signals. We used the European ancestry cohort as a discovery cohort for genome-wide significant SNP-level associations for each trait, and we used each non-European ancestry cohort as a validation cohort. We then calculated a nominal significance threshold for each trait as 0.05 divided by the number of significant variants for each trait in the European cohort that were tested in at least one other cohort. The corresponding nom-

inal significance thresholds, number of SNPs that were significant in the European ancestry cohort, and the number of SNPs that surpassed the nominal significance threshold in at least one other ancestry cohort are given in [Table S12](#). Replication counts and proportions are illustrated in [Figure S4](#) and the ranges of significant effect sizes for each ancestry trait-pair are shown in [Table S13](#). Finally, for each variant that was significant with the two-stage nominal threshold, we performed a variant-specific power calculation by using the marginal European-ancestry effect size and each non-European ancestry cohort's minor allele frequency and sample size with the method outlined in Sham and Purcell.⁹ The maximum power achieved by a variant in each cohort-trait pairing is given in [Table S14](#) and the number of variants with greater than 90% detection power are given in [Table S15](#).

Gene-level association tests

In order to test aggregated sets of SNP-level GWA effect sizes for enrichment of associated mutations with a given quantitative trait, we applied `gene-ε`²⁹ to each ancestry cohort we studied for each trait of interest, resulting in 125 sets of gene-level association statistics ([Table S3](#)). The `gene-ε` method takes two summary statistics as input: (1) SNP-level GWA marginal effect size estimates $\hat{\beta}$ derived with ordinary least-squares and (2) an LD matrix Σ empirically estimated from external data (e.g., directly from GWA study genotype data, a matrix estimated from a population with similar genomic ancestry to that of the samples analyzed in the GWA study). It is well-known that SNP-level effect size estimates can be inflated as a result of various correlation structures among genome-wide genotypes. `gene-ε` uses its input $\hat{\beta}$ to derive regularized effect size estimates through elastic net penalized regression. `gene-ε` uses the LD matrix Σ to test each gene for enrichment of SNP-level associations beyond what is expected by chance (given the number of SNPs in the gene and the LD among them), thereby identifying genes that are enriched for mutations associated with a trait of interest.^{13,14,17,33,40,41}

In practice, `gene-ε` and other enrichment analyses^{14,41,42} can be applied to any user-specified set of genomic regions, such as regulatory elements, intergenic regions, or gene sets. These gene-level enrichment analyses enable identification of traits in which genetic architecture may be heterogeneous among individuals at the SNP level across individuals by increasing sensitivity to identify interacting mutations of moderate effect on a given trait. Applying `gene-ε` in multiple ancestry cohorts allows researchers to further test whether genes associated (i.e., enriched for SNP-level associations signals given the LD matrix) with a trait of interest are the same, or vary, across ancestries. `gene-ε` takes as input a list of boundaries for all regions to be tested for enrichment of associations. In our study, we applied `gene-ε` to all genes and transcriptional elements defined in Gusev et al.⁴³ for human genome build 19.

In our gene-level analysis, SNP arrays included both genotyped and high-confidence imputed SNPs (information score ≥ 0.8) for each ancestry-trait pair. To compute the LD matrix, we first pruned highly linked SNPs so that the number of SNPs included for any chromosome was less than 35,000 SNPs—the computational limit of `gene-ε` due to the size of the LD matrix—by using the `plink` command `-indep-pairwise 100 10 0.5`. For the UK Biobank European, South Asian, and African ancestry cohorts, we then derived empirical LD estimates between each pair of SNPs for each chromosome in each cohort by using `plink` flag `-r` square applied to the empirical genotype and high-confidence imputed data. We then used

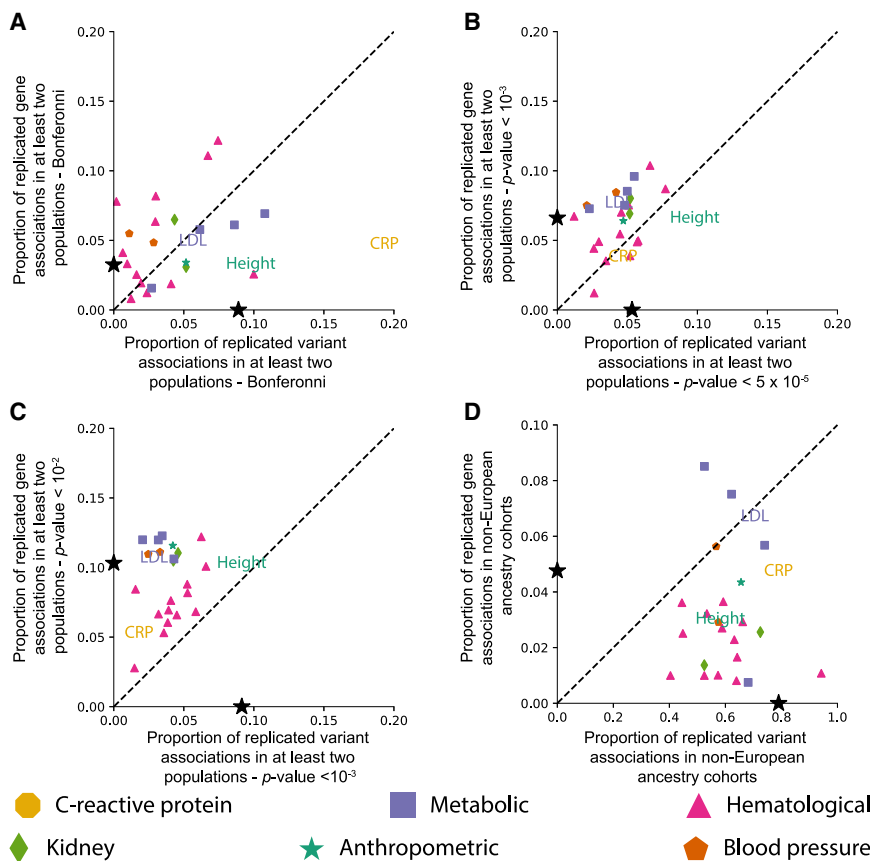


Figure 1. Less stringent significance thresholds lead to a decrease in the proportion of replicated SNP-level associations and an increase in the proportion of gene-level associations among ancestries for each of the 25 traits analyzed

(A) Proportion of all SNP-level Bonferroni-corrected genome-wide significant associations in any ancestry that replicate in at least one other ancestry is shown on the x axis (see [Table S11](#) for ancestry-trait-specific Bonferroni-corrected p value thresholds). On the y axis, we show the proportion of significant gene-level associations that were replicated for a given phenotype in at least two ancestries (see [Table S16](#) for Bonferroni-corrected significance thresholds for each ancestry-trait pair). The black stars on the x- and y-axes represent the mean proportion of replicates in SNP and gene analyses, respectively. C-reactive protein (CRP) contains the greatest proportion of replicated SNP-level associations of any of the phenotypes.

(B) The x axis indicates the proportion of SNP-level associations that surpass a nominal threshold of p value $< 10^{-5}$ in at least one ancestry cohort that replicate in at least one other ancestry cohort. The y axis indicates the proportion of gene-level associations that surpass a nominal threshold of p value $< 10^{-3}$ in at least one ancestry cohort and replicate in at least one other ancestry cohort. Nominal p value thresholds tend to decrease the

proportion of replicated SNP-level associations and tend to increase the proportion of replicated gene-level associations. The number of unique SNPs and genes that replicated in each cohort is given in [Figure S18](#).

(C) The x axis indicates the proportion of SNP-level associations that surpass a nominal threshold of p value $< 10^{-3}$ in at least one ancestry cohort that replicate in at least one other ancestry cohort. The y axis indicates the proportion of gene-level associations that surpass a nominal threshold of p value $< 10^{-2}$ in at least one ancestry cohort and replicate in at least one other ancestry cohort. The number of unique SNPs and genes that replicated in each cohort is given in [Figure S19](#).

(D) The x axis represents the proportion of variants that were significant in the European and at least one non-European ancestry cohort with an alternative significant threshold defined as 0.05 divided by the number of significant European variant associations. The y axis is the corresponding proportion of genes that were significant in at least one non-European ancestry cohort with the same threshold calculation for genes. Note that the axes in (D) are different from one another and the axes of the other panels. As shown in panels (B), (C), and (D) nominal p value thresholds tend to decrease the proportion of replicated SNP-level associations and tend to increase the proportion of replicated gene-level associations. Expansion of three letter trait codes are given in [Table S2](#) and a version of this plot with all trait names displayed as text is shown in [Figure S17](#). Figure S17 shows the same set of plots with all traits represented as text.

the ancestry-specific SNP arrays to calculate 23,603 gene-level association statistics for the European ancestry cohort, 23,671 gene-level association statistics for the South Asian ancestry cohort, and 23,575 gene-level association statistics for the African ancestry cohort.

To calculate gene-level association statistics with Biobank Japan summary statistics, we first found the intersection between SNPs included in the analysis of each trait and SNPs included in the 1000 Genomes Project phase 3 data for the sample of 93 individuals from the Japanese in Tokyo (JPT) population. Note, this intersection was different among some traits, as the genotype data in the Biobank Japan were from different studies, which in turn used different genotyping arrays. We then pruned highly linked markers for each trait separately by using the plink flag `-indep-pairwise 100 10 X` where X was determined by finding the highest possible value that led to the inclusion of less than 35,000 SNPs on each chromosome for the trait. Because of the increased density of SNPs with effect size estimates for height, X was set to prune more conservatively at X = 0.15. For all other traits, X was set to 0.5. The

number of regions for which a gene-e gene-level association statistic was calculated for each trait is given in [Table S5](#).

GWA summary statistics for the five cohorts in the PAGE study data were used as input to gene-e for each available ancestry-trait combination. The array of markers for each ancestry cohort in the PAGE study data was pruned with plink flag `-indep-pairwise 100 10 X`. X was set to the maximum value in each ancestry that ensured no chromosome contained more than 35,000 markers: X was set to 0.05 for the African American cohort, 0.08 for the Hispanic and Latin American and American Indian and Alaska Native (AIAN) cohorts, and 0.25 for the Native Hawaiian cohorts. Finally, for each ancestry-trait combination, genes that passed the Bonferroni-corrected p value ($p = 0.05/\text{number of genes tested}$) were labeled as “significant” throughout this study (see [Table S16](#) for specific thresholds).

We used LD estimates from reference panels for the ancestry cohorts where genotype data was unavailable (BioBank Japan and PAGE datasets). As discussed in other papers proposing enrichment analyses,^{17,44} the discordance between GWA summary

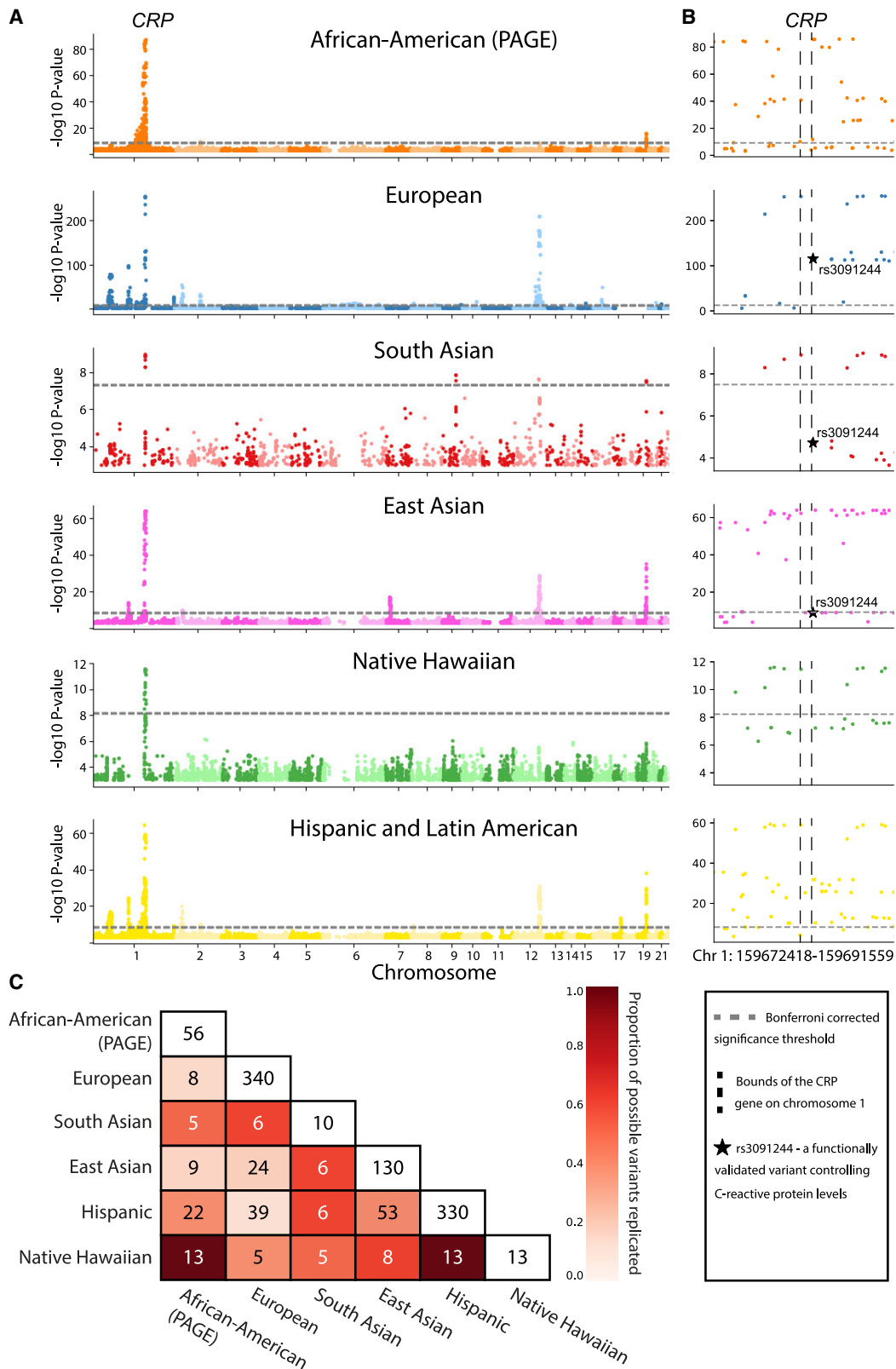


Figure 2. C-reactive protein is an exceptional trait where standard GWA analyses may be sufficient to identify shared genetic architecture among ancestry cohorts

(A) Manhattan plot for SNP-level associations with C-reactive protein levels. Ancestry-specific Bonferroni-corrected significance thresholds are shown with dashed horizontal gray lines and listed in [Table S11](#). Note that the scale of the $-\log_{10}$ -transformed p values on the y axis is different for each ancestry for clarity.

(legend continued on next page)

statistics estimated from a large cohort and LD estimates from a small reference panel may lead to increased false discovery rate and power in the application of gene- ϵ . Finally, we additionally show that gene- ϵ detects a large proportion of the same significant genes in the European ancestry cohort with a more stringent r^2 threshold of 0.1 (see [Table S17](#)).

Pathway analysis and network propagation using Hierarchical HotNet

We tested for significantly mutated subnetworks of genes in each ancestry-trait pair by using the method Hierarchical HotNet.¹⁶ Briefly, Hierarchical HotNet uses hierarchical clustering of scores (such as gene-level association statistics⁴¹ or mutations in cancer genomes^{16,45}) propagated on a protein-protein interaction network that are enriched for trait associations beyond what is expected by chance. The method enables identification of strongly connected components in the network, which are interpretable as subnetworks of interacting genes enriched for mutations associated with a trait of interest. Unlike using annotated gene lists,⁴⁶ network propagation of association statistics enables identifying novel gene sets underwriting complex traits as well as crosstalk between annotated pathways. We identified subnetworks of interacting genes enriched for associations with each trait of interest by using network propagation of gene- ϵ gene-level association statistics as input to Hierarchical HotNet.¹⁶ In this study, these gene scores were set to $-\log_{10}$ -transformed p values of gene- ϵ gene-level association test statistics (see also Nakka et al.^{41,47}). For each ancestry-trait combination, we assigned p values of 1 to genes with p values greater than 0.1 to make the resulting networks both sparse and more interpretable (again see Nakka et al.^{41,47}). In addition, ancestry-trait pairs in which less than 25 genes produced gene- ϵ p values less than 0.1 were discarded as there were an insufficient number of gene-level statistics to populate the protein-protein interaction networks.

We used three protein-protein interaction networks: ReactomeFI 2016,⁴⁸ iRefIndex 15.0,⁴⁹ and HINT+HI.^{50,51} For the ReactomeFI 2016 interaction network, interactions with confidence scores less than 0.75 were discarded. The HINT+HI interaction network consists of the combination of all interactions in HINT binary, HINT co-complex, and HuRI HI interaction networks. We ran Hierarchical HotNet (10^3 permutations) on the thresholded $-\log_{10}$ -transformed gene-level p values for each ancestry-trait combination. We restricted our further investigation to the largest subnetwork identified in each significant ancestry-trait-interaction network combination ($p < 0.05$).

Results

Multiple recent studies have interrogated the extent to which SNP-level associations for a given trait replicate

across ancestries, both empirically and under a variety of models (see Wojcik et al.,⁶ Durvasula and Lohmueller,²⁸ Shi et al.,⁴⁴ Carlson et al.,⁵² Liu et al.,¹² Eyre-Walker,⁵³ Shi et al.⁵⁴). To extensively compare variant-level associations among the seven ancestry cohorts that we analyzed, we first examined the number of genome-wide significant SNP-level associations that replicated exactly on the basis of chromosomal position and reference SNP cluster ID (rsID) in multiple ancestries (see [Figure S5A](#) and [Figure S5C](#), with Bonferroni-corrected thresholds provided in [Table S11](#)). Exact replication of at least one SNP-level association across two or more ancestries occurs in all 25 traits that were studied. The C-reactive protein (CRP) trait had the highest proportion of replicated SNP associations in multiple ancestries, with 18.95% replicating with the standard GWA framework in at least two ancestries, but has a relatively low number of unique GWA significant SNPs (2,734) when compared to other traits ([Figure 1](#)). This is most likely because the genetic architecture of CRP is sparse and highly conserved across ancestries, as is shown in [Figure 2](#). We note that the concordance of genome-wide significant SNP-level association statistics for CRP among five ancestry cohorts is exceptional. In the other 24 traits we analyzed, we did not observe any SNP-level replication among five cohorts. C-reactive protein, which is encoded by the gene of the same name located on chromosome 1, is synthesized in the liver and released into the bloodstream in response to inflammation. In our standard GWA analysis of SNP-level association signal in each ancestry cohort with CRP, rs3091244 is genome-wide significant in a single ancestry cohort. rs3091244 has been functionally validated as influencing CRP levels^{55,56} and is linked to genome-wide significant SNPs in the other two ancestries for which genotype data are available. Interestingly, all GWA significant SNP-level associations for CRP in the Native Hawaiian ancestry cohort replicate in both the African American (PAGE) and the Hispanic and Latin American cohorts (these three cohorts were all genotyped on the same array).

In the other 24 traits, the proportion of genome-wide SNP-level replications was below 10% ([Figure 1A](#)). For polygenic traits, replication of SNP-level GWA results is challenging to interpret considering the large number of GWA significant associations for the trait overall. For example, height contains the largest number of replicated SNP-level associations in our multi-ancestry analysis—but

(B) Manhattan plot of SNP-level associations around the *CRP* gene located on chromosome 1 for each ancestry (zoomed in from A). Boundaries of the *CRP* gene are shown with vertical dashed black lines. All six ancestries contain genome-wide significant SNPs in the region. Black stars in the European, South Asian, and East Asian plots represent rs3091244, a SNP that has been functionally validated as contributing to serum levels of C-reactive protein.^{55,56}

(C) Heatmap of Bonferroni-corrected significant genotyped SNPs replicated between each pair of ancestries analyzed. Here, we focus on SNPs in the 1 MB region surrounding the *CRP* gene. Entries along the diagonal represent the total number of SNP-level associations in the 1 MB region surrounding the *CRP* gene for each ancestry. The color of each cell is proportional to the percentage of SNP-level associations replicated out of all possible replications in each ancestry pair (i.e., the minimum of the diagonal entries between the pairs being considered). For example, the maximum number of genome-wide significant SNPs that can possibly replicate between the Hispanic and East Asian is 25, and 20 replicate, resulting in the cell color denoting 80% replication. A similar matrix, computed including imputed SNPs, is shown in [Figure S20](#).

these only represent 8.90% of all unique SNP-level associations with height discovered in any ancestry cohort. A more comprehensive discussion of previously associated SNPs is available for both height and CRP in the [supplemental information](#). The number of SNPs that replicate among cohorts vary by trait and, as a proportion of the total number of significant SNP-level association signals, is typically less than 10% ([Figure S5](#)).

We also explored how varying the SNP-level significance threshold for each ancestry cohort influences the replication of SNP-level associations by using the standard GWA framework ([Figures 1B and 1C](#)). We performed power calculations for a range of set effect sizes and minor allele frequencies (according to the design and discussion in Sham and Purcell⁹) to identify cohorts where GWA studies lack power to identify associations with a nominal significance threshold of 5×10^{-8} . The two largest cohorts we studied here, the European ancestry cohort and East Asian ancestry cohort, are sufficiently large to identify true SNP associations regardless of choice of effect size or minor allele frequency ([Figure S3](#)). Conversely, in the two smallest cohorts we studied, the AIAN and Native Hawaiian cohorts, GWA studies would lack power to detect true SNP associations with either small effect ($\beta \leq 0.1$) sizes or low minor allele frequencies ($MAF < 0.05$) ([Figure S3](#)).

We then applied a two-stage GWA study design with a less stringent nominal significance threshold for replication in the non-European ancestry cohorts; the resulting thresholds are shown in [Table S12](#). The nominal significance threshold was calculated as 0.05 divided by the number of Bonferroni-corrected significant SNPs in the European ancestry cohort that were tested in at least one other ancestry cohort. Using the European ancestry cohort for discovery of associations, we calculated the proportion of associated SNPs that were nominally significant in at least one non-European ancestry cohort ([Figure 1D](#)). As expected, the proportion of SNP-level replication increased across all 25 traits that were studied (maximum percentage of replication was 94.23% for Basophil count, 49 of 52 SNPs; minimum percentage of replication was 40.39% for hemoglobin, 580 of 1,436 SNPs). Number and proportion of replicated SNP-level associations with this framework are shown in [Figure S4](#). These results are in agreement with our results from the application of two fine-mapping methods, SuSiE¹⁷ and PESCA,⁴⁴ to the SNP-level summary statistics of the European and East Asian ancestry cohorts; this analysis also indicated widespread homogeneity in direction of effect among significant SNPs (described in the [supplemental information, Tables S18–S22](#)).

Enrichment analyses aggregate SNP-level association statistics with predefined SNP sets, genes, and pathways to identify regions of the genome enriched for trait associations beyond what is expected by chance. Published enrichment analyses have demonstrated the ability to identify trait associations that go unidentified with standard SNP-level GWA analysis.^{13,14,17,57–60} The standard GWA method is known to have a high false discovery

rate (FDR),^{61,62} which enrichment analyses can mitigate. Our analyses in [Figure S6](#) and [Figure S7](#) illustrate that two methods—regression with summary statistics (RSS),¹⁷ a fully Bayesian method, and gene- ϵ ²⁹—control FDR particularly well both in the presence and absence of population structure. However, [Figure S8](#) and [Table S23](#) illustrate that both GWA study and gene- ϵ are limited by the sample size of the cohort of interest. Specifically, when the sample size is set to 2,000 individuals, power is low and FDRs are high for both the standard GWA framework and gene- ϵ . Enrichment methods increase power for identifying biologically interpretable trait associations in studies with smaller sample sizes and with heterogeneous genetic architecture than do present-day GWA studies and therefore can be particularly useful when analyzing multi-ancestry genetic datasets with merged phenotype data. For example, Nakka et al.⁴¹ identified an association between *ST3GAL3* and attention-deficit/hyperactivity disorder (ADHD) by using methods that aggregated SNP-level signals across genes and networks. ADHD is a trait with heritability estimates as high as 75% that had no known genome-wide significant SNP-level associations at the time; Nakka et al.⁴¹ studied genotype data from just 3,319 individuals with cases, 2,455 controls and 2,064 trios.⁶³ A study by Demontis et al.⁶⁴ later found a SNP-level association in the *ST3GAL3* gene but was only able to do so with a cohort an order of magnitude larger (20,183 individuals diagnosed with ADHD and 35,191 controls, totaling 55,374 individuals).

Because non-European GWA ancestry cohorts usually have much smaller sample sizes compared to studies with individuals of European ancestry, enrichment analyses offer a unique opportunity to boost statistical power and identify biologically relevant genetic associations with traits of interest by using multi-ancestry datasets. In a simulation study with synthetic phenotypes generated from the European and African ancestry cohorts in the UK Biobank, we show that gene- ϵ is able to identify significantly associated genes even in smaller cohorts ($N = 10,000$ and $N = 4,967$ in the European and African ancestry cohorts, respectively) without the inflated FDR that is often exhibited by the standard GWA framework ([Figures S9 and S10](#)). Additionally, in these simulations, gene- ϵ correctly identifies “causal” genes that are commonly associated in both cohorts ([Figures S11 and S12](#)). These simulations illustrate the utility of modeling LD (and in the case of gene- ϵ , additionally shrinking inflated effect sizes) information to identify enrichment of SNP-level associations in predefined SNP sets.

In an analysis performed by Ben-Eghan et al.³⁰ on 45 studies analyzing UK Biobank data, the second most commonly stated reason for omitting non-European cohorts in applied GWA analyses was the lack of power for identifying SNP-level GWA signals. We tested for gene-level associations in each of the 25 complex traits in each ancestry cohort for which we had data ([Tables S1–Table S10](#)) and identified associations in genes and

transcriptional elements shared across ancestries for every trait. All of our analyses discussed here used gene- ϵ (see performance comparison with other enrichment analyses in Cheng et al.¹³ and Figures S9–S12), an empirical Bayesian approach that aggregates SNP-level GWA summary statistics, where p values for each gene are derived by constructing an empirical null distribution based on the eigenvalues of a gene-specific partitioning of the LD matrix (for more details, see Cheng et al.¹³). Our analyses show that several hematological traits have a higher rate of significant gene-level associations that replicate across multiple ancestry cohorts than SNP-level associations that replicate across ancestry cohorts (Figure 1B). These include platelet count (PLC), mean corpuscular hemoglobin (MCH), mean corpuscular hemoglobin concentration (MCHC), hematocrit, hemoglobin, mean corpuscular volume (MCV), red blood cell count (RBC), and neutrophil count (Figure S5F). Focusing on platelet count as an example, we identify 65 genes that are significantly enriched for associations in multiple ancestries when tested with gene- ϵ (see Table S16 for details on Bonferroni thresholds we used to correct for the number of genes tested; Table S24 displays gene- ϵ for the shared significant genes in non-European ancestry cohorts).¹³ Fifty-five of these genes are significantly associated in both the European and East Asian ancestry cohorts, and the remaining ten all replicate in other pairs of ancestry cohorts. Overall, each of the six ancestry cohorts in our analysis share at least one significant gene with another ancestry cohort, as shown in Figure S13. Our analysis of platelet count illustrates how the implementation of gene-level enrichment analyses can lead to the identification of shared elements of genetic trait architecture among ancestry cohorts that would have not been identified with the standard SNP-level GWA framework alone. Additionally, gene-level enrichment analyses yield statistically significant results that are biologically interpretable across ancestry cohorts even when sample sizes were highly variable.

Results from gene-level enrichment analyses can be further propagated on protein-protein interaction networks to identify interacting genes enriched for association signals.⁴⁵ Often, studies use network propagation as a way to incorporate information from multiple “omics” databases in order to identify significantly mutated gene subnetworks or modules contributing to a particular disease.⁶⁵ An unexplored extension of network propagation is how it can be used with multi-ancestry GWA datasets to identify significantly mutated subnetworks that are shared or ancestry specific.⁴⁷

To conduct network propagation of gene-level association results in our analyses, we applied the Hierarchical HotNet method¹⁶ to gene- ϵ gene-level association statistics for each trait-ancestry dataset. In Figure 3, we display the significant (p value < 0.01) network results for triglyceride levels in three ancestry cohorts: European, East Asian, and Native Hawaiian (networks separated by ancestry are available in Figure S14). In both the European and East Asian

cohorts, we identify enrichment of mutations in a highly connected subnetwork of genes in the apolipoprotein family. In addition, we identify a gene subnetwork enriched for mutations in the East Asian and Native Hawaiian cohorts that interacts with the significantly mutated subnetwork identified in both the European and East Asian cohorts. For instance, beta-secretase 1 (*BACE1*) is a genome-wide significant gene-level association in the East Asian cohort but does not contain SNPs previously associated with triglycerides in any ancestry cohort in the GWAS Catalog. *BACE1* has gene- ϵ significant p values in both the East Asian ancestry cohort (p = 3.57×10^{-13}) and European ancestry cohort (p = 5.55×10^{-17}). *BACE1* was significant at the gene level but contained no previously associated SNPs in any cohort in the GWAS Catalog. *BACE1* plays a role in the metabolism of amyloid beta precursor protein and is known to play a role in amyloid precursor protein (APP) metabolism.⁶⁶ Additionally, both *APOL1* and *HBA1* were identified as significantly associated with triglycerides via gene- ϵ in our analysis of the Native Hawaiian ancestry cohort, and both genes were part of significant subnetworks identified by Hierarchical HotNet in the European and Native Hawaiian ancestry cohorts. It is important to underscore that the results from the Native Hawaiian ancestry cohort are based on a relatively small sample size (N = 1,915). While small sample size can increase the FDR in the gene- ϵ (Figure S8), we highlight the networks identified as enriched for associations with triglycerides in the Native Hawaiian ancestry cohort due to their proximity and biological connection to the networks identified in the well-powered European and East Asian ancestry cohorts. Furthermore, there were no variant-level associations for triglyceride levels that were significant in both the European and Native Hawaiian cohorts (Tables S14 and S15). If analysis had stopped at the variant level, the shared signal of association would have gone unidentified. Details on replicated SNP-level and gene-level associations among ancestries for triglyceride levels are shown in Figure S15 and Figure S16, respectively. While the identification of these subnetworks is predicated on the use of LD panels derived from 1000 Genomes populations as references, we find widespread validation of SNP-level associations with triglyceride levels in many of the genes included in the significant subnetworks (see GWAS Catalog results in Table S25 and gene- ϵ p values for each gene included in the subnetwork in Table S26).

SNP-level and gene-level association results are further discussed for both platelet count and triglyceride levels in the supplemental information. Our results indicate that network propagation methods, such as Hierarchical HotNet, can identify subnetworks of genes on known protein-protein interaction networks that are enriched for significant gene-level associations beyond what is expected by chance. As is the case with triglyceride levels in the European, East Asian, and Native Hawaiian cohorts analyzed in this study, application of pathway enrichment analyses offers the potential to identify subnetworks of interacting

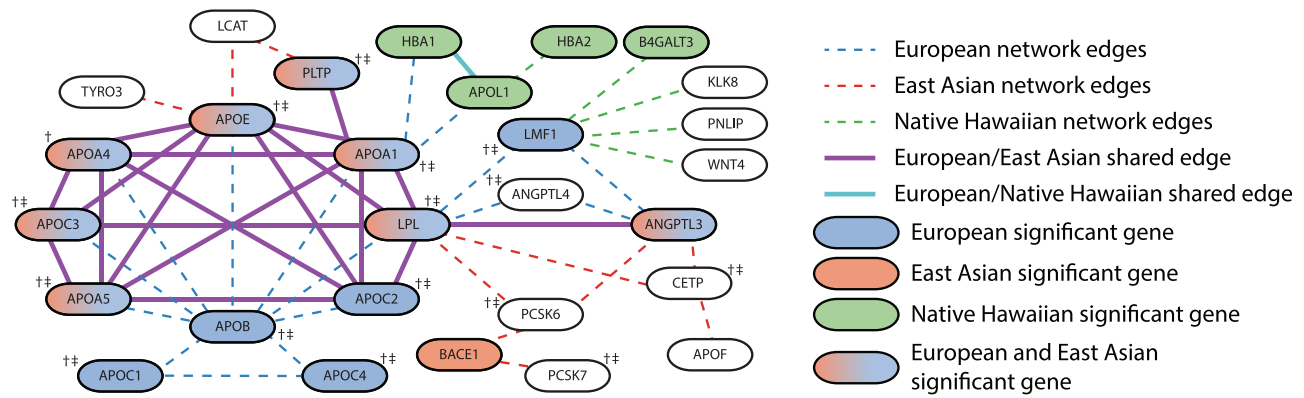


Figure 3. A subnetwork of apolipoprotein genes is significantly enriched for mutations in European, East Asian, and Native Hawaiian ancestries associated with triglyceride levels

The largest significantly altered subnetwork (p value < 0.05) for triglyceride levels contains overlapping gene subnetworks for each of the European, East Asian, and Native Hawaiian ancestries when analyzed independently with Hierarchical HotNet.¹⁶ Each node in the network represents a gene. The shading of each node indicates the statistical significance of the association of that gene with triglyceride levels in a particular cohort. Two genes are connected if their protein products interact based on the ReactomeFl 2016⁴⁸ (European, East Asian) or iRefIndex 15.0⁴⁹ (Native Hawaiian) protein-protein interaction networks. Several genes from the apolipoprotein gene family are significantly associated with triglyceride levels in both the European and East Asian cohorts (see [data and code availability](#)). Additionally, the interactions between them form a highly connected subnetwork. Smaller subnetworks identified in the Native Hawaiian cohort are distal modules that are connected to the subnetwork detected in the European cohort. Not all genes in the largest significantly altered subnetwork for the Native Hawaiian ancestry group are shown for visualization purposes (127 not pictured here). Genes that contain SNPs previously associated to triglyceride levels in a European cohort in the GWAS Catalog are indicated with †. Similarly, genes that contain SNPs previously associated with triglyceride levels in a non-European cohort in the GWAS Catalog are indicated with ‡. The studies identifying these associations are given in [Table S25](#).

genes that are enriched for gene-level association signals in multiple ancestry cohorts.

Discussion

Many recent studies have proposed changes to multi-ancestry GWA study design^{2,5,6,28,30–32,67–69}. In this analysis, we have focused on the potential of *methods* to increase the insight gained into complex trait architecture from multi-ancestry GWA datasets via the generation of biologically interpretable hypotheses. We demonstrate the potential gains of moving beyond standard SNP-level GWA analysis by using 25 quantitative complex traits among seven human ancestry cohorts in three large biobanks: BioBank Japan, the UK Biobank, and the PAGE consortium database ([Tables S1–S10](#)). Ultimately, we believe that studying complex traits demands analysis across multiple genomic scales and ancestries in order to gain biological insight into complex trait architecture and ultimately achieve personalized medicine.

As has been previously noted,^{5,31} non-European ancestry cohorts are often excluded from GWA analyses of multi-ancestry biobanks; complementing the analyses of Ben-Eghan et al.,³⁰ we find that 80.13% of UK Biobank studies over the last 9 years only report significant SNP-level associations in the white British cohort ([Figures S1 and S2](#)), despite the tens of thousands of individuals of non-European ancestry sampled in that dataset. Unless this practice is curbed by the biomedical research community, it will exacerbate already existing disparities in

healthcare across diverse communities. There are undoubted benefits from increased sampling in a given ancestry for association mapping with the standard GWA framework, but it is still unknown the extent to which results from larger GWA and fine-mapping studies using European-ancestry genomes will generalize to the entire human population.^{2,26}

As long as sample sizes of non-European ancestry cohorts in GWA studies remain relatively small, researchers tend to not analyze these data fully, making it imperative to consider alternative tests to the standard GWA framework in order to fully leverage the data available for studying the genetic basis of human complex traits. Two-stage GWA studies with nominal significance thresholds in replication cohorts offer one approach for identifying replicated associations. In addition, application of multi-ancestry fine-mapping methods such as PESCA⁴⁴ support the results of recent analyses from Mathieson³⁶ that even when SNP-level significance is not observed in multiple ancestry cohorts, the direction of effect is generally the same. These methods continue to rely on the statistical detection of association from individual SNPs. Given that multi-ancestry biobank datasets have variable power to detect SNP-level associations given differences in sample size and minor allele frequencies across cohorts ([Figure S3](#)), many researchers simply ignore non-European ancestry samples in GWA studies,^(2,5,6,30) potentially perpetuating health disparities and limiting our understanding of the genetic basis of complex traits and any heterogeneity in genetic trait architecture.^{44,47} For these reasons, we strongly recommend drawing on enrichment

analyses to study genetic associations with a trait of interest, as enrichment analyses offer the opportunity for generating interpretable hypotheses regarding the shared biological mechanisms underwriting complex traits by using large-scale multi-ancestry datasets with variable sample sizes. Enrichment analyses offer a biologically interpretable way of boosting power to detect genetic architecture without alterations to the original design of a study.

There are multiple other technical considerations for conducting multi-ancestry association analyses that we do not consider here, which future studies may explore further in the context of SNP-level association studies and enrichment analyses. First, because we are analyzing some datasets for which we did not have access to genotype data (BioBank Japan and PAGE study data), we relied on reference panels to estimate LD, which is not ideal for enrichment analyses (as has been explored by Zhu and Stephens,¹⁷ Shi et al.⁴⁴). While we draw on the published literature to validate our findings of shared genetic architecture underlying the complex traits studied here (Table S25), our pipelines highlight the importance of managed access to individual-level genotype data for gaining insight into the genetic basis of complex traits. Second, we have not addressed the downstream consequences of using self-identified ancestry to define cohorts in large-scale GWA studies (but see Willer et al.,⁷⁰ Lin et al.,⁷¹ Yang et al.,⁷² Urbut et al.⁷³). Third, each sample we analyzed has also experienced environmental exposures that may influence the statistical detection of genetic associations, and some of those environmental exposures may be correlated with genomic ancestry.^{19,74–76} Interrogation of the influence of gene by environment interactions on complex traits must be done with highly controlled experiments, which can in turn help prioritize traits in which association studies will be interpretable and useful. Lastly, we underscore that increasing sample size in GWA studies alone will not resolve these fundamental biological questions: the proportion of phenotypic variance explained by associations discovered as sample sizes increase in GWA studies has largely reached diminishing returns,⁴² and gene-by-environment interactions are increasingly influential, and estimable, in large biobanks with cryptic relatedness.^{77,78}

Many recent methodological advances that leverage GWA summary statistics have focused on testing the co-localization of causal SNPs (e.g., fine mapping^{79–82}), the non-additive effects of SNP-level interactions (i.e., epistasis^{83,84}), and multivariate GWA tests.^{73,84–86} While these methods can be extended and applied to multi-ancestry GWA analyses, they still focus on SNP-level signals of genetic trait architecture (see also Brown et al.,⁸⁷ Galinsky et al.⁸⁸). Unlike the traditional GWA method, enrichment analyses increase statistical power by aggregating SNP-level signals of genetic associations and allowing for genetic heterogeneity in SNP-level trait architecture across samples as well as offering the opportunity for immediate insights into trait architecture with existing datasets. These methods have been comparatively underused in multi-ancestry GWA studies. Application of enrichment methods to small cohorts is prone to the same

statistical limitations as the standard GWA framework, namely, less power to detect true associations and elevated false positive rates when applied to small sample sizes (Figure S8, Table S23). However, enrichment of associations can be assessed at multiple biological scales—genes, gene sets, and networks—thereby allowing for biologically informed insight into trait architecture when small sample sizes are studied in conjunction with better powered cohorts, generating targeted hypotheses for biological validation. Thus, comparison of results from enrichment analyses offer the opportunity to identify therapeutic targets in ancestries where sample sizes are limited.

While many studies note that differences in LD across ancestries affect transferability of effect size estimates,^{6,52,89–91} recent studies in population genetics have additionally debated how various selection pressures and genetic drift may hamper transferability of GWA results across ancestries (see for example, Edge and Rosenberg,^{21,22} Novembre and Barton,²⁴ Harpak and Przeworski,²⁶ Durvasula and Lohmueller,²⁸ Mostafavi et al.²⁹). Future GWA studies should be coupled with approaches from studies of how evolutionary processes shape the genetic architecture of complex traits.^{26,34,53,92}

Two open questions must be tackled when studying complex trait architecture in the multi-ancestry biobank era: (1) to what extent is the true genetic trait architecture (causal SNPs and/or their effects on a trait of interest) heterogeneous across cohorts^{6,93} and (2) which components of GWA results (e.g., p values, estimated effect size, direction of effect sizes) are transferable across ancestries at any genomic scale? Continued application of the standard SNP-level GWA approach will not answer these questions. However, enrichment methods that aggregate SNP-level effects, test for effect size heterogeneity, and leverage genomic annotations and gene interaction networks offer opportunities to directly test these fundamental questions. Methods can and should play an important role as biomedical research shifts current paradigms to extend the benefits of personalized medicine beyond people of European ancestry.

Additionally, biomedical researchers should continue to pressure both funding agencies and institutions to diversify their sampling efforts in the name of inclusion and addressing—instead of exacerbating—genomic health disparities. In addition to those efforts, we believe existing and new methods can increase the return on investment in multi-ancestry biobanks, ensure that every bit of information from these datasets is studied, and prioritize biological mechanism above SNP-level statistical association signals by identifying associations that are robust across ancestries.

Data and code availability

All scripts and publicly available data from GWA, gene, and pathway association tests are available at https://github.com/ramachandran-lab/multiancestry_enrichment. Results from PESCA analyses were provided through personal correspondence by Huwenbo Shi.

Supplemental information

Supplemental information can be found online at <https://doi.org/10.1016/j.ajhg.2022.03.005>.

Acknowledgments

We thank Kirk Lohmueller and Alicia R. Martin for helpful comments on an earlier version of this manuscript as well as the Crawford and Ramachandran Labs for helpful discussions. This research was conducted in part with computational resources and services at the Center for Computation and Visualization at Brown University as well as with the UK Biobank Resource under application number 22419. The Population Architecture Using Genomics and Epidemiology (PAGE) program is funded by the National Human Genome Research Institute (NHGRI) with co-funding from the National Institute on Minority Health and Health Disparities (NIMHD). The WHI program is funded by the National Heart, Lung, and Blood Institute, National Institutes of Health, U.S. Department of Health and Human Services through contracts 75N92021D00001, 75N92021D00002, 75N92021D00003, 75N92021D00004, and 75N92021D00005. The HCHS/SOL study was carried out as a collaborative study supported by contracts from the National Heart, Lung and Blood Institute (NHLBI) to the University of North Carolina (N01-HC65233), University of Miami (N01-HC65234), Albert Einstein College of Medicine (N01-HC65235), Northwestern University (N01-HC65236), and San Diego State University (N01-HC65237). S.P.S. was a trainee supported under the Brown University Predoctoral Training Program in Biological Data Science (NIH T32 GM128596). L.C. acknowledges the support of an Alfred P. Sloan Research Fellowship and a David & Lucile Packard Fellowship for Science and Engineering. This work was also supported by US National Institutes of Health R01 GM118652 and National Institutes of Health R35 GM139628 to S.R. S.R. acknowledges additional support from National Science Foundation CAREER Award DBI-1452622.

Declaration of interests

C.G. owns stock in 23andMe. E.K. and C.G. are members of the scientific advisory board for Encompass Bioscience. E.K. consults for Illumina.

Received: November 1, 2021

Accepted: March 2, 2022

Published: March 28, 2022

Web resources

gene-e, <https://github.com/ramachandran-lab/genee>

Hierarchical HotNet, <https://github.com/raphael-group/hierarchical-hotnet>

PESCA, <https://github.com/huwenboshi/pesca>

RSS, <https://github.com/stephenslab/rss>

References

1. Nagai, A., Hirata, M., Kamatani, Y., Muto, K., Matsuda, K., Kiyohara, Y., Ninomiya, T., Tamakoshi, A., Yamagata, Z., Mushiroda, T., et al.; BioBank Japan Cooperative Hospital Group (2017). Overview of the BioBank Japan Project: Study design and profile. *J. Epidemiol.* *27* (3S), S2–S8.
2. Martin, A.R., Gignoux, C.R., Walters, R.K., Wojcik, G.L., Neale, B.M., Gravel, S., Daly, M.J., Bustamante, C.D., and Kenny, E.E. (2017). Human demographic history impacts genetic risk prediction across diverse populations. *Am. J. Hum. Genet.* *100*, 635–649.
3. Sankar, P.L., and Parker, L.S. (2017). The Precision Medicine Initiative's All of Us Research Program: an agenda for research on its ethical, legal, and social issues. *Genet. Med.* *19*, 743–750.
4. Bycroft, C., Freeman, C., Petkova, D., Band, G., Elliott, L.T., Sharp, K., Motyer, A., Vukcevic, D., Delaneau, O., O'Connell, J., et al. (2018). The UK Biobank resource with deep phenotyping and genomic data. *Nature* *562*, 203–209.
5. Martin, A.R., Kanai, M., Kamatani, Y., Okada, Y., Neale, B.M., and Daly, M.J. (2019). Clinical use of current polygenic risk scores may exacerbate health disparities. *Nat. Genet.* *51*, 584–591.
6. Wojcik, G.L., Graff, M., Nishimura, K.K., Tao, R., Haessler, J., Gignoux, C.R., Highland, H.M., Patel, Y.M., Sorokin, E.P., Avery, C.L., et al. (2019). Genetic analyses of diverse populations improves discovery for complex traits. *Nature* *570*, 514–518.
7. Sohail, M., Maier, R.M., Ganna, A., Bloemendal, A., Martin, A.R., Turchin, M.C., Chiang, C.W., Hirschhorn, J., Daly, M.J., Patterson, N., et al. (2019). Polygenic adaptation on height is overestimated due to uncorrected stratification in genome-wide association studies. *eLife* *8*, e39702.
8. Berg, J.J., Harpak, A., Sinnott-Armstrong, N., Joergensen, A.M., Mostafavi, H., Field, Y., Boyle, E.A., Zhang, X., Racimo, F., Pritchard, J.K., and Coop, G. (2019). Reduced signal for polygenic adaptation of height in UK Biobank. *eLife* *8*, e39725.
9. Sham, P.C., and Purcell, S.M. (2014). Statistical power and significance testing in large-scale genetic studies. *Nat. Rev. Genet.* *15*, 335–346.
10. Price, A.L., Spencer, C.C.A., and Donnelly, P. (2015). Progress and promise in understanding the genetic basis of common diseases. *Proc. Biol. Sci.* *282*, 20151684.
11. Visscher, P.M., Wray, N.R., Zhang, Q., Sklar, P., McCarthy, M.I., Brown, M.A., and Yang, J. (2017). 10 years of gwas discovery: biology, function, and translation. *Am. J. Hum. Genet.* *101*, 5–22.
12. Liu, J.Z., van Sommeren, S., Huang, H., Ng, S.C., Alberts, R., Takahashi, A., Ripke, S., Lee, J.C., Jostins, L., Shah, T., et al.; International Multiple Sclerosis Genetics Consortium; and International IBD Genetics Consortium (2015). Association analyses identify 38 susceptibility loci for inflammatory bowel disease and highlight shared genetic risk across populations. *Nat. Genet.* *47*, 979–986.
13. Cheng, W., Ramachandran, S., and Crawford, L. (2020). Estimation of non-null SNP effect size distributions enables the detection of enriched genes underlying complex traits. *PLoS Genet.* *16*, e1008855.
14. Wu, M.C., Lee, S., Cai, T., Li, Y., Boehnke, M., and Lin, X. (2011). Rare-variant association testing for sequencing data with the sequence kernel association test. *Am. J. Hum. Genet.* *89*, 82–93.
15. Rajabli, F., Feliciano, B.E., Celis, K., Hamilton-Nelson, K.L., Whitehead, P.L., Adams, L.D., Bussies, P.L., Manrique, C.P., Rodriguez, A., Rodriguez, V., et al. (2018). Ancestral origin of ApoE ϵ 4 Alzheimer disease risk in Puerto Rican and African American populations. *PLoS Genet.* *14*, e1007791.
16. Reyna, M.A., Leiserson, M.D.M., and Raphael, B.J. (2018). Hierarchical HotNet: identifying hierarchies of altered subnetworks. *Bioinformatics* *34*, i972–i980.

17. Zhu, X., and Stephens, M. (2017). Bayesian large-scale multiple regression with summary statistics from genome-wide association studies. *Ann. Appl. Stat.* *11*, 1561–1592.
18. Pritchard, J.K., and Przeworski, M. (2001). Linkage disequilibrium in humans: models and data. *Am. J. Hum. Genet.* *69*, 1–14.
19. Berg, J.J., and Coop, G. (2014). A population genetic signal of polygenic adaptation. *PLoS Genet.* *10*, e1004412.
20. Jakobsson, M., Edge, M.D., and Rosenberg, N.A. (2013). The relationship between F_{ST} and the frequency of the most frequent allele. *Genetics* *193*, 515–528.
21. Edge, M.D., and Rosenberg, N.A. (2014). Upper bounds on F_{ST} in terms of the frequency of the most frequent allele and total homozygosity: the case of a specified number of alleles. *Theor. Popul. Biol.* *97*, 20–34.
22. Edge, M.D., and Rosenberg, N.A. (2015). A general model of the relationship between the apportionment of human genetic diversity and the apportionment of human phenotypic diversity. *Hum. Biol.* *87*, 313–337.
23. Hormozdiari, F., Zhu, A., Kichaev, G., Ju, C.J., Segrè, A.V., Joo, J.W.J., Won, H., Sankararaman, S., Pasaniuc, B., Shifman, S., and Eskin, E. (2017). Widespread allelic heterogeneity in complex traits. *Am. J. Hum. Genet.* *100*, 789–802.
24. Novembre, J., and Barton, N.H. (2018). Tread lightly interpreting polygenic tests of selection. *Genetics* *208*, 1351–1355.
25. Rosenberg, N.A., Edge, M.D., Pritchard, J.K., and Feldman, M.W. (2018). Interpreting polygenic scores, polygenic adaptation, and human phenotypic differences. *Evol. Med. Public Health* *2019*, 26–34.
26. Harpak, A., and Przeworski, M. (2021). The evolution of group differences in changing environments. *PLoS Biol.* *19*, e3001072.
27. Pereira, L., Mutesa, L., Tindana, P., and Ramsay, M. (2021). African genetic diversity and adaptation inform a precision medicine agenda. *Nat. Rev. Genet.* *22*, 284–306.
28. Durvasula, A., and Lohmueller, K.E. (2021). Negative selection on complex traits limits phenotype prediction accuracy between populations. *Am. J. Hum. Genet.* *108*, 620–631.
29. Mostafavi, H., Harpak, A., Agarwal, I., Conley, D., Pritchard, J.K., and Przeworski, M. (2020). Variable prediction accuracy of polygenic scores within an ancestry group. *eLife* *9*, e48376.
30. Ben-Eghan, C., Sun, R., Hleap, J.S., Diaz-Papkovich, A., Munter, H.M., Grant, A.V., Dupras, C., and Gravel, S. (2020). Don't ignore genetic data from minority populations. *Nature* *585*, 184–186.
31. Popejoy, A.B., and Fullerton, S.M. (2016). Genomics is failing on diversity. *Nature* *538*, 161–164.
32. Bustamante, C.D., Burchard, E.G., and De la Vega, F.M. (2011). Genomics for the world. *Nature* *475*, 163–165.
33. Zhu, X., and Stephens, M. (2018). Large-scale genome-wide enrichment analyses identify new trait-associated genes and pathways across 31 human phenotypes. *Nat. Commun.* *9*, 4361.
34. Boyle, E.A., Li, Y.I., and Pritchard, J.K. (2017). An expanded view of complex traits: from polygenic to omnigenic. *Cell* *169*, 1177–1186.
35. Sinnott-Armstrong, N., Naqvi, S., Rivas, M., and Pritchard, J.K. (2021). GWAS of three molecular traits highlights core genes and pathways alongside a highly polygenic background. *eLife* *10*, e58615.
36. Mathieson, I. (2021). The omnigenic model and polygenic prediction of complex traits. *Am. J. Hum. Genet.* *108*, 1558–1563.
37. Chang, C.C., Chow, C.C., Tellier, L.C., Vattikuti, S., Purcell, S.M., and Lee, J.J. (2015). Second-generation PLINK: rising to the challenge of larger and richer datasets. *Gigascience* *4*, 7.
38. Abraham, G., Qiu, Y., and Inouye, M. (2017). FlashPCA2: principal component analysis of Biobank-scale genotype datasets. *Bioinformatics* *33*, 2776–2778.
39. Bulik-Sullivan, B.K., Loh, P.R., Finucane, H.K., Ripke, S., Yang, J., Patterson, N., Daly, M.J., Price, A.L., Neale, B.M.; and Schizophrenia Working Group of the Psychiatric Genomics Consortium (2015). LD Score regression distinguishes confounding from polygenicity in genome-wide association studies. *Nat. Genet.* *47*, 291–295.
40. Wu, M.C., Kraft, P., Epstein, M.P., Taylor, D.M., Chanock, S.J., Hunter, D.J., and Lin, X. (2010). Powerful SNP-set analysis for case-control genome-wide association studies. *Am. J. Hum. Genet.* *86*, 929–942.
41. Nakka, P., Raphael, B.J., and Ramachandran, S. (2016). Gene and network analysis of common variants reveals novel associations in multiple complex diseases. *Genetics* *204*, 783–798.
42. Zhang, Y., Qi, G., Park, J.H., and Chatterjee, N. (2018). Estimation of complex effect-size distributions using summary-level statistics from genome-wide association studies across 32 complex traits. *Nat. Genet.* *50*, 1318–1326.
43. Gusev, A., Ko, A., Shi, H., Bhatia, G., Chung, W., Penninx, B.W., Jansen, R., de Geus, E.J., Boomsma, D.I., Wright, F.A., et al. (2016). Integrative approaches for large-scale transcriptome-wide association studies. *Nat. Genet.* *48*, 245–252.
44. Shi, H., Burch, K.S., Johnson, R., Freund, M.K., Kichaev, G., Mancuso, N., Manuel, A.M., Dong, N., and Pasaniuc, B. (2020). Localizing Components of Shared Transethnic Genetic Architecture of Complex Traits from GWAS Summary Data. *Am. J. Hum. Genet.* *106*, 805–817.
45. Leiserson, M.D., Vandin, F., Wu, H.-T., Dobson, J.R., and Raphael, B.R. (2014). Pan-cancer identification of mutated pathways and protein complexes. *Cancer Res.* *74*, 5324.
46. Subramanian, A., Tamayo, P., Mootha, V.K., Mukherjee, S., Ebert, B.L., Gillette, M.A., Paulovich, A., Pomeroy, S.L., Golub, T.R., Lander, E.S., and Mesirov, J.P. (2005). Gene set enrichment analysis: a knowledge-based approach for interpreting genome-wide expression profiles. *Proc. Natl. Acad. Sci. USA* *102*, 15545–15550.
47. Nakka, P., Archer, N.P., Xu, H., Lupo, P.J., Raphael, B.J., Yang, J.J., and Ramachandran, S. (2017). Novel gene and network associations found for acute lymphoblastic leukemia using case-control and family-based studies in multiethnic populations. *Cancer Epidemiol. Biomarkers Prev.* *26*, 1531–1539.
48. Fabregat, A., Sidiropoulos, K., Garapati, P., Gillespie, M., Hausmann, K., Haw, R., Jassal, B., Jupe, S., Korninger, F., McKay, S., et al. (2016). The reactome pathway knowledgebase. *Nucleic Acids Res.* *44* (D1), D481–D487.
49. Razick, S., Magklaras, G., and Donaldson, I.M. (2008). iRefIndex: a consolidated protein interaction database with provenance. *BMC Bioinformatics* *9*, 405.
50. Das, J., and Yu, H. (2012). HINT: High-quality protein interactomes and their applications in understanding human disease. *BMC Syst. Biol.* *6*, 92.
51. Rolland, T., Taşan, M., Charloteaux, B., Pevzner, S.J., Zhong, Q., Sahni, N., Yi, S., Lemmens, I., Fontanillo, C., Mosca, R.,

- et al. (2014). A proteome-scale map of the human interactome network. *Cell* 159, 1212–1226.
52. Carlson, C.S., Matise, T.C., North, K.E., Haiman, C.A., Fesinmeyer, M.D., Buyske, S., Schumacher, F.R., Peters, U., Franceschini, N., Ritchie, M.D., et al.; PAGE Consortium (2013). Generalization and dilution of association results from European GWAS in populations of non-European ancestry: the PAGE study. *PLoS Biol.* 11, e1001661.
 53. Eyre-Walker, A. (2010). Evolution in health and medicine Sackler colloquium: Genetic architecture of a complex trait and its implications for fitness and genome-wide association studies. *Proc. Natl. Acad. Sci. USA* 107 (Suppl 1), 1752–1756.
 54. Shi, H., Gazal, S., Kanai, M., Koch, E.M., Schoech, A.P., Sievert, K.M., Kim, S.S., Luo, Y., Amariuta, T., Huang, H., et al. (2021). Population-specific causal disease effect sizes in functionally important regions impacted by selection. *Nat. Commun.* 12, 1098.
 55. Szalai, A.J., Wu, J., Lange, E.M., McCrory, M.A., Langefeld, C.D., Williams, A., Zakharkin, S.O., George, V., Allison, D.B., Cooper, G.S., et al. (2005). Single-nucleotide polymorphisms in the C-reactive protein (CRP) gene promoter that affect transcription factor binding, alter transcriptional activity, and associate with differences in baseline serum CRP level. *J. Mol. Med. (Berl.)* 83, 440–447.
 56. Zhang, S.-C., Wang, M.-Y., Feng, J.-R., Chang, Y., Ji, S.-R., and Wu, Y. (2020). Reversible promoter methylation determines fluctuating expression of acute phase proteins. *eLife* 9, e51317.
 57. Browning, B.L., and Browning, S.R. (2007). Efficient multilocus association testing for whole genome association studies using localized haplotype clustering. *Genet. Epidemiol.* 31, 365–375.
 58. Liu, J.Z., McRae, A.F., Nyholt, D.R., Medland, S.E., Wray, N.R., Brown, K.M., Hayward, N.K., Montgomery, G.W., Visscher, P.M., Martin, N.G., Macgregor, S.; and AMFS Investigators (2010). A versatile gene-based test for genome-wide association studies. *Am. J. Hum. Genet.* 87, 139–145.
 59. de Leeuw, C.A., Mooij, J.M., Heskes, T., and Posthuma, D. (2015). MAGMA: generalized gene-set analysis of GWAS data. *PLoS Comput. Biol.* 11, e1004219.
 60. Zhang, Q.S., Browning, B.L., and Browning, S.R. (2015). Genome-wide haplotypic testing in a Finnish cohort identifies a novel association with low-density lipoprotein cholesterol. *Eur. J. Hum. Genet.* 23, 672–677.
 61. Storey, J.D., and Tibshirani, R. (2003). Statistical significance for genomewide studies. *Proc. Natl. Acad. Sci. USA* 100, 9440–9445.
 62. Stephens, M. (2017). False discovery rates: a new deal. *Biostatistics* 18, 275–294.
 63. Neale, B.M., Medland, S.E., Ripke, S., Asherson, P., Franke, B., Lesch, K.P., Faraone, S.V., Nguyen, T.T., Schäfer, H., Holmans, P., et al.; Psychiatric GWAS Consortium: ADHD Subgroup (2010). Meta-analysis of genome-wide association studies of attention-deficit/hyperactivity disorder. *J. Am. Acad. Child Adolesc. Psychiatry* 49, 884–897.
 64. Demontis, D., Walters, R.K., Martin, J., Mattheisen, M., Als, T.D., Agerbo, E., Baldursson, G., Belliveau, R., Bybjerg-Grauholm, J., Bækvad-Hansen, M., et al.; ADHD Working Group of the Psychiatric Genomics Consortium (PGC); Early Life-course & Genetic Epidemiology (EAGLE) Consortium; and 23andMe Research Team (2019). Discovery of the first genome-wide significant risk loci for attention deficit/hyperactivity disorder. *Nat. Genet.* 51, 63–75.
 65. Cowen, L., Ideker, T., Raphael, B.J., and Sharan, R. (2017). Network propagation: a universal amplifier of genetic associations. *Nat. Rev. Genet.* 18, 551–562.
 66. Perneczky, R., Alexopoulos, P.; and Alzheimer's Disease euroimaging Initiative (2014). Cerebrospinal fluid BACE1 activity and markers of amyloid precursor protein metabolism and axonal degeneration in Alzheimer's disease. *Alzheimers Dement.* 10 (5, Suppl), S425–S429, 429.e1.
 67. Hindorff, L.A., Bonham, V.L., Brody, L.C., Ginoza, M.E.C., Hutter, C.M., Manolio, T.A., and Green, E.D. (2018). Prioritizing diversity in human genomics research. *Nat. Rev. Genet.* 19, 175–185.
 68. Sinnott-Armstrong, N., Tanigawa, Y., Amar, D., Mars, N., Benner, C., Aguirre, M., Venkataraman, G.R., Wainberg, M., Ollila, H.M., Kiiskinen, T., et al.; FinnGen (2021). Genetics of 35 blood and urine biomarkers in the UK Biobank. *Nat. Genet.* 53, 185–194.
 69. Peterson, R.E., Kuchenbaecker, K., Walters, R.K., Chen, C.Y., Popejoy, A.B., Periyasamy, S., Lam, M., Iyegbe, C., Strawbridge, R.J., Brick, L., et al. (2019). Genome-wide association studies in ancestrally diverse populations: opportunities, methods, pitfalls, and recommendations. *Cell* 179, 589–603.
 70. Willer, C.J., Li, Y., and Abecasis, G.R. (2010). METAL: fast and efficient meta-analysis of genomewide association scans. *Bioinformatics* 26, 2190–2191.
 71. Lin, D.-Y., Tao, R., Kalsbeek, W.D., Zeng, D., Gonzalez, F., 2nd, Fernández-Rhodes, L., Graff, M., Koch, G.G., North, K.E., and Heiss, G. (2014). Genetic association analysis under complex survey sampling: the Hispanic Community Health Study/Study of Latinos. *Am. J. Hum. Genet.* 95, 675–688.
 72. Yang, J., Zaitlen, N.A., Goddard, M.E., Visscher, P.M., and Price, A.L. (2014). Advantages and pitfalls in the application of mixed-model association methods. *Nat. Genet.* 46, 100–106.
 73. Urbut, S.M., Wang, G., Carbonetto, P., and Stephens, M. (2019). Flexible statistical methods for estimating and testing effects in genomic studies with multiple conditions. *Nat. Genet.* 51, 187–195.
 74. Vrieze, S.I., Iacono, W.G., and McGue, M. (2012). Confluence of genes, environment, development, and behavior in a post-gwas world. *Dev. Psychopathol.* 24, 1195–1214.
 75. Gage, S.H., Davey Smith, G., Ware, J.J., Flint, J., and Munafò, M.R. (2016). G = e: What gwas can tell us about the environment. *PLoS Genet.* 12, e1005765.
 76. Borrell, L.N., Elhawary, J.R., Fuentes-Afflick, E., Witonsky, J., Bhakta, N., Wu, A.H.B., Bibbins-Domingo, K., Rodríguez-Santana, J.R., Lenoir, M.A., Gavin, J.R., 3rd, et al. (2021). Race and genetic ancestry in medicine - a time for reckoning with racism. *N. Engl. J. Med.* 384, 474–480.
 77. Young, A.I., Frigge, M.L., Gudbjartsson, D.F., Thorleifsson, G., Bjornsdottir, G., Sulem, P., Masson, G., Thorsteinsdottir, U., Stefansson, K., and Kong, A. (2018). Relatedness disequilibrium regression estimates heritability without environmental bias. *Nat. Genet.* 50, 1304–1310.
 78. Young, A.I., Benonisdottir, S., Przeworski, M., and Kong, A. (2019). Deconstructing the sources of genotype-phenotype associations in humans. *Science* 365, 1396–1400.
 79. Hormozdiari, F., Kostem, E., Kang, E.Y., Pasaniuc, B., and Eskin, E. (2014). Identifying causal variants at loci with multiple signals of association. *Genetics* 198, 497–508.
 80. Hormozdiari, F., van de Bunt, M., Segrè, A.V., Li, X., Joo, J.W.J., Bilow, M., Sul, J.H., Sankaraman, S., Pasaniuc, B., and Eskin,

- E. (2016). Colocalization of GWAS and eQTL Signals Detects Target Genes. *Am. J. Hum. Genet.* *99*, 1245–1260.
81. LaPierre, N., Taraszka, K., Huang, H., He, R., Hormozdiari, F., and Eskin, E. (2021). Identifying causal variants by fine mapping across multiple studies. *PLoS Genet.* *17*, e1009733.
 82. Wang, G., Sarkar, A., Carbonetto, P., and Stephens, M. (2020). A simple new approach to variable selection in regression, with application to genetic fine mapping. *J. R. Stat. Soc. Series B Stat. Methodol.* *82*, 1273–1300.
 83. Crawford, L., Zeng, P., Mukherjee, S., and Zhou, X. (2017). Detecting epistasis with the marginal epistasis test in genetic mapping studies of quantitative traits. *PLoS Genet.* *13*, e1006869.
 84. Turchin, M.C., and Stephens, M. (2019). Bayesian multivariate reanalysis of large genetic studies identifies many new associations. *PLoS Genet.* *15*, e1008431.
 85. Zhou, X., and Stephens, M. (2012). Genome-wide efficient mixed-model analysis for association studies. *Nat. Genet.* *44*, 821–824.
 86. Stephens, M. (2013). A unified framework for association analysis with multiple related phenotypes. *PLoS ONE* *8*, e65245.
 87. Brown, B.C., Ye, C.J., Price, A.L., Zaitlen, N.; and Asian Genetic Epidemiology Network Type 2 Diabetes Consortium (2016). Transethnic genetic-correlation estimates from summary statistics. *Am. J. Hum. Genet.* *99*, 76–88.
 88. Galinsky, K.J., Reshef, Y.A., Finucane, H.K., Loh, P.R., Zaitlen, N., Patterson, N.J., Brown, B.C., and Price, A.L. (2019). Estimating cross-population genetic correlations of causal effect sizes. *Genet. Epidemiol.* *43*, 180–188.
 89. Bitarello, B.D., and Mathieson, I. (2020). Polygenic scores for height in admixed populations. *G3* *10*, 4027–4036.
 90. Marnetto, D., Pärna, K., Läll, K., Molinaro, L., Montinaro, F., Haller, T., Metspalu, M., Mägi, R., Fischer, K., and Pagani, L. (2020). Ancestry deconvolution and partial polygenic score can improve susceptibility predictions in recently admixed individuals. *Nat. Commun.* *11*, 1628.
 91. Huang, H., Ruan, Y., Feng, Y.-C.A., Chen, C.-Y., Lam, M., Sawa, A., Martin, A., Qin, S., and Ge, T. (2021). Improving polygenic prediction in ancestrally diverse populations. Preprint at medRxiv. <https://doi.org/10.1101/2020.12.27.20248738>.
 92. Hayward, L.K., and Sella, G. (2019). Polygenic adaptation after a sudden change in environment. Preprint at bioRxiv. <https://doi.org/10.1101/792952>.
 93. McClellan, J., and King, M.C. (2010). Genetic heterogeneity in human disease. *Cell* *141*, 210–217.

The American Journal of Human Genetics, Volume 109

Supplemental information

Enrichment analyses identify shared associations

for 25 quantitative traits in over 600,000

individuals from seven diverse ancestries

Samuel Pattillo Smith, Sahar Shahamatdar, Wei Cheng, Selena Zhang, Joseph Paik, Misa Graff, Christopher Haiman, T.C. Matise, Kari E. North, Ulrike Peters, Eimear Kenny, Chris Gignoux, Genevieve Wojcik, Lorin Crawford, and Sohini Ramachandran

S1 Supplemental Note for Smith et al. 2021 - “Enrichment analyses identify shared associations for 25 quantitative traits in over 600,000 individuals from seven diverse ancestries”

S0.1 SNP-level results for height and C-reactive protein

In [Figure S5A](#) and [Figure S5D](#), we found that, across 25 traits analyzed, height had the greatest number of genome-wide significant SNP-level associations (76,910 unique associations) in at least one ancestry. Of these SNP-level associations, 8.90% (7,377 SNPs) replicate based off of rsID in at least two ancestry cohorts. Height is not the only trait in which the standard GWA SNP-level association test detects associations that replicate extensively across ancestries. In fact, SNP-level associations replicate in each of the 25 continuous traits that we analyze in this study.

We analyzed SNP-level associations with C-reactive protein in six ancestry cohorts: African-American (PAGE), European, South Asian, East Asian, Native Hawaiian, and Hispanic and Latin American cohorts. C-reactive protein is an example of a trait with a sparse and highly conserved genetic architecture across ancestries, as shown in [Figure 2](#). Many SNPs within the *CRP* gene have been previously associated with C-reactive protein plasma levels^{[4](#)[3](#)}. In our analysis, rs3091244 is genome-wide significant in only the European ancestry cohort, and has been functionally validated as influencing C-reactive protein levels^{[4](#)[5](#)}. The SNP rs3091244 is located in a promoter region slightly upstream of *CRP*, and it has clinical implications for both atrial fibrillation^{[6](#)} and lupus erythematosus^{[7](#)} (European $p = 1.54 \times 10^{-116}$; East Asian $p = 1.15 \times 10^{-9}$).

We expanded our search for replicated GWA SNP-level association signals across ancestry cohorts by scanning for 1 Mb regions that contained associations to the same phenotype in two or more ancestries—a process often referred to as “clumping”. These windows were centered at every unique genome-wide significant SNP in any ancestry for a given trait (we refer the 1Mb window around the significant SNP as a “clump”, [Figure S5B](#) and [Figure S5E](#)). In addition to the largest number of unique SNP-level associations, height also had the largest proportion of clumps containing a significant SNP-level GWA association signal that replicated in at least two ancestry cohorts (see [Figure S5B](#) and [Figure S5E](#)). The three traits with the greatest proportion of clumps containing SNP-level GWA signals that replicate in multiple ancestry cohorts were height (77.09% of clumps), urate (65.89%), and low density lipoprotein (54.40%).

In addition to the SNP-level associations on chromosome 1 surrounding the *CRP* gene across all six ancestry cohorts (displayed in [Figure 2](#)), there are other regions of the genome that contain significant GWA associations with C-reactive protein that replicate in multiple ancestry cohorts. On chromosome 2, there is a cluster of four SNPs significantly associated with C-reactive protein levels in the European, East Asian, and

32 Hispanic and Latin American ancestry cohorts. Of these, rs1260326 (European $p = 1.01 \times 10^{-55}$; East Asian
33 $p = 1.70 \times 10^{-9}$; Hispanic and Latin American $p = 1.24 \times 10^{-20}$), rs780094 (European $p = 9.95 \times 10^{-51}$;
34 East Asian $p = 1.70 \times 10^{-9}$; Hispanic and Latin American $p = 1.14 \times 10^{-16}$), and rs6734238 (African-
35 American (PAGE) $p = 3.04 \times 10^{-10}$; European $p = 8.38 \times 10^{-34}$; South Asian $p = 2.17 \times 10^{-9}$) were
36 statistically significant in three of the six ancestry cohorts that we analyzed. Each of these three SNPs has
37 been previously associated with C-reactive protein levels in a European ancestry cohort^{[8][10]}. Of these three
38 SNPs, only one (rs6734238) had previously been replicated in other ancestries (in African-American, and
39 Hispanic and Latin American cohorts^[11]).

40 On chromosome 19 there are 23 SNPs that are associated with CRP in the African-American PAGE,
41 European, and Hispanic and Latin American ancestry cohorts. Two other SNPs are associated with C-
42 reactive protein in the African-American (PAGE), European, and Hispanic and Latin American cohorts,
43 as well as the East Asian ancestry cohort. One of these two SNPs, rs7310409 (African-American (PAGE)
44 $p = 8.57 \times 10^{-9}$; European $p = 3.57 \times 10^{-210}$; East Asian $p = 2.72 \times 10^{-27}$; Hispanic and Latin American
45 $p = 5.35 \times 10^{-29}$) located in the HNF1 homeobox A (*HNF1A*) gene, has been previously associated with
46 C-reactive protein levels in only a European ancestry cohort^{[9][10]}. Three additional significant SNPs in our
47 analysis have been previously associated with European ancestry cohorts in previous studies, including:
48 rs1169310^[11] (European $p = 1.52 \times 10^{-172}$; East Asian $p = 1.28 \times 10^{-18}$; Hispanic and Latin American
49 $p = 1.17 \times 10^{-27}$), rs1183910^{[8][12]} (European $p = 5.50 \times 10^{-177}$; East Asian $p = 3.16 \times 10^{-29}$; Hispanic and
50 Latin American $p = 7.47 \times 10^{-29}$), and rs7953249^[13] (European $p = 1.19 \times 10^{-177}$; East Asian $p = 1.10 \times 10^{-19}$;
51 Hispanic and Latin American $p = 4.80 \times 10^{-29}$). Two SNPs, rs2259816 (European $p = 2.77 \times 10^{-172}$;
52 East Asian $p = 9.33 \times 10^{-18}$; Hispanic and Latin American $p = 1.90 \times 10^{-27}$) and rs7979473 (African
53 $p = 1.49 \times 10^{-9}$; East Asian $p = 6.06 \times 10^{-29}$; Hispanic and Latin American $p = 1.56 \times 10^{-30}$), have been
54 previously associated with C-reactive protein in both African-American and Hispanic and Latin American
55 ancestry cohorts^[11]. There is one final group of three SNPs associated with C-reactive protein in the African-
56 American (PAGE), European, East Asian, and Hispanic and Latin American ancestry cohorts on chromosome
57 19. One of them, rs4420638 (East Asian $p = 9.93 \times 10^{-29}$; Hispanic and Latin American $p = 2.03 \times 10^{-30}$),
58 has been previously associated in a European ancestry cohort^{[8][10][12]}. These four regions indicate a highly
59 conserved SNP-level architecture of C-reactive protein across six ancestry cohorts. Interestingly, we were
60 unable to replicate associations with C-reactive protein across ancestries at the gene or pathway levels.

61 Gene and pathway association results

62 Three genes, *GP6*, *RDH13*, and *AGPAT5*, were significantly associated with platelet count (PLC) in the
63 African-American (PAGE) ancestry cohort and the East Asian ancestry cohort Figure S13. Of these, no

64 significant SNPs in glycoprotein VI platelet (*GP6*) have been reported in the GWAS catalog for either
65 ancestry cohort. However, a single SNP within *GP6*, rs1613662, has previously been associated with mean
66 platelet volume in a GWA study analyzing a European ancestry cohort¹⁴. *GP6* plays a critical role in
67 platelet aggregation, and mutations have been previously associated with fetal loss¹⁵. Retinol dehydrogenase
68 13 (*RDH13*) has no reported GWAS catalog associations with platelet count, but is within 60kb of a SNP
69 significantly associated with platelet aggregation¹⁶. Of the three genes significantly associated with PLC
70 in both the European and AIAN cohorts, 1-Acylglycerol-3-Phosphate O-Acyltransferase 5 (*AGPAT5*) is a
71 member of a gene family known to play a role in immunity and inflammation response¹⁷.

72 Alcohol dehydrogenase 2 (*ALDH2*) has additionally been associated with hypertension in an elderly
73 Japanese cohort¹⁸. A member of the RAS oncogene family (*RAB8A*) has been shown to play a role in
74 the inhibition of inflammatory response. In contrast, cut like homeobox 2 *CUX2* contains a significantly
75 associated SNP in the array used in this study for the East Asian ancestry cohort, but it has no previous
76 associations in a European ancestry cohort. However, *CUX2* is significantly associated at the gene-level in
77 both the European and East Asian ancestry cohorts. Although not reported as being associated with PLC
78 in the GWAS Catalog, a single SNP, rs61745424 which encodes a missense mutation, has been previously
79 identified as being related to the trait¹⁹. The gene- ϵ association statistics for the seven genes significantly
80 associated with PLC are available in [Table S24](#).

81 Finally, a single gene, acyl-CoA dehydrogenase family member 10 (*ACAD10*) associated in our gene-level
82 analysis of PLC, was significant in both the European and East Asian ancestry cohorts (European gene-
83 $\epsilon p = 1.47 \times 10^{-10}$; East Asian gene- $\epsilon p = 2.00 \times 10^{-10}$) but contained no previous associations in the GWAS
84 catalog. The African-American and Hispanic and Latin American ancestry cohorts analyzed in Qayyum
85 et al.²⁰ both contain SNPs within *ACAD10* that are significantly associated with PLC.

86 In our analysis of triglyceride levels in six ancestry cohorts (African-American (PAGE), European, East
87 Asian, South Asian, Hispanic and Latin American, and Native Hawaiian), we identified shared genetic
88 architecture at the SNP, gene, and subnetwork level. Replicated SNPs and genes between the six ancestry
89 cohorts are shown in [Figure S15](#) [Figure S16](#). We focus our discussion of results at the network level in
90 the European, East Asian, and Native Hawaiian ancestry cohorts (Figure [3](#)). In the European and East
91 Asian ancestry cohorts, we identified 55 shared genome-wide significant associations at the gene-level. Of
92 these results, eight genes lie in the same significantly mutated subnetwork (Hierarchical HotNet $p < 10^{-3}$)
93 when analyzing each ancestry cohort independently. Five of those eight genes belong to the apolipoprotein
94 family of genes, including: apolipoprotein A1 (*APOA1*), apolipoprotein A4 (*APOA4*), apolipoprotein A5
95 (*APOA5*), apolipoprotein C3 (*APOC3*), apolipoprotein E (*APOE*). Specifically, the apolipoprotein play a
96 central role in lipoprotein biosynthesis and transport. All of these genes contain SNPs previously associated

97 with triglyceride levels in a European ancestry cohort^{21,26}. All five genes also contain SNPs previously
98 associated with triglyceride levels in non-European ancestry cohorts. Specifically, *APOA1*, *APOC3*, and
99 *APOE* each contain SNPs previously associated with triglyceride levels in African-American and Hispanic
100 and Latin American ancestry cohorts^{21,22}. *APOA5* has previously been associated to triglyceride levels in
101 an East Asian, African-American, and Hispanic and Latin American ancestry cohorts^{24,27}.

102 The other three genes that were significantly associated with triglyceride levels in the European and East
103 Asian ancestry cohorts are members of the largest significantly mutated subnetwork including phospholipid
104 transfer protein (*PLTP*; European gene- ϵ $p = 4.29 \times 10^{-9}$; East Asian gene- ϵ $p = 6.66 \times 10^{-15}$), lipoprotein
105 lipase (*LPL*; European gene- ϵ $p = 4.08 \times 10^{-13}$; East Asian gene- ϵ $p = 1.00 \times 10^{-20}$), and angiopoietin like 3
106 (*ANGPTL3*; European gene- ϵ $p = 8.86 \times 10^{-8}$; East Asian gene- ϵ $p = 1.00 \times 10^{-20}$). *PLTP* has previously
107 been associated with triglyceride levels in European, African-American, and Hispanic and Latin American
108 ancestry cohorts^{21,22,24,28,32}. *LPL* is one of the most well-studied genes in the regulation of triglyceride levels.
109 It has previously been associated with triglyceride levels in European ancestry cohorts^{21,26,28,32,32,45}, East
110 Asian ancestry cohorts^{27,46}, and African ancestry cohorts as well as Hispanic and Latin American ancestry
111 cohorts^{21,24,28,29,42,44,45,47,48}. The final gene that was genome-wide significant in both the European and
112 East Asian ancestry cohorts, *ANGPTL3*, has no previous associations in the GWAS catalog and presents
113 a novel candidate gene within the network. While not significant in any gene-level analysis, *ANGPTL4*
114 (European gene- ϵ $p = 1.00 \times 10^{-20}$; East Asian gene- ϵ $p = 9.99 \times 10^{-1}$) is from the same family is present
115 in the largest subnetwork in the European cohort and also has also been previously identified as having
116 associations in European, African, and Hispanic and Latin American ancestry cohorts^{24,28,42,44,45,49}.

117 In our analysis of the European ancestry cohort from the UK Biobank, we additionally identified a set of
118 eight genes that are connected to the core network discussed above. One of these genes is *ANGPTL4*, which
119 we discussed above. Five of these genes were significant at the gene-level in the European ancestry cohort,
120 including four apolipoprotein genes (*APOC1*; European gene- ϵ $p = 1.67 \times 10^{-16}$, *APOC2*; European gene-
121 ϵ $p = 3.57 \times 10^{-13}$, *APOC4*; European gene- ϵ $p = 3.72 \times 10^{-13}$, and *APOB*; European gene- ϵ $p = 1.00 \times 10^{-20}$)
122 and lipase maturation factor 1 (*LMF1*; European gene- ϵ $p = 8.03 \times 10^{-7}$). Each of these genes have been
123 previously associated with triglyceride levels in a European ancestry cohort²⁴. Additional associations
124 were also found in that same study which conducted a meta-analysis of European, African-American, and
125 Hispanic and Latin American ancestry cohorts. The final two genes included in the significantly mutated
126 subnetwork of the European ancestral cohort, *APOL1* and *HBA1*, were not were not identified as genome-
127 wide significant by gene- ϵ and have no previous SNP-level associations with triglyceride levels in the GWAS
128 Catalog. Interestingly, both *APOL1* (Native Hawaiian gene- ϵ $p = 8.89 \times 10^{-11}$) and *HBA1* (Native Hawaiian
129 gene- ϵ $p = 2.46 \times 10^{-10}$) were both identified as genome-wide significant by gene- ϵ in our analysis of the Native

130 Hawaiian ancestry cohort and the interaction between them was identified in our Hierarchical HotNet⁵⁰
131 analysis as present in both the European and Native Hawaiian ancestry cohorts.

132 In addition to *APOL1* and *HBA1*, six more genes are connected to the core network of genes that overlap
133 in the East Asian and European significantly mutated subnetworks. Of these, both *HBA2* and *B4GALT3* are
134 significant at the gene-level in the Native Hawaiian ancestry cohort alone. They are each connected to genes
135 identified in both the European and Native Hawaiian ancestry cohorts as members of the largest significantly
136 mutated subnetwork. The final three genes include kallikrein related peptidase 8 (*KLK8*), pancreatic lipase
137 *PNLIP*, and wnt family member 4 (*WNT4*) which were not significant at the gene-level and did not contain
138 previous SNP-level associations in the GWAS catalog.

139 Three of the genes within the network identified in the East Asian ancestry cohort contain previously
140 associated SNPs in both European and non-European ancestry cohorts, including: cholesteryl ester transfer
141 protein (*CETP*), proprotein convertase subtilisin/kexin type 6 (*PCSK6*), and proprotein convertase subtil-
142 isin/kexin type 7 (*PCSK7*)²¹²⁹. The final three genes in the significantly mutated subnetwork identified in
143 the East Asian ancestry cohort were not significant at the gene-level and do not contain previously associated
144 SNPs in the GWAS catalog in any ancestral cohort. Lecithin-cholesterol acyltransferase (*LCAT*) is involved
145 in cholesterol biosynthesis and apolipoprotein F (*APOF*) encodes one of the minor apolipoprotein genes
146 present in plasma. Finally, tyrosine-protein kinase receptor 3 (*TYRO3*) plays a role in ligand recognition
147 and cell metabolism⁵¹. The gene- ε p -values in each ancestry cohort for each of the 28 genes discussed here
148 are shown in [Table S26](#)

149 Supplemental Figures

UK Biobank Studies from 2012 to 2020

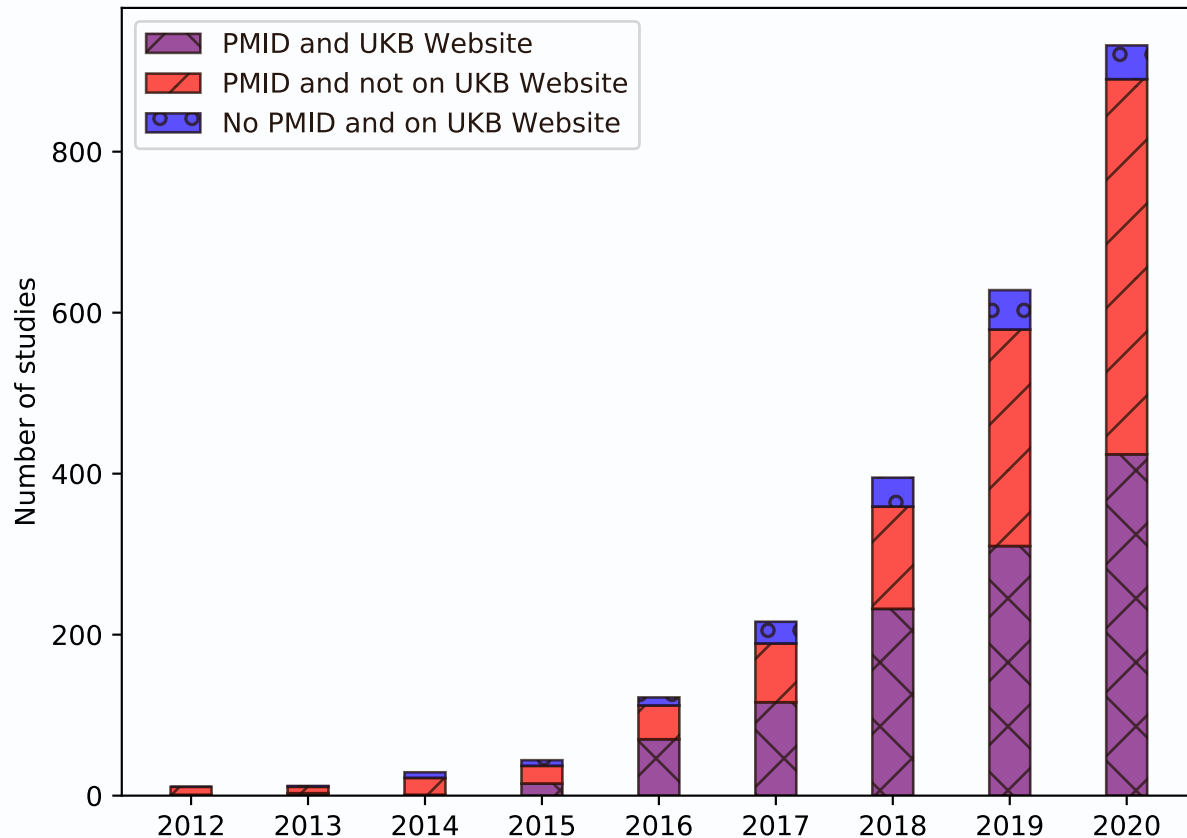


Figure S1: Number of publications we identified using UK Biobank data from 2012 to 2020. Studies identified using PMIDs as described in the Supplemental Information. Studies that are displayed on the UK Biobank website (<https://www.ukbiobank.ac.uk/>) and identified on PubMed are shown in purple. Studies listed on the UK Biobank website but do not have a PMID are shown in blue, and studies only identified using PubMed but not listed on the UK Biobank website are shown in red. The protocols for identifying studies both on PubMed and the UK Biobank website are detailed in the Supplemental Information. Data from both the UK Biobank website and PubMed were accessed on January 12, 2021.

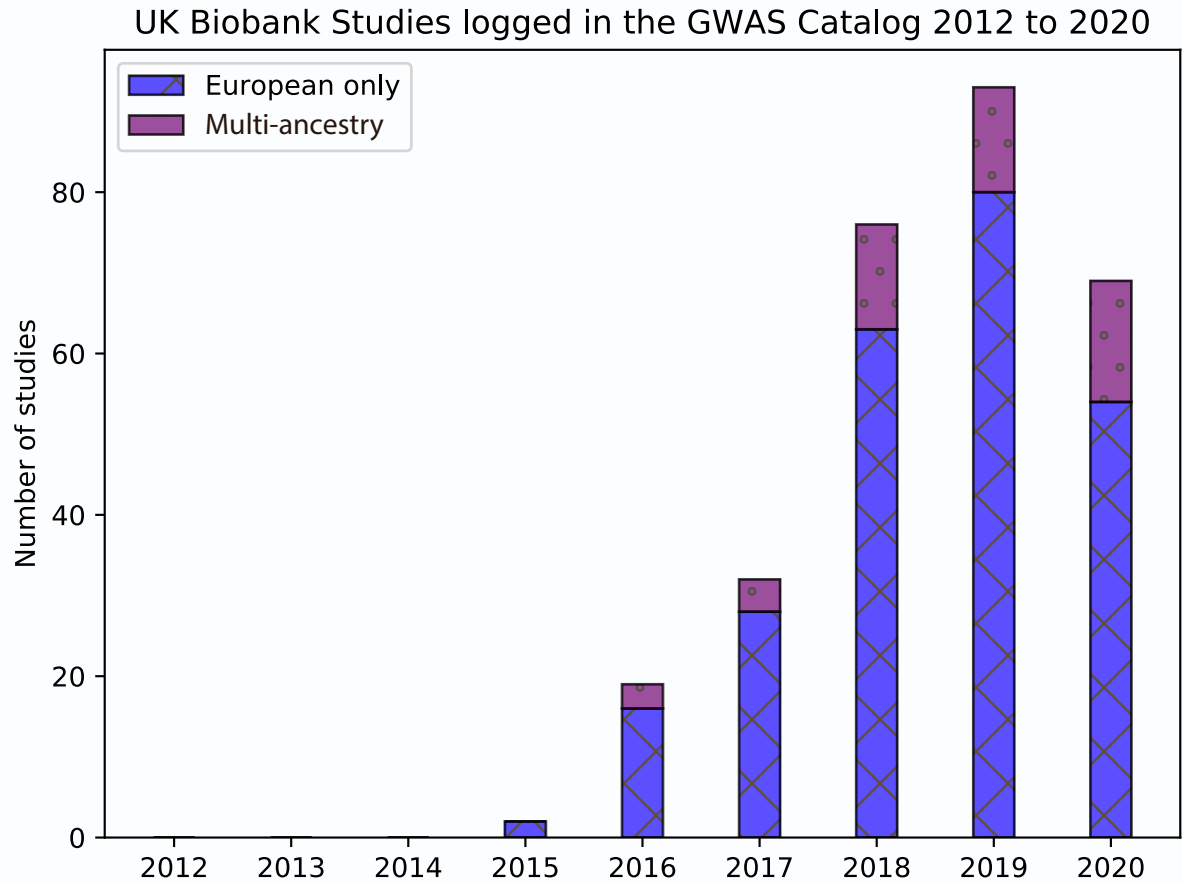


Figure S2: Number of studies published using UK Biobank data from 2012 to 2020 that have available metadata in the GWAS Catalog. Our protocols for identifying studies from the GWAS Catalog are detailed in the Supplemental Information. Multi-ancestry studies are shown in purple and include those that list samples of more than one ancestral group in the GWAS catalog (as defined according to the protocol using Popejoy and Fullerton⁵², available on the GitHub page https://github.com/ramachandran-lab/redefining_replication). Studies that only list samples of European ancestry in the GWAS catalog are shown in blue. Every multi-ancestry analysis includes samples of European ancestry and of at least one other ancestry. GWAS Catalog data was accessed on January 10, 2021 from the website <https://www.ebi.ac.uk/gwas/docs/file-downloads> using the final release file of 2020 (see file named `gwas_catalog.v1.0.2-associations_e100_r2020-12-15.tsv`).

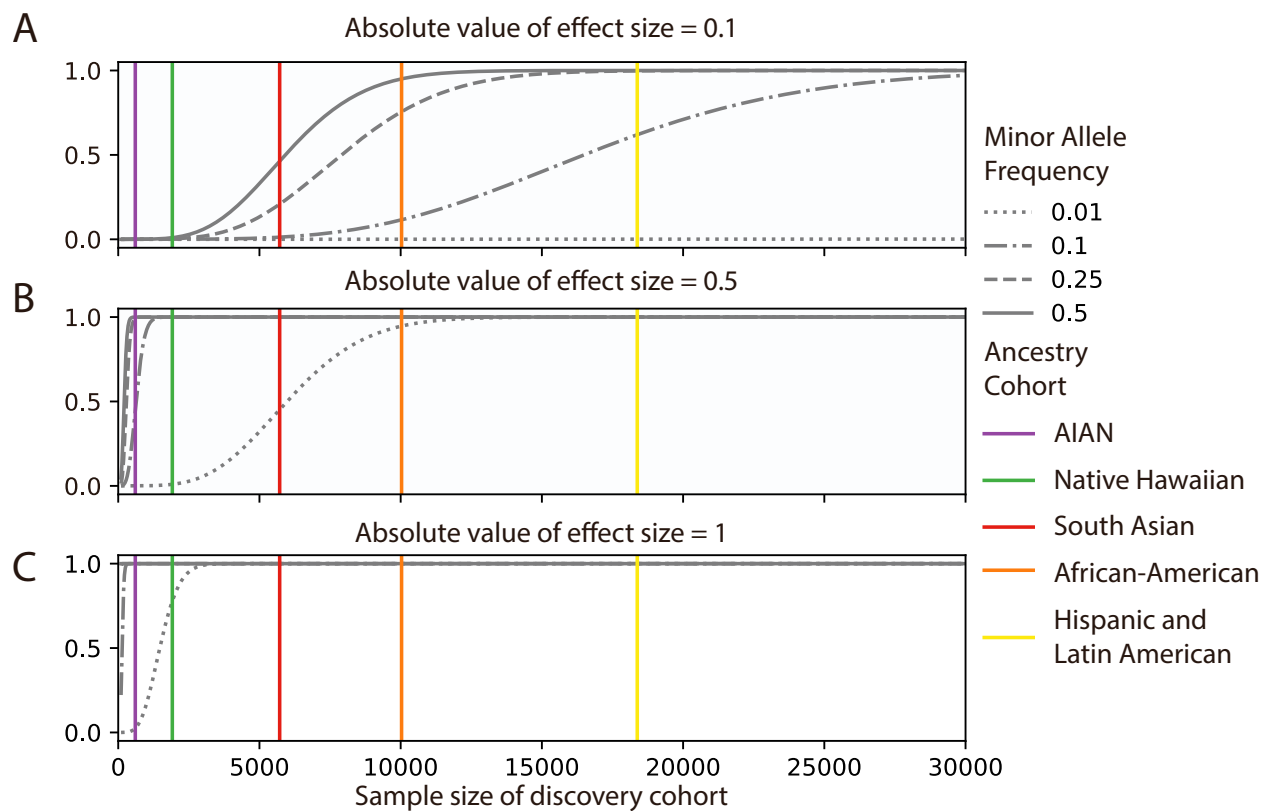


Figure S3: Power calculations for the standard GWA framework as a function of sample sizes using a range of effect sizes and minor allele frequencies. A. For an absolute value of effect size equal to 0.1 we performed power calculations for the standard GWA framework for cohorts with sample sizes of up to 30,000 individuals. Similar plots for absolute value of effect size set to 0.5 and 1 are shown in **B.** and **C.**, respectively. A full description of the power calculations is given in the Materials and Methods.

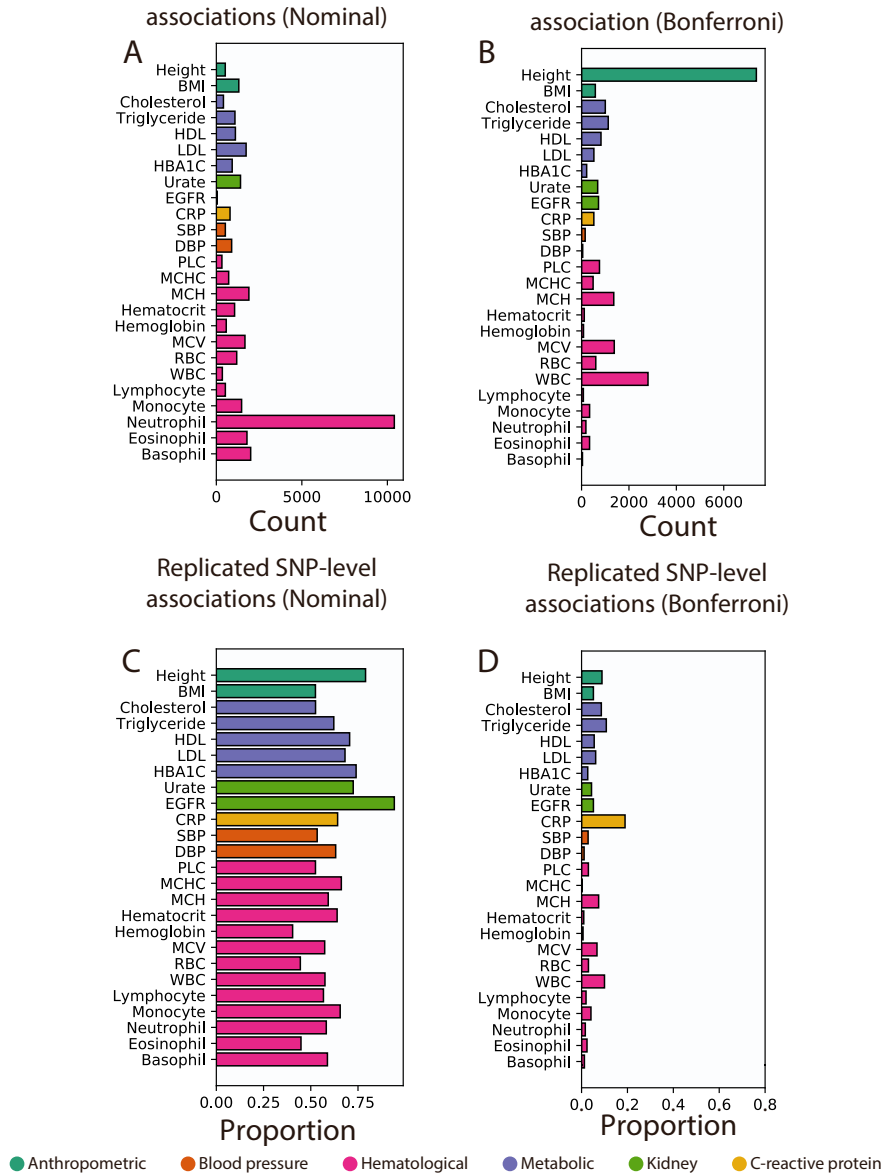


Figure S4: Summaries of replicated SNP-level associations when using two-stage GWA study design a nominal significance threshold. (A) Number and (C) proportion of nominally significant SNPs associated with a phenotype in the European ancestry cohort that were replicated in at least one other ancestry cohorts using a nominal p -value threshold calculated as 0.05 divided by the number of SNPs significantly associated with that trait in the European ancestry cohort. The corresponding thresholds for each trait are listed in [Table S12](#). For ease of comparison, (B) number and (D) proportion of Bonferroni significant SNP-level associations that replicate among ancestry cohorts using the ancestry-trait Bonferroni-correction thresholds shown [Table S11](#). Expansion of three letter trait codes are given in [Table S2](#). Expansion of three letter trait codes are given in [Table S2](#).

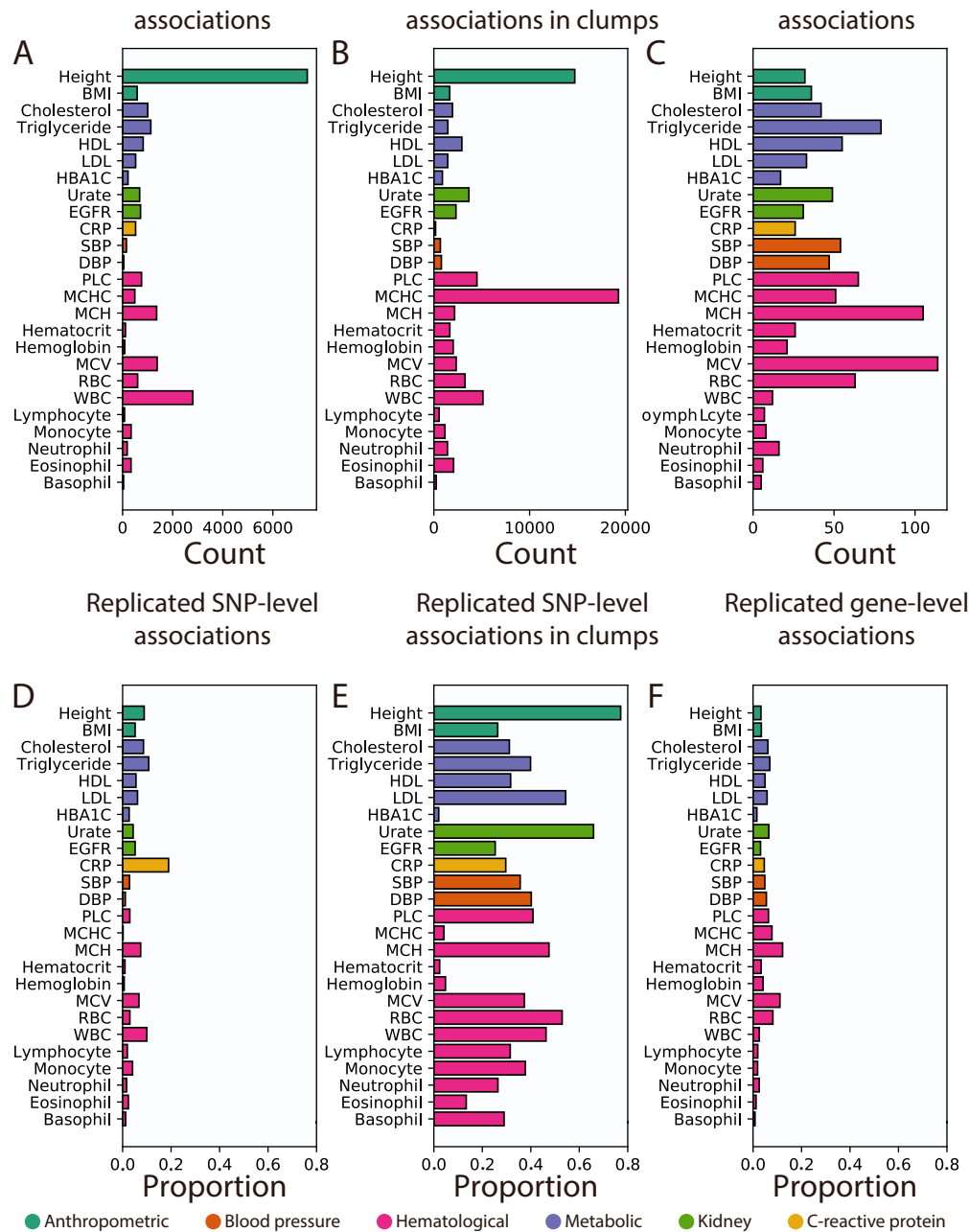


Figure S5: Summaries of replicated associations at multiple genomic scales among ancestry cohorts for all 25 traits analyzed using Bonferroni-corrected thresholds. Expansion of three letter trait codes are given in [Table S2](#). (A) Number and (D) proportion of genome-wide significant SNPs associated with a phenotype in at least one ancestry cohort that were replicated in at least two ancestry cohorts. In all 25 traits, genome-wide significant SNPs replicate in at least two ancestry cohorts. Height contains over 7,000 replicated SNPs among the seven ancestry cohorts analyzed, illustrating its highly polygenic architecture. For many traits across all categories, with the exception of other biochemical (i.e., CRP), the replication rate of genes is higher in gene-level associations than at the SNP-level. (B) Number and (E) proportion of 1Mb windows, or “clumps”, that contain at least one genome-wide significant SNP-level associations for a given phenotype in at least two ancestry cohorts. (C) Number and (F) proportion of genome-wide significant gene-level associations that replicate among ancestry cohorts. Replicated associations in hematological are common at the gene-level in hematological and metabolic traits. For instance, in three of the four cohorts with mean corpuscular hemoglobin (MCH) measurements *HBA1* and *HBA2* were identified as significant associated with MCH in the African, European, and East Asian ancestry cohorts [Table S3](#). The denominator of the proportion is calculated as the total number of unique SNPs, clumps, or genes that are significantly associated with a trait in at least on ancestral cohort. Note that D and F correspond to Figure [1A](#) and B, with an altered x-axis upper limit of 0.8 in this figure.

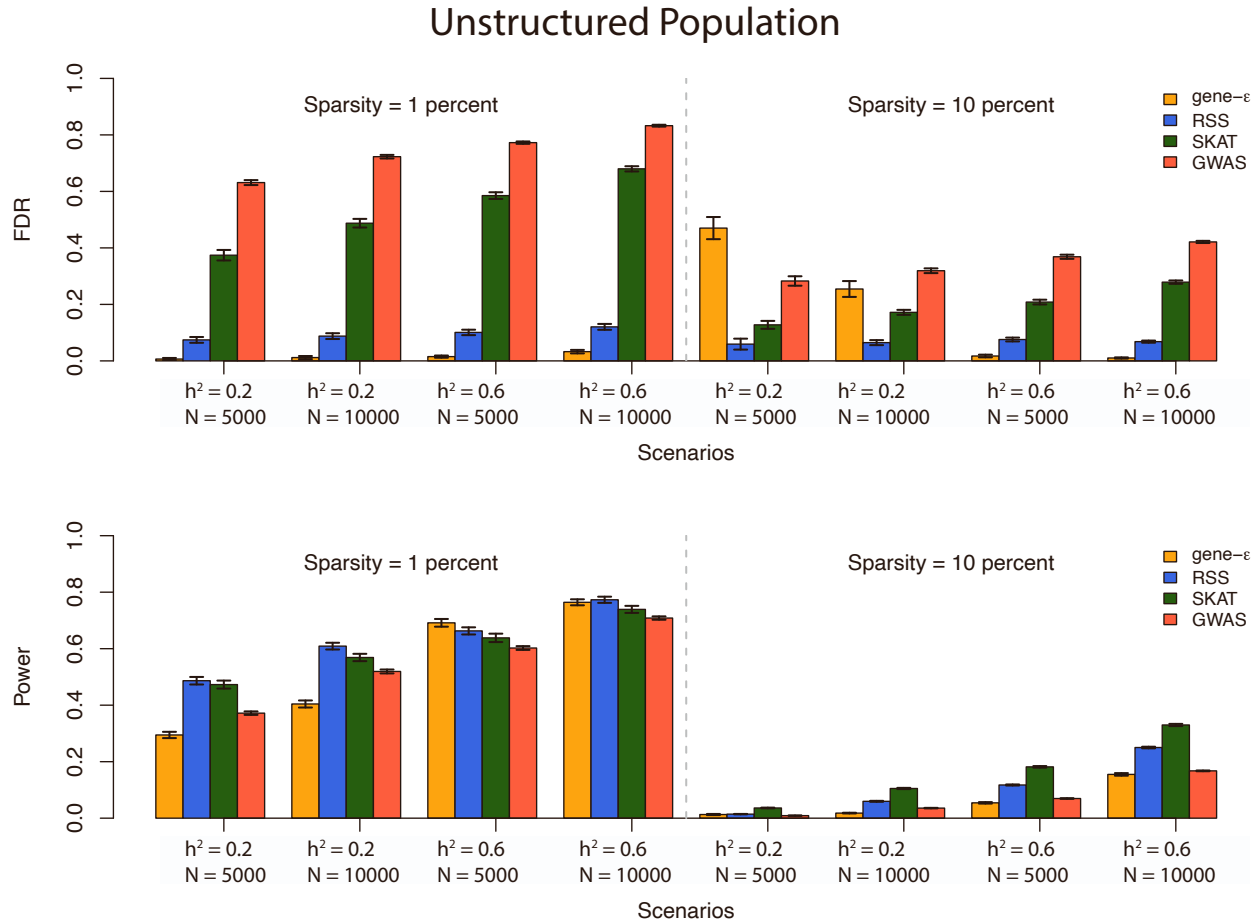


Figure S6: gene- ϵ outperforms and controls false discovery rate (FDR) better than other association methods in simulations with varying heritability and sample size. Simulations were designed to assess gene versus SNP-level association false discovery rate (FDR) and power in an unstructured population as described by the protocols in the Supplemental Information. The top and bottom panels show the FDR and power of four different association methods on 100 simulated datasets, respectively. We compared performance of three gene-level association test methods (gene- ϵ ⁵³, RSS⁵⁴, SKAT⁵⁵) with outputs from the standard GWA association test under different simulation parameters (sample size N , narrow-sense heritability h^2 , and sparsity). We define sparsity as the proportion of SNPs that are ground-truth causal. Standard errors across the simulated replicates are shown using black whisker plots. Simulation protocol is described in the Supplemental Information.

Structured Population

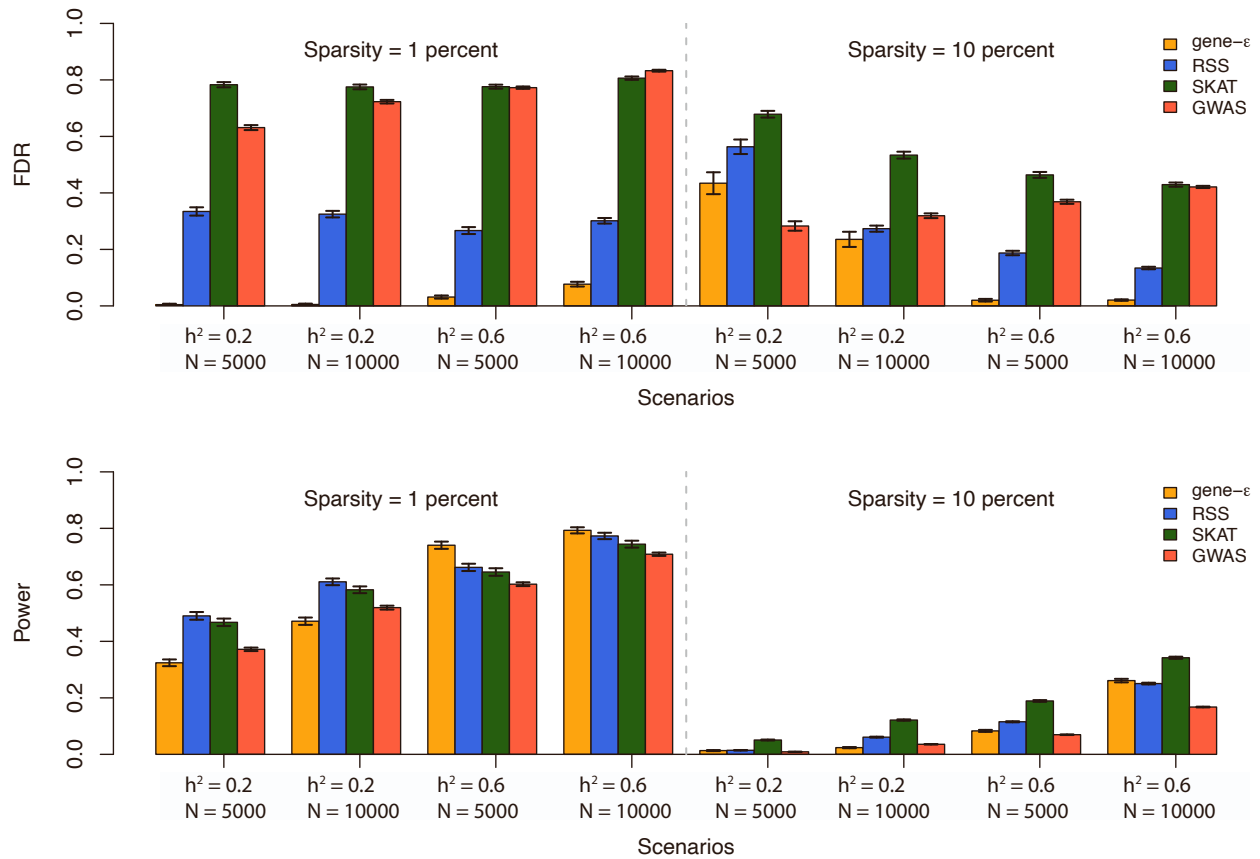


Figure S7: gene- ϵ outperforms and controls false discovery rate (FDR) better than other association methods in simulations with varying heritability and sample size. Simulations are designed to assess gene versus SNP-level association false discovery rate (FDR) and power in an structured population as described by the protocols in the Supplemental Information. The top and bottom panels show the FDR and power of four different association methods on 100 simulated datasets, respectively. We compared performance of three gene-level association test methods (gene- ϵ ⁵³, RSS⁵⁴, SKAT⁵⁵) with outputs from the standard GWA association test under different simulation parameters (sample size N , narrow-sense heritability h^2 , and sparsity). We define sparsity as the proportion of SNPs that are designated to be causal. Standard errors across the simulated replicates are shown using black whisker plots.

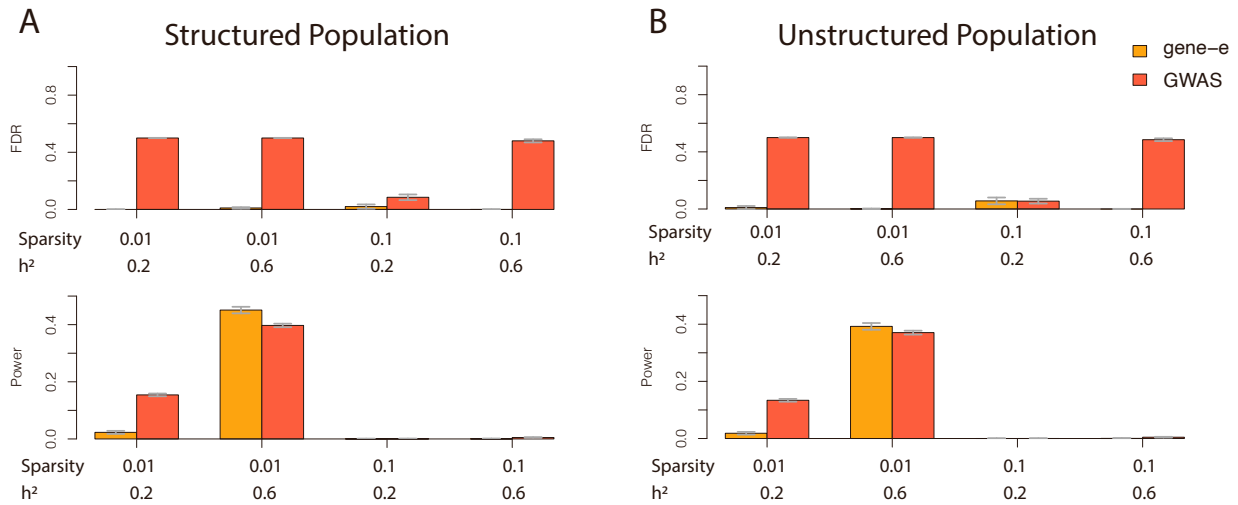


Figure S8: gene- ϵ outperforms and controls false discovery rate (FDR) better than the standard GWA framework in simulations with varying heritability and sparsity. All simulations were done with 2,000 individuals to test the power of gene- ϵ to detect associations in a small cohort. The FDR (top) and power (bottom) for each parameter set are calculated across 100 simulated replicates. A. Results from simulated populations where population structure is present. B. Results from simulated populations when population structure is not present. Mean power and false discovery rate, as well as corresponding standard errors, are shown in [Table S23](#) for clarity.

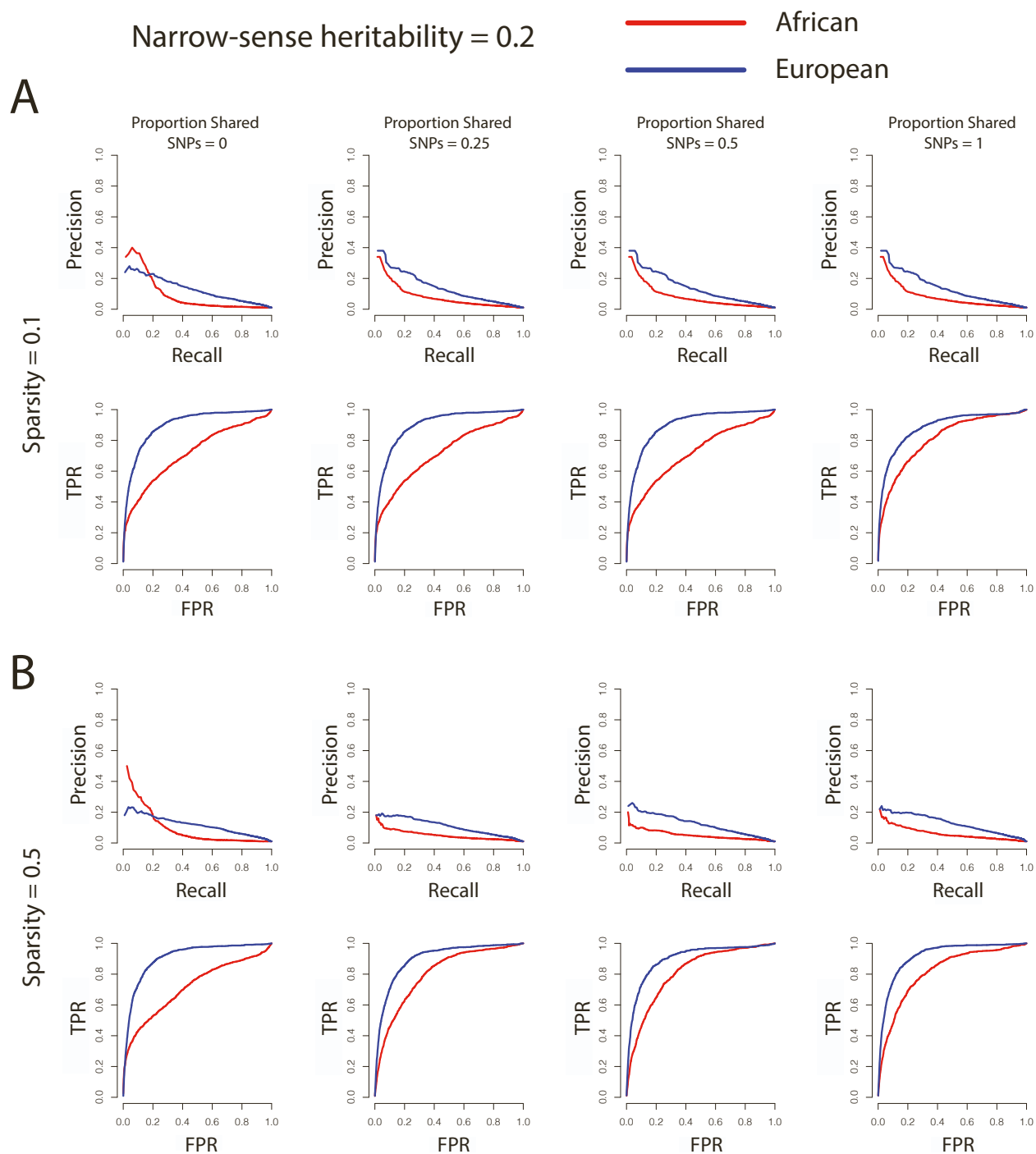


Figure S9: gene- ϵ identifies associated genes in two simulated ancestry cohorts under a variety of genetic architectures with low narrow sense heritability. **A.** Precision-recall (top row) and receiver operating curves (bottom row) for gene- ϵ analysis of cohorts simulated using genotypes from individuals of European ($N = 10,000$; blue line) and African ($N = 4,967$; red line) ancestry, respectively. Narrow-sense heritability was set to $h^2 = 0.2$ in each simulation. Sparsity of causal SNPs was set to a proportion of 0.1 and the proportion of causal SNPs shared was tested at different values. 50 replicates of each set of simulations under each parameter were performed. **B.** Precision-recall (top row) and receiver operating curves (bottom row) for gene- ϵ analysis of 50 replicated simulations of a European and African cohort using a causal SNP sparsity of 0.5.

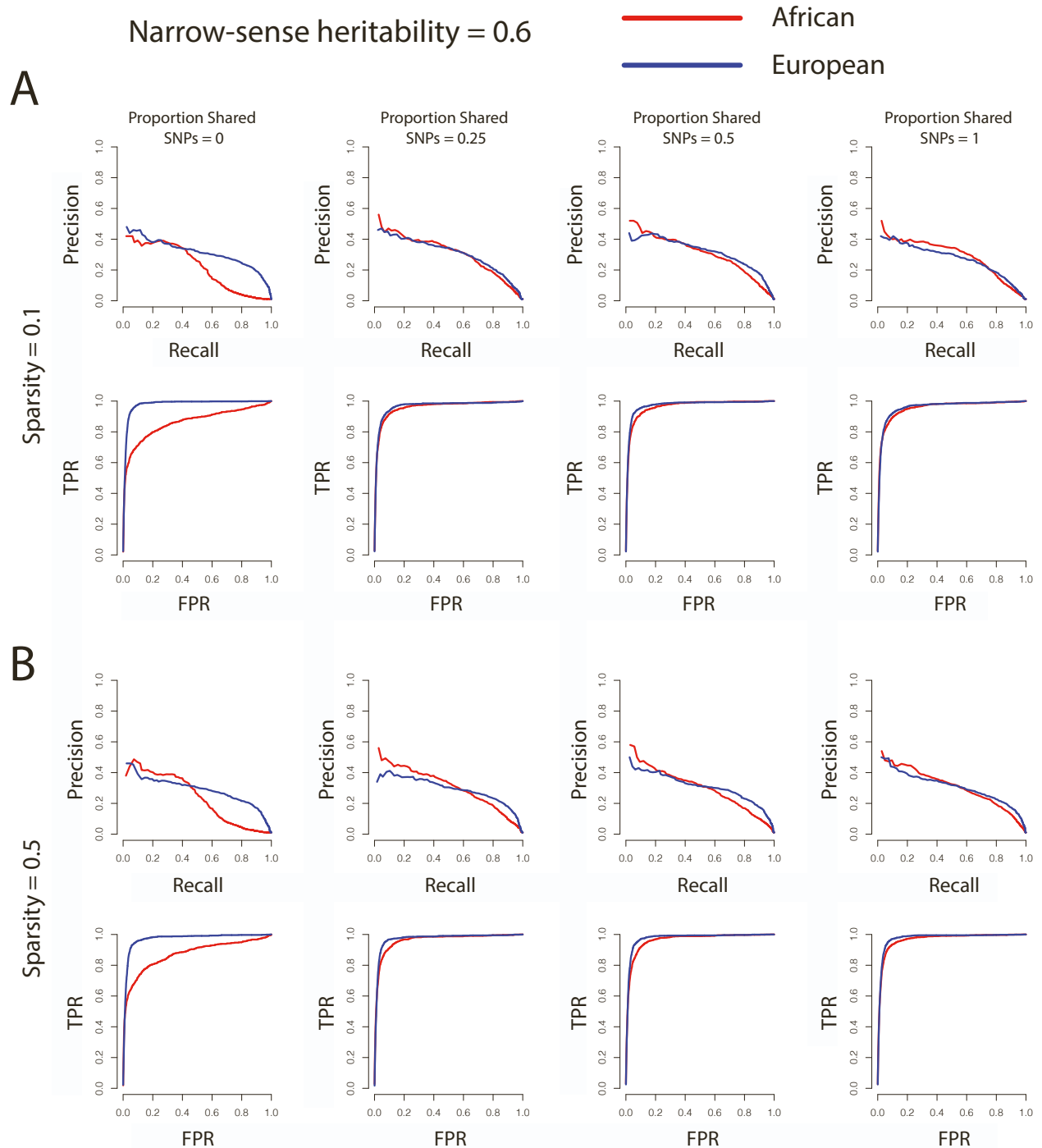


Figure S10: gene- ϵ identifies associated genes in two simulated ancestry cohorts under a variety of genetic architectures with high narrow sense heritability. A. Precision-recall (top row) and receiver operating curves (bottom row) for gene- ϵ analysis of cohorts simulated using genotypes from individuals of European ($N = 10,000$; blue line) and African ($N = 4,967$; red line) ancestry, respectively. Narrow-sense heritability was set to $h^2 = 0.6$ in each simulation. Sparsity of causal SNPs was set to a proportion of 0.1 and the proportion of causal SNPs shared was tested at different values. 50 replicates of each set of simulations under each parameter were performed. **B.** Precision-recall (top row) and receiver operating curves (bottom row) for gene- ϵ analysis of 50 replicated simulations of a European and African cohort using a causal SNP sparsity of 0.5.

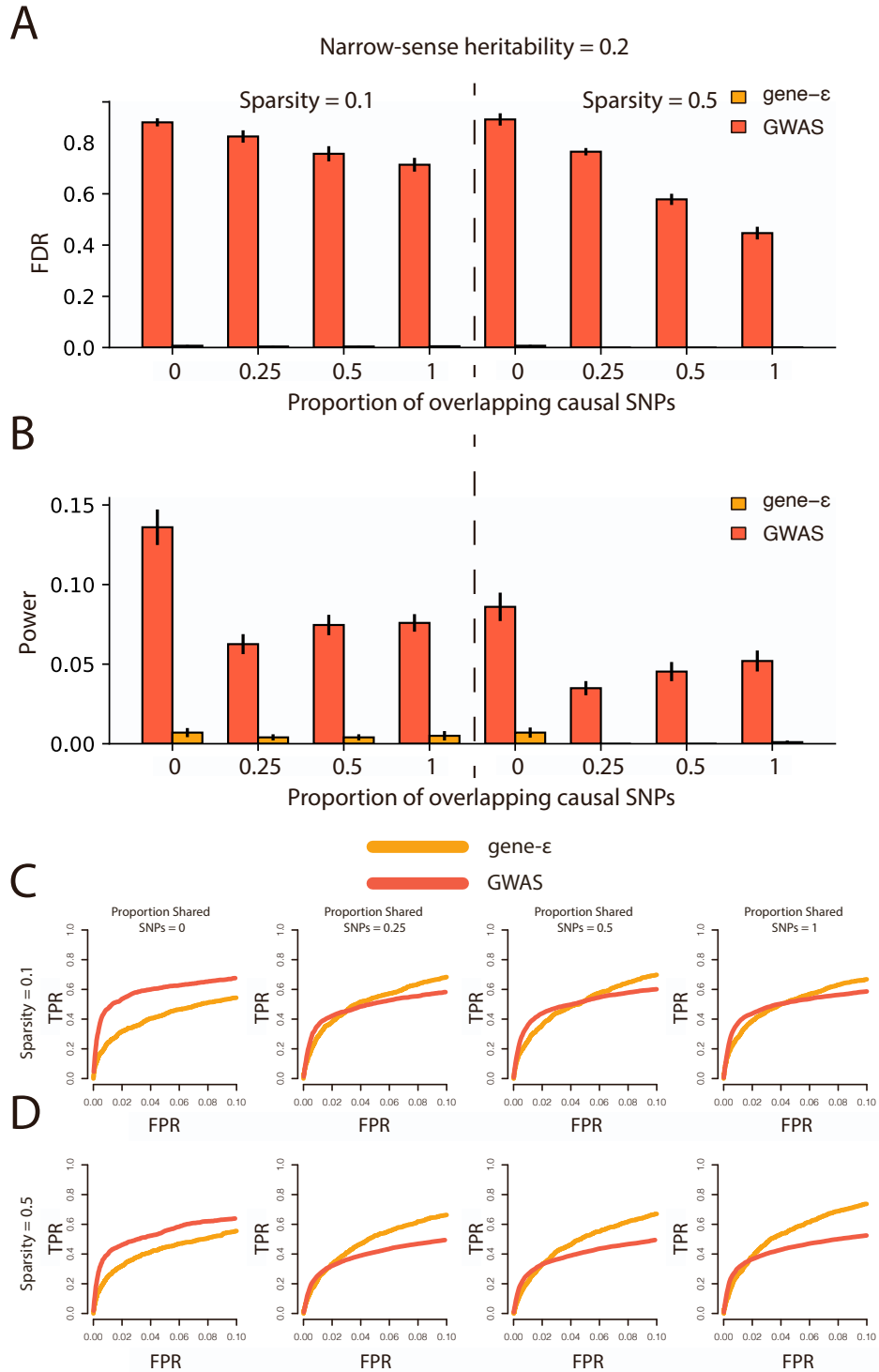


Figure S11: gene- ϵ (orange) has a lower false discovery rate for identification of shared genetic determinants between cohorts than the standard GWA framework (red). Narrow-sense heritability (percent variance explained by the genotype matrix) was set to $h^2 = 0.2$ for all simulations. **A.** False discovery rate of shared genetic determinants between two ancestry cohorts using varying levels of causal SNP sparsity and proportion of shared causal SNPs between the cohorts. **B.** Power of gene- ϵ and the standard GWA framework to detect shared genetic determinants between two cohorts. Error bars were calculated using the results from 50 simulations of each parameter set of sparsity and proportion of shared causal SNPs for both FDR(**A**) and Power(**B**). **C.** Receiver operating curves corresponding to simulations of genetic architecture when causal SNP sparsity is equal to 0.1 (corresponding to the left-hand panels of **A** and **B**). **D.** Receiver operating curves corresponding to simulations of genetic architecture when causal SNP

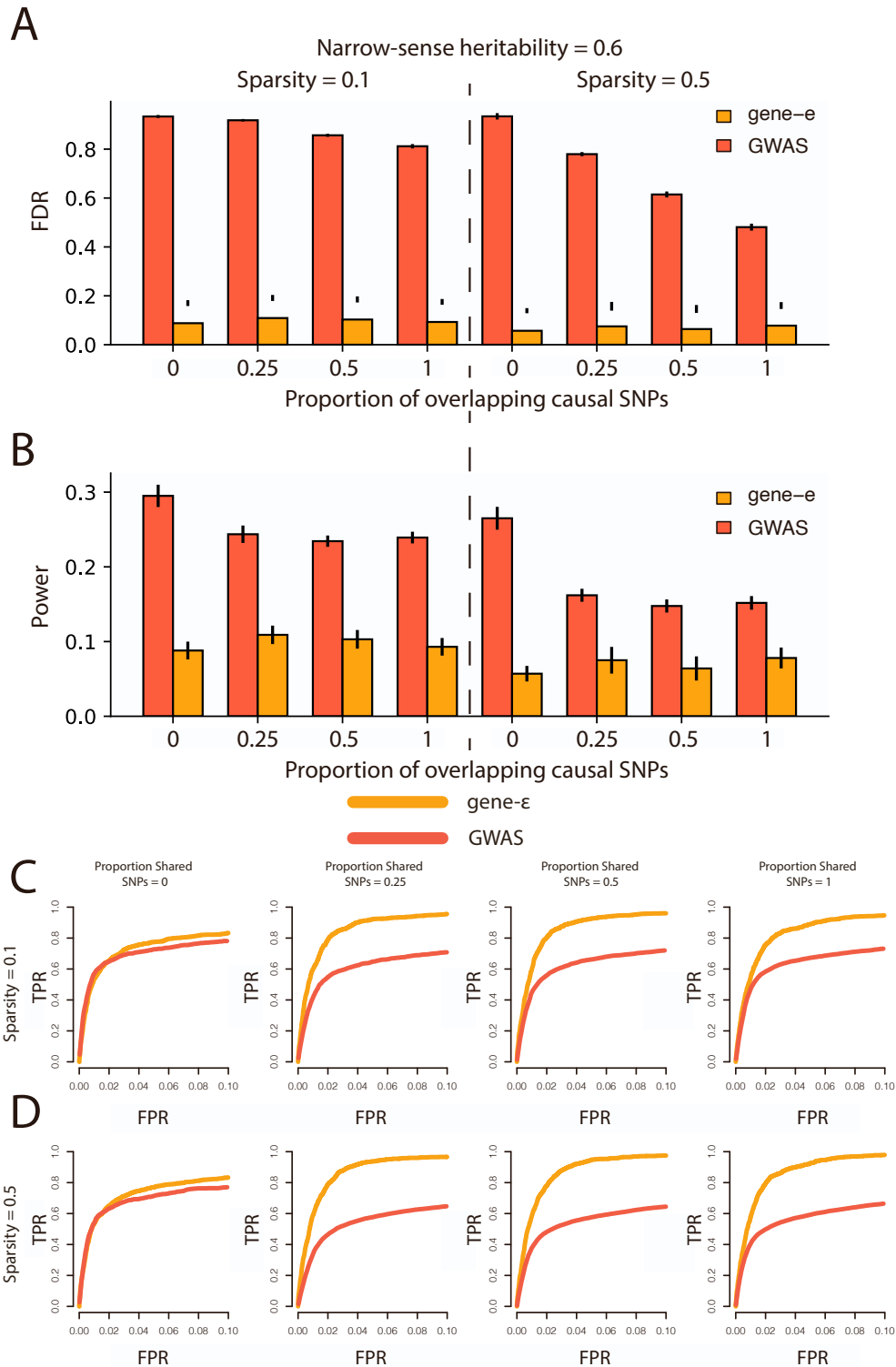


Figure S12: gene- ϵ (orange) has a lower false discovery rate for identification of shared genetic determinants between cohorts than the standard GWA framework (red). Narrow-sense heritability (percent variance explained by the genotype matrix) was set to $h^2 = 0.6$ for all simulations. **A.** False discovery rate of shared genetic determinants between two ancestry cohorts using varying levels of causal SNP sparsity and proportion of shared causal SNPs between the cohorts. **B.** Power of gene- ϵ and the standard GWA framework to detect shared genetic determinants between two cohorts. Error bars were calculated using the results from 50 simulations of each parameter set of sparsity and proportion of shared causal SNPs for both FDR(**A**) and Power(**B**). **C.** Receiver operating curves corresponding to simulations of genetic architecture when causal SNP sparsity is equal to 0.1 (corresponding to the left-hand panels of **A** and **B**). **D.** Receiver operating curves corresponding to simulations of genetic architecture when causal SNP sparsity is equal to 0.5 (corresponding to the right-hand panels of **A** and **B**).

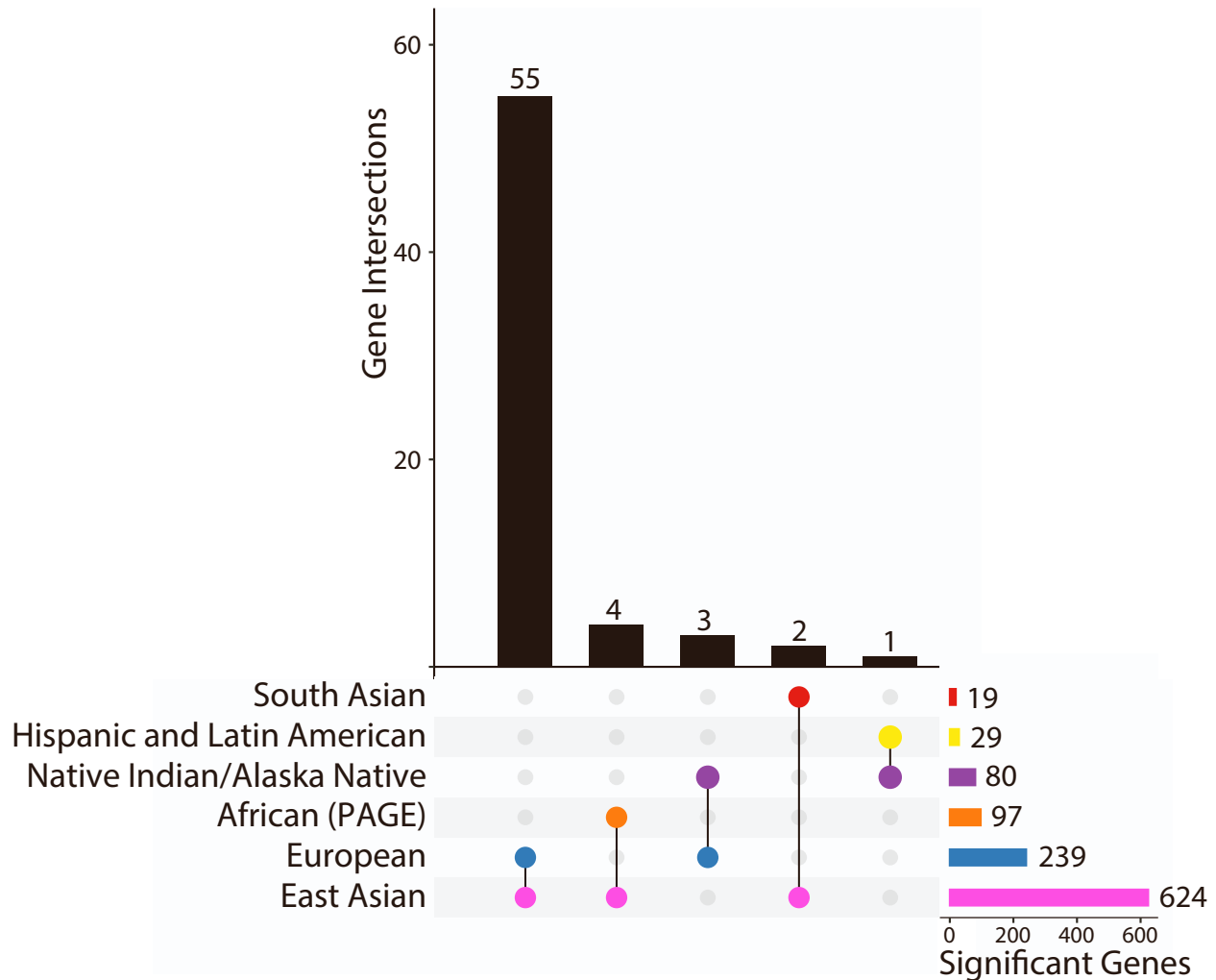


Figure S13: All six ancestries have gene-level associations with platelet count that replicate in at least one other ancestry. Total number of genome-wide significant genes in each ancestry, after correcting for total number of regions tested, are given in the bar plot located in the bottom right (significance thresholds are given in [Table S16](#) sample sizes are given in [Table S6](#)-[Table S9](#)). Shared gene-level association statistics between pairs of ancestries are shown in the vertical bar plot; the pair of ancestries represented by each bar can be identified using the dots and links below the barplot. Of the 65 genome-wide significant gene-level association statistics that replicate in at least two ancestry cohorts, only 25 contain SNPs that have been previously associated with platelet count in at least one ancestry in at least one study in the GWAS catalog (<https://www.ebi.ac.uk/gwas/home>) This plot was generated using the UpSetR package⁵⁶.

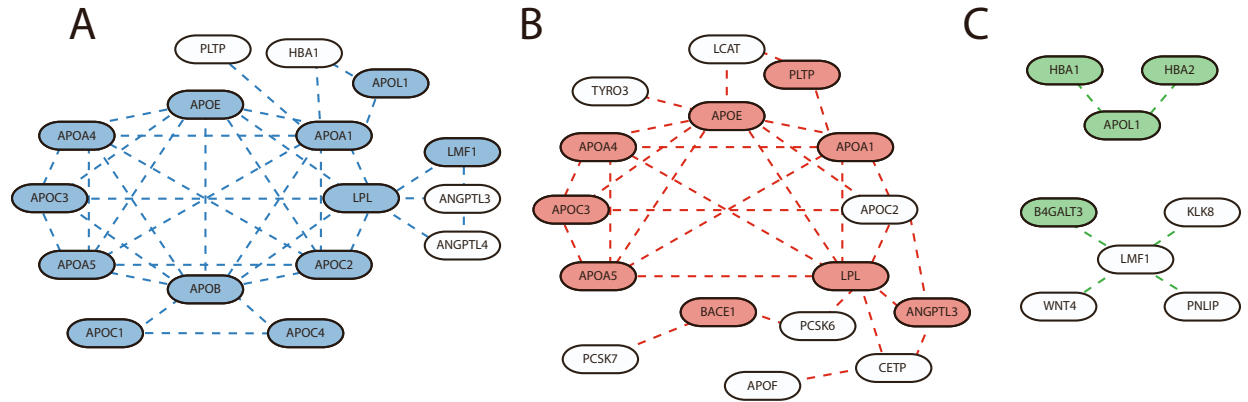


Figure S14: Significantly mutated subnetworks associated with triglyceride levels identified in the (A) European, (B) East Asian, and (C) Native Hawaiian ancestry cohorts. Significantly mutated subnetworks were identified using the Hierarchical HotNet method⁵⁰. Genes that were identified in each ancestry as significantly associated with triglyceride levels using the gene- ϵ method are shaded using ancestry-specific color coding (also used in Figure 3) European—blue, East Asian—pink, Native Hawaiian—green). Significantly mutated subnetworks in the (A) European and (B) East Asian cohorts were identified using the ReactomeFl⁵⁷ protein-protein interaction network, and the significantly mutated subnetwork in the (C) the Native Hawaiian cohort was identified using the iRefIndex 15.0⁵⁸ protein-protein interaction networks. Genes that are present in any of the significantly mutated subnetworks that contain SNPs previously associated with triglyceride levels in the GWAS Catalog are listed with corresponding citations in Table S25.

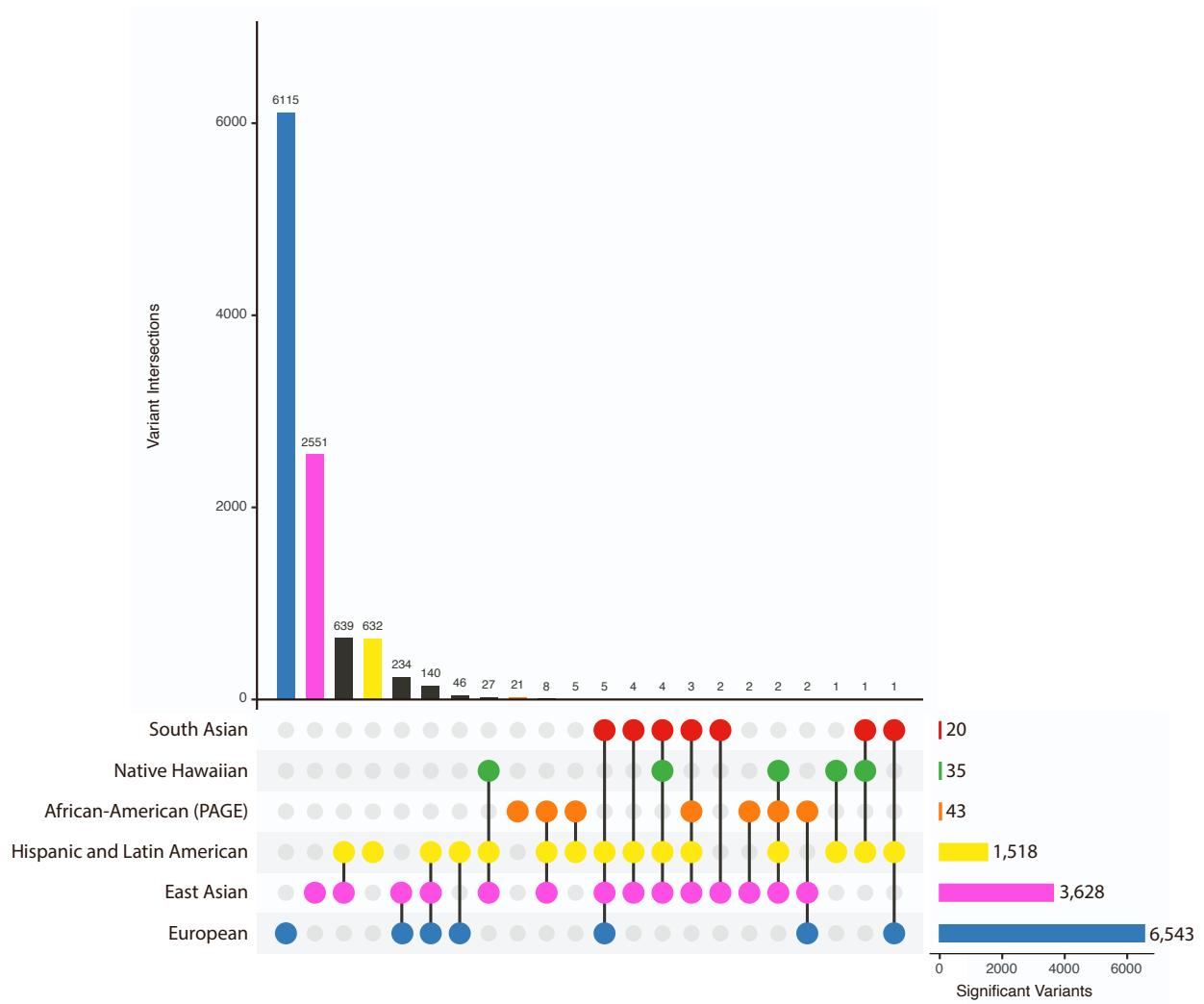


Figure S15: Shared SNP-level associations with triglyceride levels in six ancestral cohorts. Total number of genome-wide significant genes in each ancestry, after correcting for total number of regions tested, are given in the bar plot located in the bottom right (significance thresholds are given in [Table S11](#) and sample sizes are given in [Table S6](#) - [Table S9](#)). Shared SNP-level association statistics between pairs of ancestries are shown in the vertical bar plot. The pair of ancestries represented by each bar can be identified using the dots and links below the vertical barplot. This plot was generated using the UpSetR package⁵⁶.

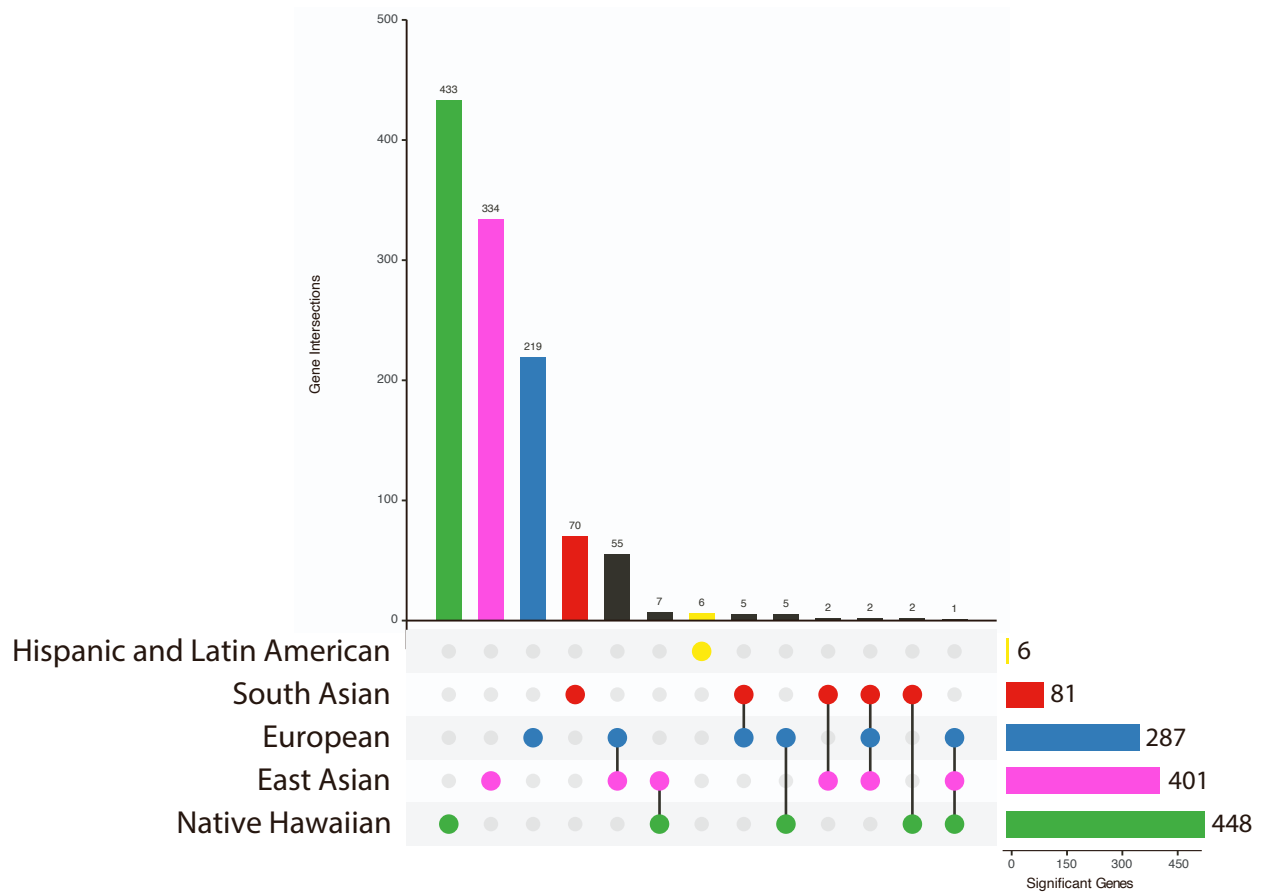


Figure S16: Shared gene-level associations with triglyceride levels in five ancestral cohorts. Total number of genome-wide significant genes in each ancestry, after correcting for total number of regions tested, are given in the bar plot located in the bottom right (significance thresholds are given in [Table S16](#) and sample sizes are given in [Table S6](#) - [Table S9](#)). Shared gene-level association statistics between pairs of ancestries are shown in the vertical bar plot. The pair of ancestries represented by each bar can be identified using the dots and links below the vertical barplot. This plot was generated using the UpSetR package⁵⁶.

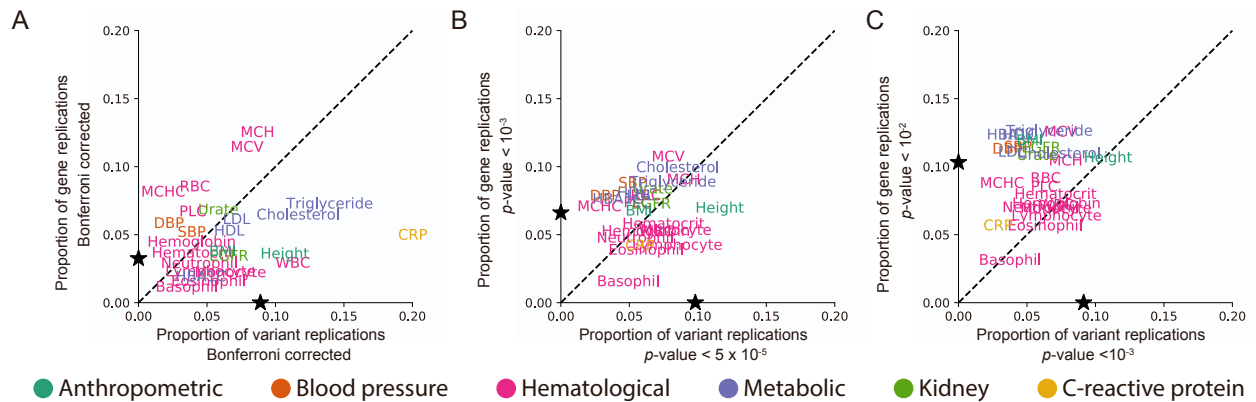


Figure S17: Less stringent significance thresholds lead to a decrease in the proportion of replicated SNP-level associations and an increase in the proportion of gene-level associations among ancestries for each of the 25 traits analyzed. **A.** Proportion of all SNP-level Bonferroni-corrected genome-wide significant associations in any ancestry that replicate in at least one other ancestry is shown on the x-axis (see [Table S11](#) for ancestry-trait specific Bonferroni corrected p -value thresholds). On the y-axis we show the proportion of significant gene-level associations that were replicated for a given phenotype in at least two ancestries (see [Table S16](#) for Bonferroni corrected significance thresholds for each ancestry-trait pair). The black stars on the x- and y-axes represent the mean proportion of replicates in SNP and gene analyses, respectively. C-reactive protein (CRP) contains the greatest proportion of replicated SNP-level associations of any of the phenotypes. **B.** The x-axis indicates the proportion of SNP-level associations that surpass a nominal threshold of p -value $< 10^{-5}$ in at least one ancestry cohort that replicate in at least one other ancestry cohort. The y-axis indicates the proportion of gene-level associations that surpass a nominal threshold of p -value $< 10^{-3}$ in at least one ancestry cohort and replicate in at least one other ancestry cohort. Nominal p -value thresholds tend to decrease the proportion of replicated SNP-level associations and tend to increase the proportion of replicated gene-level associations. The number of unique SNPs and genes that replicated in each cohort is given in [Figure S18](#). **C.** The x-axis indicates the proportion of SNP-level associations that surpass a nominal threshold of p -value $< 10^{-3}$ in at least one ancestry cohort that replicate in at least one other ancestry cohort. The y-axis indicates the proportion of gene-level associations that surpass a nominal threshold of p -value $< 10^{-2}$ in at least one ancestry cohort and replicate in at least one other ancestry cohort. The number of unique SNPs and genes that replicated in each cohort is given in [Figure S19](#). As shown in panel **B**, nominal p -value thresholds tend to decrease the proportion of replicated SNP-level associations and tend to increase the proportion of replicated gene-level associations. Expansion of three letter trait codes are given in [Table S2](#).

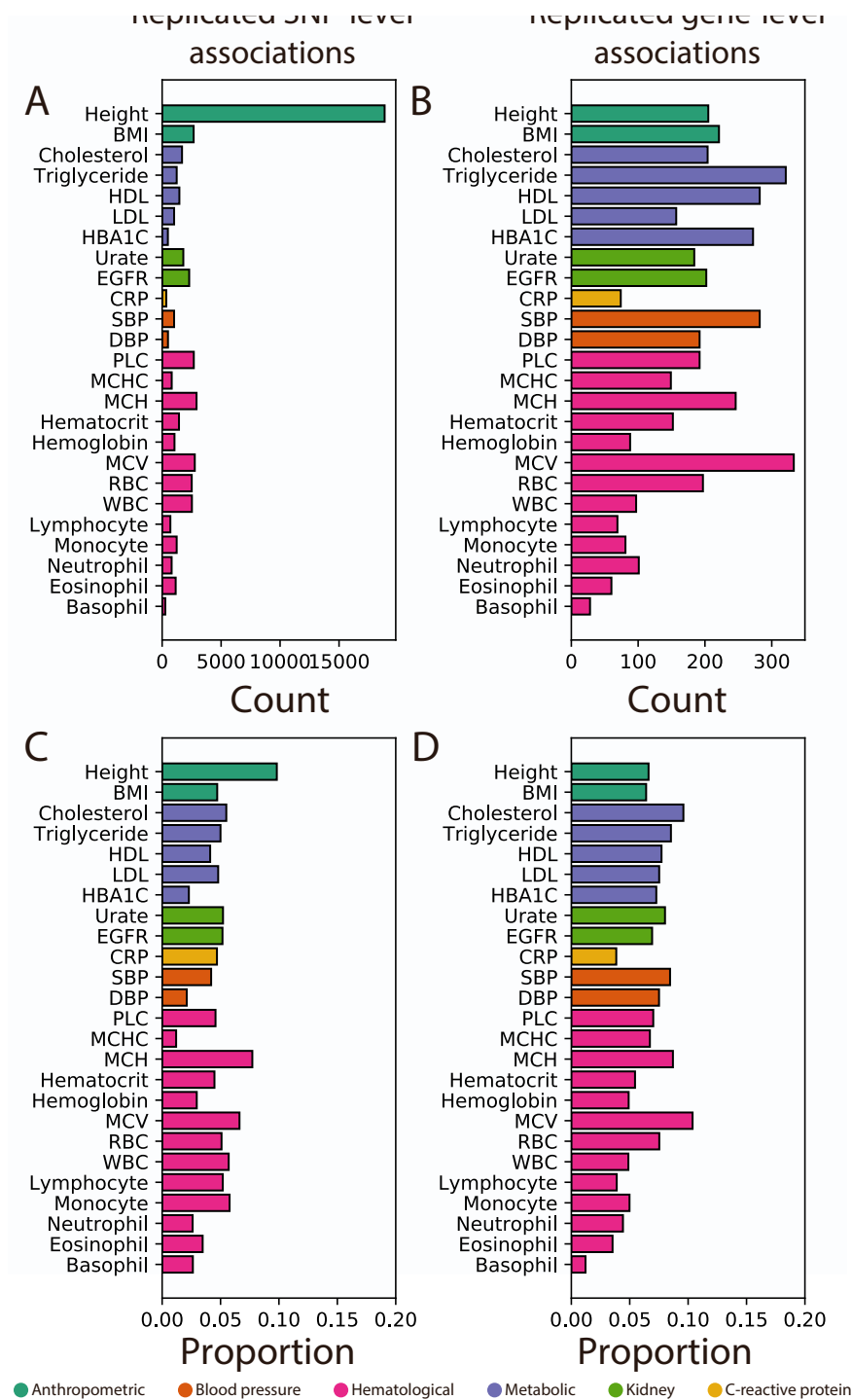


Figure S18: Summaries of replicated associations at multiple genomic scales among ancestry cohorts for all 25 traits analyzed using nominal p -value thresholds (SNP p -value $< 5 \times 10^{-5}$, gene p -value $< 10^{-3}$). (A) Number and (C) proportion of genome-wide significant SNPs associated with a phenotype in at least one ancestry cohort that were replicated in at least two ancestry cohorts using a nominal p -value threshold of 5×10^{-5} . (B) Number and (D) proportion of genome-wide significant gene-level associations that replicate among ancestry cohorts using a nominal p -value threshold of 10^{-3} . Expansion of three letter trait codes are given in [Table S2](#).

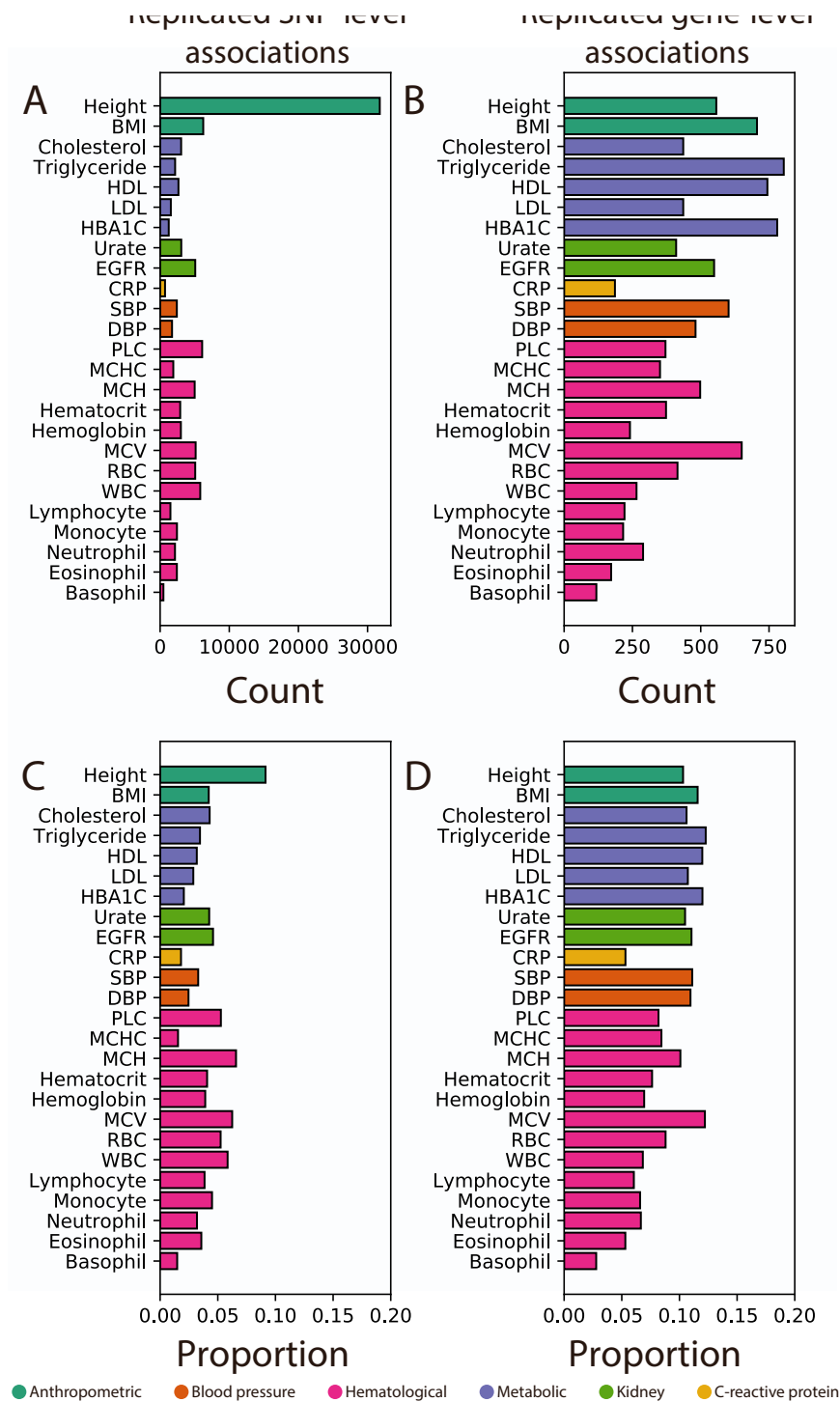


Figure S19: Summaries of replicated associations at multiple genomic scales among ancestry cohorts for all 25 traits analyzed using nominal p -value thresholds (SNP p -value $< 10^{-3}$, gene p -value $< 10^{-2}$). (A) Number and (C) proportion of genome-wide significant SNPs associated with a phenotype in at least one ancestry cohort that were replicated in at least two ancestry cohorts using a nominal p -value threshold of 10^{-3} . (B) Number and (D) proportion of genome-wide significant gene-level associations that replicate among ancestry cohorts using a nominal p -value threshold of 10^{-2} . Expansion of three letter trait codes are given in [Table S2](#). Expansion of three letter trait codes are given in [Table S2](#).

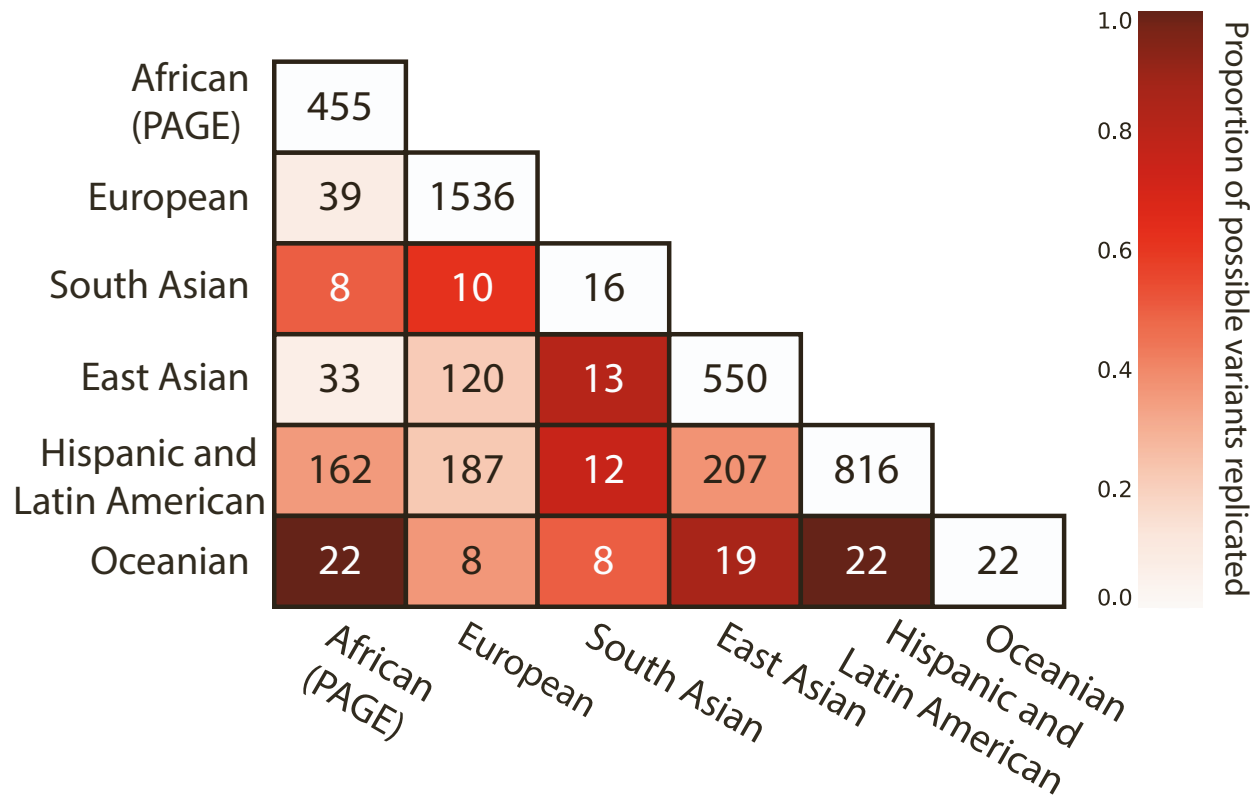
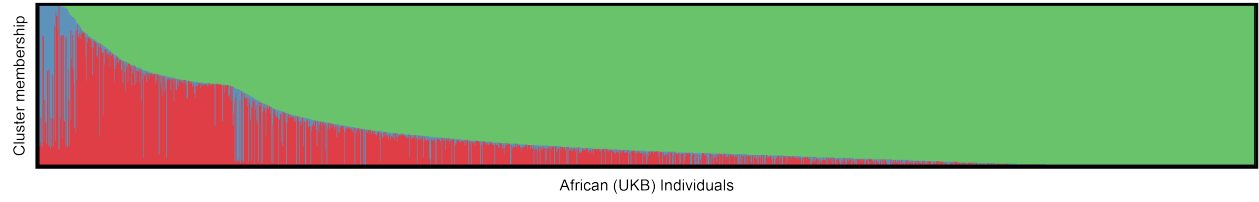


Figure S20: Pairwise replication of SNP-level association signals for C-reactive protein in six ancestral cohorts using genotype and imputed data. Imputed data was available and included in this analysis for each of the six cohorts. The inclusion of imputed SNPs in GWA analysis of C-reactive protein increases both the number of significant SNPs in each ancestry (along the diagonal) as well as the number of replicating significant SNP-level associations among pairs of ancestry cohorts (lower triangular). The corresponding analysis of pairwise SNP-level replication using only genotype data from each cohort is shown in Figure 2C.



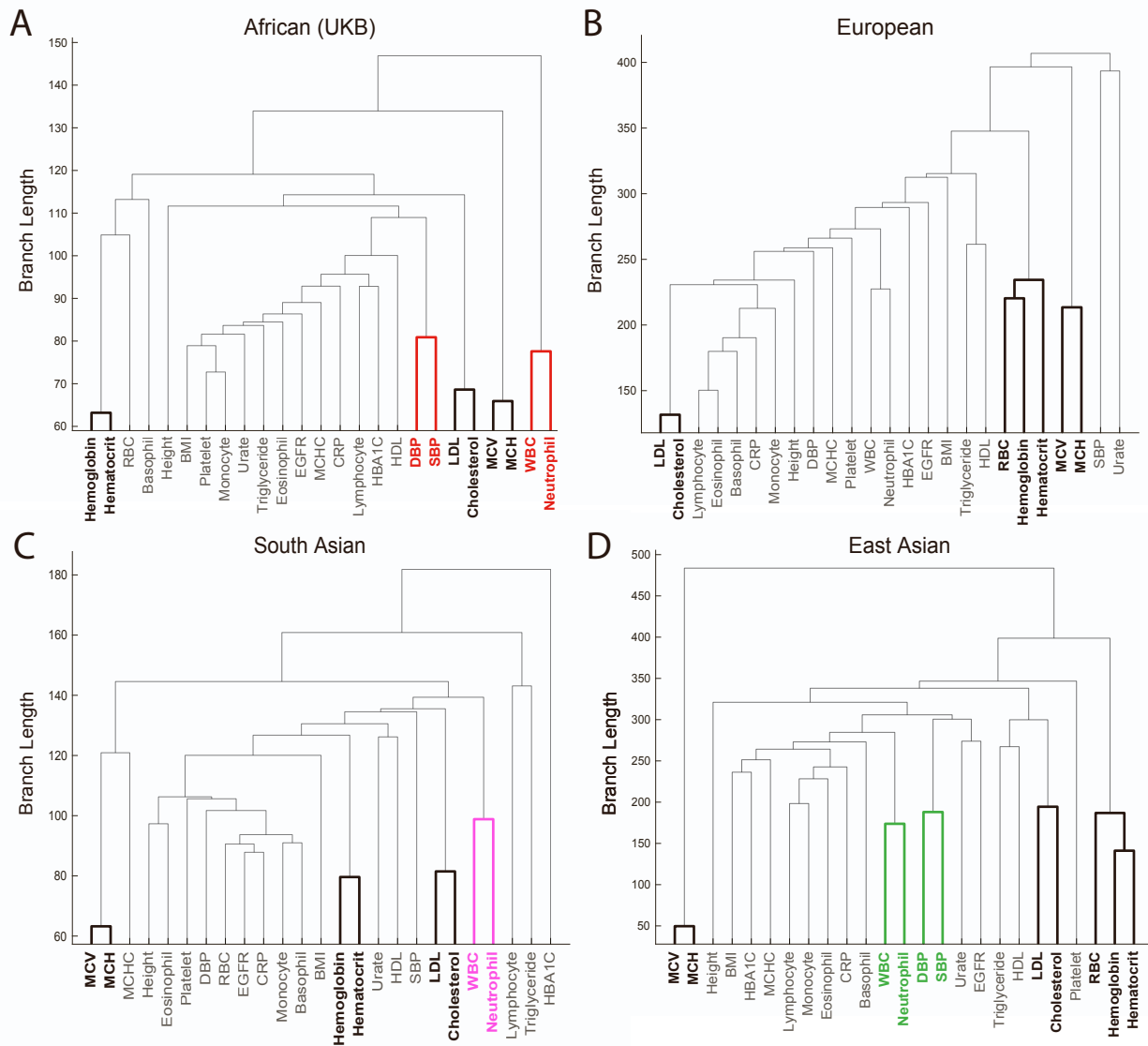


Figure S21: Multiple prioritized trait clusters with shared core genetic trait architecture replicate in the (A) African (UKB), (B) European, (C) South Asian, and (D) East Asian ancestry cohorts. The WINGS algorithm identified prioritized phenotype clusters in each of these ancestry cohorts, denoted in each dendrogram as clades with emboldened lines. Three clusters of phenotypes were found in all ancestries (shown and labeled in black), comprising: mean corpuscular volume (MCV) and mean corpuscular hemoglobin (MCH), hemoglobin and hematocrit, and the metabolic traits low-density lipoprotein (LDL) and cholesterol levels. In both the European and East Asian ancestry cohorts, red blood cell count (RBC) was also a member of the hemoglobin and hematocrit phenotype cluster. Two other phenotype clusters were identified in at least two ancestry cohorts. One of these clusters contains white blood cell count (WBC) and neutrophil count, and the other contains diastolic and systolic blood pressure (DBP and SBP). These two clusters are color-coded according to the ancestry cohorts in which they are prioritized. The WINGS algorithm was applied to traits from each ancestry cohort separately as described in the Supplemental Information.

Ancestry cohort label in this study	Study	Label from original study	Sample Size	Number of SNPs
European	UK Biobank	Self-identified white british	349,411	1,933,096
East Asian	Biobank Japan	East Asian	19,190 - 206,692	4,823,101 - 6,628,005
Hispanic and Latin American	PAGE	Admixed Hispanic and Latin American	15,522 - 21,955	8,576,622 - 8,822,607
African-American (PAGE)	PAGE	African-American	3,750 - 17,280	12,107,345 - 12,274,127
South Asian	UK Biobank	Self-identified South Asian	5,716	958,375
African (UKB)	UK Biobank	African	4,967	578,320
Native Hawaiian	PAGE	Native Hawaiian	1,777 - 3,938	6,656,996 - 6,966,169
American Indian/Alaska Native	PAGE	AIAN	574 - 645	3,970,247 - 8,504,923

Table S1: Ancestry cohorts analyzed in this study. In studies where GWA summary statistics were available to us, sample size and number of SNPs differ due to original study design. The specific sample size and number of SNPs for each trait in studies from Biobank Japan and PAGE are provided in [Table S5](#), [Table S10](#).

Trait Name	Code
Body mass index	BMI
High density lipoprotein	HDL
Low density lipoprotein	LDL
Hemoglobin A1c	HBA1C
Estimated glomerular filtration rate	EGFR
C-reactive protein	CRP
Systolic blood pressure	SBP
Diastolic blood pressure	DBP
Platelet count	PLC
Mean corpuscular hemoglobin concentration	MCHC
Mean corpuscular hemoglobin	MCH
Mean corpuscular volume	MCV
Red blood cell count	RBC
White blood cell count	WBC

Table S2: Abbreviations used throughout this study for 14 quantitative traits analyzed in this study. The remaining 11 traits analyzed were Basophil count, Cholesterol, Eosinophil count, Height, Hematocrit, Hemoglobin, Lymphocyte count, Monocyte count, Neutrophil count, and Triglyceride levels, respectively. These are not abbreviated in the main text.

Trait Name or Code	AIAN	Native Hawaiian	Hispanic
BMI	Yes	Yes	Yes
Basophil count	No	No	No
CRP	Yes	Yes	Yes
Cholesterol	Yes	Yes	Yes
DBP	Yes	No	Yes
EGFR	Yes	No	Yes
Eosinophil count	No	No	No
HBA1C	Yes	Yes	Yes
HDL	Yes	Yes	Yes
Height	Yes	Yes	Yes
Hematocrit	No	No	No
Hemoglobin	No	No	No
LDL	Yes	Yes	Yes
Lymphocyte count	No	No	No
MCH	Yes	No	Yes
MCHC	No	No	No
MCV	No	No	No
Monocyte count	No	No	No
Neutrophil count	No	No	No
PLC	Yes	No	Yes
RBC	No	No	No
SBP	Yes	No	Yes
Triglyceride	No	Yes	Yes
Urate	No	No	No
WBC	Yes	No	Yes

Table S3: Traits assayed in the PAGE study data by ancestry cohort. Data were available for each of the 25 listed traits in the UK Biobank European, South Asian, and African cohorts, as well as, the East Asian cohort from the Biobank Japan. Thus, each trait was analyzed in a minimum of four ancestries and a maximum of seven ancestries.

Trait	Number of significant SNPs in at least the European or East Asian cohort	Number of SNPs with same direction of effect	Percentage of SNPs with same direction of effect
BMI	6,374	4,456	69.91
Basophil	884	520	58.82
CRP	694	463	66.71
Cholesterol	3,451	2,379	68.94
DBP	1,962	1,320	67.28
EGFR	7,129	5,038	70.67
Eosinophil	5,890	3,608	61.26
HBA1C	3,030	2,206	72.81
HDL	5,995	4,077	68.01
Height	33,577	22,090	65.79
Hematocrit	5,382	3,602	66.93
Hemoglobin	5,280	3,601	68.20
LDL	2,521	1,929	76.56
Lymphocyte	2,214	1,237	55.87
MCH	6,763	4,674	69.11
MCHC	1,760	1,124	63.86
MCV	7,489	5,208	69.54
Monocyte	3,929	2,565	65.28
Neutrophil	5,431	3,850	70.89
PLC	11,014	7,161	65.02
RBC	9,211	6,263	67.99
SBP	1,807	1,182	65.41
Triglyceride	3,743	2,686	71.76
WBC	6,017	4,105	68.22
Urate	5,864	3,787	64.58

Table S4: Effect size homogeneity in variants identified as significant in the European or East Asian cohorts. In each of the 25 traits analyzed in this study a majority of variants that are significant in at least the European or East Asian cohorts had the same direction of effect in the other ancestry cohort.

Trait Name or Code	Sample Size	Total SNPs	Pruned SNPs	Regions	Citations
Basophil count	62,076	5,653,566	410,465	23,106	59
BMI	158,284	5,653,566	410,465	23,085	60
CRP	75,391	5,608,701	408,166	23,108	59
DBP	136,615	5,653,566	410,465	23,085	59
eGFR	143,658	5,608,701	408,166	23,108	59
Eosinophil count	62,076	5,653,566	410,465	23,106	59
HDL	70,657	5,608,701	408,166	23,108	59
Height	159,095	6,296,332	354,647	23,679	61
Hematocrit	108,757	5,653,566	410,465	23,106	59
Hemoglobin	108,769	5,653,566	410,465	23,085	59
HbA1c	75,391	5,608,701	408,166	23,108	59
LDL	72,866	5,608,701	408,166	23,108	59
Lymphocyte count	62,076	5,653,566	410,465	23,106	59
MCH	108,054	5,653,566	410,465	23,106	59
MCHC	108,738	5,653,566	410,465	23,106	59
MCV	108,526	5,653,566	410,465	23,085	59
Monocyte count	62,076	5,653,566	410,465	23,106	59
Neutrophil count	62,076	5,653,566	410,465	23,106	59
PLC	108,208	5,653,566	410,465	23,085	59
RBC	108,794	5,653,566	410,465	23,085	59
SBP	136,597	5,653,566	410,465	23,085	59
Cholesterol	128,305	5,608,701	408,166	23,108	59
Triglyceride	105,597	5,608,701	410,465	23,108	59
Urate	109,029	5,608,701	408,166	23,108	59
WBC	107,694	5,653,566	408,166	23,085	59

Table S5: Number of individuals, total SNPs, pruned SNPs used for gene- ϵ , and genes and transcription factors (regions) included in the analysis for each trait in Biobank Japan data. Regions were defined using the hg19 list provided in Gusev et al.[62](#).

Trait Name or Code	Sample Size	Total SNPs	Pruned SNPs	Regions
BMI	17,127	12,139,115	404,401	24,216
CRP	8,349	12,274,126	404,572	24,206
DBP	11,380	12,148,801	405,188	24,218
eGFR	8,261	12,128,273	403,371	24,207
Hemoglobin A1c	17,127	12,139,115	404,401	24,215
HDL	10,085	12,114,827	404,089	24,201
Height	17,280	12,139,907	404,522	24,201
LDL	9,720	12,107,344	403,740	24,218
MCHC	3,750	12,132,232	405,558	24,217
PLC	8,850	12,131,935	404,497	24,193
SBP	11,380	12,148,801	405,188	24,218
Cholesterol	10,137	12,110,337	403,674	24,222
Triglyceride	9,980	12,110,879	403,455	24,206
WBC	8,802	12,126,732	404,579	24,219

Table S6: Number of individuals, total SNPs, pruned SNPs used for gene- ϵ , and genes and transcription factors (regions) included in the analysis for each trait in the African-American cohort of the PAGE study data.

Trait Name or Code	Sample Size	Total SNPs	Pruned SNPs	Region Count
BMI	21,955	8,812,436	432,762	24,138
CRP	15,912	8,576,621	397,941	24,118
DBP	21,549	8,784,112	430,360	24,126
Estimated glomerular filtration rate	18,548	8,702,426	422,598	24,123
HbA1c	21,955	8,812,436	432,762	24,138
HDL	17,751	8,583,603	412,771	24,122
Height	22,187	8,822,606	433,604	24,132
LDL	17,373	8,588,800	413,074	24,116
MCHC	15,522	8,763,739	427,208	24,132
PLC	18,949	8,612,804	415,201	24,115
SBP	21,549	8,784,112	430,360	24,126
Cholesterol	17,802	8,586,887	412,830	24,115
Triglyceride	17,856	8,594,121	413,546	24,104
WBC	18,206	8,603,503	414,462	24,123

Table S7: Number of individuals, total SNPs, pruned SNPs used for gene- ϵ , and genes and transcription factors (regions) included in the analysis for each trait in the Hispanic and Latin American cohort of the PAGE study data.

Trait Name or Code	Sample Size	Total SNPs	Pruned SNPs	Regions
BMI	645	8,374,976	421,826	24,124
CRP	574	8,504,922	417,287	24,136
DBP	636	8,376,521	421,528	24,136
eGFR	602	8,336,044	417,540	24,132
Hemoglobin A1c	645	8,374,976	421,826	24,124
HDL	604	8,315,912	415,939	24,121
Height	645	8,375,624	421,750	24,117
LDL	591	8,360,719	419,544	24,123
MCHC	620	3,970,246	62,339	17,381
PLC	603	8,294,302	414,530	24,133
Systolic blood pressure	636	8,376,521	421,528	24,136
Cholesterol	604	8,586,887	415,939	24,121
WBC	602	8,289,567	414,462	24,133

Table S8: Number of individuals, total SNPs, pruned SNPs used for gene- ϵ , and genes and transcription factors (regions) included in the analysis for each trait in the AIAN cohort of the PAGE study data.

Trait Name or Code	Sample Size	Total SNPs	Pruned SNPs	Regions
BMI	3,936	6,664,738	415,221	23,885
CRP	1,777	6,966,169	428,517	23,834
Hemoglobin A1c	3,936	6,664,738	415,221	23,885
HDL	1,912	6,656,996	416,255	23,894
Height	3,938	6,660,920	415,172	23,878
LDL	1,900	6,662,802	416,810	23,895
Cholesterol	1,915	6,660,807	416,425	23,899
Triglycerides	1,915	6,660,807	416,425	23,899

Table S9: Number of individuals, total SNPs, pruned SNPs used for gene- ϵ , and genes and transcription factors (regions) included in the analysis for each trait in the Native Hawaiian (Native Hawaiian) cohort of the PAGE study data.

Trait Name or Code	Sample Size	Total SNPs	Pruned SNPs	Regions
BMI	4,647	15,362,633	433,356	24,085
CRP	1,811	14,374,461	428,656	24,116
DBP	1,086	12,470,507	416,273	24,112
eGFR	150	8,314,417	337,167	24,017
HbA1c	4,647	15,362,633	433,356	24,085
HDL	2,378	13,413,244	428,598	24,072
Height	4,679	15,366,710	433,005	24,103
LDL	2,316	13,327,313	428,741	24,075
MCHC	128	8,089,136	315,583	23,946
PLC	541	10,528,072	421,929	24,098
SBP	1,086	12,470,507	416,273	24,112
Cholesterol	2,387	13,436,190	428,656	24,078
Triglyceride	2,381	13,423,953	429,246	24,073
WBC	543	10,570,051	421,776	24,095

Table S10: Number of individuals, total SNPs, pruned SNPs used for gene- ϵ , and genes and transcription factors (regions) included in the analysis for each trait in the Asian cohort of the PAGE study data.

Trait Name or Code	African or African-American ($\times 10^{-8}$)	East Asian ($\times 10^{-8}$)	AIAN ($\times 10^{-8}$)	Native Hawaiian ($\times 10^{-9}$)	Hispanic ($\times 10^{-8}$)
Basophil count	8.646*	8.844	NA	NA	NA
BMI	0.412	8.844	0.597	7.502	5.674
CRP	0.407	8.915	0.588	7.176	5.830
Cholesterol	0.414	8.915	0.601	7.507	5.823
DBP	0.412	8.844	0.597	NA	5.692
EGFR	0.412	8.915	0.600	NA	5.746
Eosinophil count	8.646*	8.844	NA	NA	NA
HBA1C	0.412	8.915	0.597	7.502	5.674
HDL	0.413	8.915	0.601	7.511	5.825
Height	0.412	7.941	0.597	7.506	5.667
Hematocrit	8.646*	8.844	NA	NA	NA
Hemoglobin	8.646*	8.844	NA	NA	NA
LDL	0.413	8.914	0.598	7.504	5.822
Lymphocyte count	8.646*	8.843	NA	NA	NA
MCH	8.646*	8.844	NA	NA	NA
MCHC	0.412	8.844	1.259	NA	5.705
MCV	8.646*	8.844	NA	NA	NA
Monocyte count	8.646*	8.844	NA	NA	NA
Neutrophil count	8.646*	8.844	NA	NA	NA
PLC	0.412	8.844	0.603	NA	5.805
RBC	8.646*	8.844	NA	NA	NA
SBP	0.412	8.844	0.597	NA	5.692
Triglyceride	0.413	8.915	NA	7.507	5.818
Urate	8.646*	8.915	NA	NA	NA
WBC	0.412	8.844	NA	NA	5.812

Table S11: Bonferroni p -value threshold corrected for number of SNP-level association tests performed for each ancestry-trait pair. Thresholds are calculated as 0.05 divided by the number of SNPs tested in each ancestry-trait pair. The term "NA" indicates that there was no data for that ancestry-trait pair. The threshold for Bonferroni-corrected significance was the same for every trait in the European (p -value $< 2.587 \times 10^{-8}$) and South Asian (p -value $< 5.217 \times 10^{-8}$) cohorts from the UK Biobank. Traits for which the UK Biobank African cohort was used are denoted with a *; otherwise, the African-American cohort from the PAGE study data was used. See [Table S2](#) for expansion of trait codes.

Trait Name or Code	Nominal Significance Threshold	Number of Variants Tested	Number of Replicated Variants	Proportion of Replicated Variants	Unidentified non-European Associations
MCV	1.46×10^{-05}	3,414	2,008	0.588	7,830
PLC	1.25×10^{-05}	3,998	1,792	0.448	6,073
Height	2.80×10^{-06}	17,877	10,406	0.582	37,360
BMI	2.22×10^{-05}	2,254	1,478	0.656	2,762
DBP	5.37×10^{-05}	931	528	0.567	719
SBP	8.17×10^{-05}	612	352	0.575	1,315
WBC	1.87×10^{-05}	2,680	1,192	0.445	17,800
RBC	1.71×10^{-05}	2,918	1,674	0.574	3514
Hemoglobin	3.48×10^{-05}	1,436	5,80	0.404	368
Hematocrit	2.99×10^{-05}	1,670	1,068	0.640	524
MCH	1.56×10^{-05}	3,214	1,904	0.592	7,851
MCHC	4.58×10^{-05}	1,091	722	0.662	26,507
Lymphocyte	8.03×10^{-05}	623	327	0.525	536
Monocyte	3.53×10^{-05}	1,418	896	0.632	1,568
Neutrophil	5.07×10^{-05}	987	527	0.534	1,550
Eosinophil	4.00×10^{-05}	1,249	802	0.642	2,143
Basophil	9.62×10^{-04}	52	49	0.942	2,017
Urate	2.56×10^{-05}	1,951	1,414	0.725	6,530
Triglyceride	3.99×10^{-05}	1,254	928	0.740	3,902
Cholesterol	1.96×10^{-05}	2,557	1,742	0.681	2,847
LDL	3.16×10^{-05}	1,580	1,115	0.706	1,735
HDL	2.86×10^{-05}	1,751	1,089	0.622	4,737
HBA1C	6.31×10^{-05}	7,92	4,16	0.525	899
EGFR	2.00×10^{-05}	2,506	1,315	0.525	2,227

Table S12: Nominal p -value threshold corrected for number of Bonferroni-corrected SNP-level associations found in the European ancestry cohort. To illustrate how SNP-level statistical replication among ancestry cohorts is prohibited by external factors (e.g. sample sizes, genotype array design), We calculated the number of SNP-level replications when thresholds for non-European cohorts are calculated as 0.05 divided by the number of significant SNPs in the European cohort. This design is analogous to a two-stage GWA framework, where non-European ancestry cohorts are not used for discovery and associations discovered in the European ancestry cohort are used to find replicates. Replication of SNP-level association signals increases when less stringent thresholds are used. Number of variants that were tested in the European ancestry cohort and at least one another cohort were included in this calculation and are given here. We also include the number of variants that were identified in non-European ancestry cohorts using a Bonferroni-corrected significance threshold to illustrate how this study design may miss signals in other ancestries. See [Table S2](#) for expansion of trait codes.

Gene	European	East Asian	South Asian	African-American	Hispanic and Latin American	AIAN	Native Hawaiian
MCV	0.013-0.153	0.024-0.153	0.136-0.268	0.113-0.522	NA	NA	NA
PLC	0.0132-0.190	0.024-0.140	0.124-0.171	5.715-17.196	3.732-18.805	100.736-100.736	0.0
Height	0.009-0.115	0.0178-0.150	NA	0.064-0.267	0.051-0.113	NA	NA
BMI	0.0133-0.113	0.020-0.110	NA	0.068-0.068	0.064-0.101	NA	NA
DBP	0.0136-0.070	0.022-0.074	NA	NA	0.787-0.806	NA	NA
SBP	0.0129-0.066	0.022-0.064	NA	NA	4.64-4.643	NA	NA
WBC	0.0135-0.122	0.024-0.104	0.117-0.145	0.027-0.198	0.018-0.112	NA	NA
RBC	0.012-0.107	0.025-0.142	NA	0.115-0.297	NA	NA	NA
Hemoglobin	0.0108-0.129	0.025-0.083	NA	0.162-0.232	NA	NA	NA
Hematocrit	0.011-0.093	0.024-0.085	NA	0.241-0.241	NA	NA	NA
MCH	0.013-0.159	0.024-0.153	0.104-0.277	0.109-0.541	NA	NA	NA
MCHC	0.014-0.115	0.024-0.106	NA	0.152-1.28	0.088-0.489	0.118-9.222	MA
Lymphocyte	0.014-0.078	0.033-0.264	0.503-0.503	0.647-0.647	NA	NA	NA
Monocyte	0.0133-0.195	0.0329-0.123	NA	0.423-0.423	NA	NA	NA
Neutrophil	0.014-0.160	0.033-0.106	0.123-0.142	0.108-0.518	NA	NA	NA
Eosinophil	0.013-0.149	0.033-0.188	NA	NA	NA	NA	NA
Basophil	0.014-0.120	0.033-0.167	0.363-0.581	0.241-0.626	NA	NA	NA
Urate	0.0112-0.097	0.024-0.346	0.092-0.251	0.104-0.682	NA	NA	NA
Triglyceride	0.013-0.204	0.0247-0.318	0.113-0.311	0.043-0.616	0.032-0.159	NA	0.102-0.169
Cholesterol	0.013-0.309	0.023-0.285	0.118-0.268	4.280-30.434	2.734-15.098	NA	NA
LDL	0.0136-0.121	0.030-0.514	0.139-0.367	3.785-29.006	2.371-18.999	16.273-33.101	14.133-16.297
HDL	0.013-0.296	0.030-0.529	0.106-0.369	1.368-23.818	0.838-32.374	NA	22.726-46.409
HBA1C	0.013-0.090	0.039-0.139	NA	0.068-0.068	0.064-0.101	NA	NA
EGFR	0.0133-0.195	0.021-0.095	0.119-0.162	NA	1.102-1.102	12.494-27.656	0.0
CRP	0.0137-0.122	0.0300-0.127	0.106-0.263	0.094-0.418	0.0626-0.434	NA	0.211-0.254

Table S13: Range of effect sizes for significant SNPs in each ancestry cohort.

Trait Name or Code	African	South Asian	Native Hawaiian	AIAN	Hispanic and Latin American
Hemoglobin	1.464×10^{-7}	NA	0.0	0.0	0.0
Height	0.999	7.930×10^{-5}	0.0006	NA	0.948
PLC	0.958	0.0006	0.0	NA	0.993
MCV	0.1123	0.0004	0.0	0.0	0.0
BMI	0.079	0.056	0.005	NA	0.970
DBP	0.0009	NA	0.0	NA	0.015
SBP	9.078×10^{-6}	NA	0.0	NA	0.027
WBC	0.227	0.048	0.0	NA	0.914
RBC	0.001	0.010	0.0	0.0	0.0
Hematocrit	1.287×10^{-7}	NA	0.0	0.0	0.0
MCH	0.321	0.016	0.0	0.0	0.0
MCHC	0.001	NA	0.0	6.814×10^{-8}	0.285
Lymphocyte	NA	4.931×10^{-6}	0.0	0.0	0.0
Monocyte	0.093	0.137	0.0	0.0	0.0
Neutrophil	1.722×10^{-7}	6.244×10^{-6}	0.0	0.0	0.0
Eosinophil	0.044	1.499×10^{-5}	0.0	0.0	0.0
Basophil	NA	9.739×10^{-5}	0.0	0.0	0.0
Urate	0.002	0.005	0.0	0.0	0.0
Triglyceride	0.462	0.171	NA	0.0	0.997
Cholesterol	0.897	0.210	NA	NA	0.998
LDL	0.963	NA	NA	NA	0.997
HDL	0.345	0.146	NA	NA	0.930
HBA1C	NA	NA	3.092×10^{-6}	NA	0.024
EGFR	NA	0.031	0.0	NA	0.886
CRP	0.267	0.137	0.002	1.686×10^{-5}	0.981

Table S14: Maximum power under the standard GWA framework to detect variants that were significant in both the European ancestry cohort and at least one other cohort. For each ancestry-trait pair, power calculations were performed for all variants that were significant using a Bonferroni-corrected significance threshold and were significant in the corresponding ancestry (sorted by column). Power was calculated assuming the marginal European effect size to be the true effect size. Non-European ancestry minor allele frequencies and sample sizes were used in the power calculations. Calculations were performed using then framework defined in Sham and Purcell⁶³. Comparisons where a variant had power to detect greater than 0.9 are shown in bold.

Trait Name or Code	African	South Asian	Native Hawaiian	AIAN	Hispanic and Latin American
Hemoglobin	0(1)	NA	0.0	0.0	0.0
Height	4(56)	0(2)	0(5)	NA	16(408)
PLC	1(163)	0(8)	0.0	NA	6(262)
MCV	0(18)	0(7)	0.0	0.0	0.0
BMI	0(3)	0(1)	0(35)	NA	48(212)
DBP	0(1)	NA	0.0	NA	0(109)
SBP	0(1)	NA	0.0	NA	0(99)
WBC	0(71)	0(25)	0.0	NA	35(104)
RBC	0(3)	0(3)	0.0	0.0	0.0
Hematocrit	0(1)	NA	0.0	0.0	0.0
MCH	0(22)	0(8)	0.0	0.0	0.0
MCHC	0(3)	NA	0.0	0(135)	0(110)
Lymphocyte	NA	0(7)	0.0	0.0	0.0
Monocyte	0(1)	0(2)	0.0	0.0	0.0
Neutrophil	0(2)	0(32)	0.0	0.0	0.0
Eosinophil	0(7)	0(1)	0.0	0.0	0.0
Basophil	NA	0(2)	0.0	0.0	0.0
Urate	0(1)	0(8)	0.0	0.0	0.0
Triglyceride	0(30)	0(61)	NA	0.0	124(311)
Cholesterol	0(85)	0(11)	NA	NA	16(943)
LDL	7(132)	NA	NA	NA	17(634)
HDL	0(21)	0(31)	NA	NA	2(241)
HBA1C	NA	NA	0(39)	NA	0(73)
EGFR	NA	0(86)	0.0	NA	0(5)
CRP	0(136)	0(32)	0(27)	0(8)	12(358)

Table S15: Number of variants that had greater than 90% power under the standard GWA framework that were significant in the European ancestry cohort and at least one other cohort. Numbers in parentheses are the total number of variants that could be compared between the European and corresponding (column) ancestry cohort. Power was calculated assuming the marginal European effect size to be the true effect size. Non-European ancestry minor allele frequencies and sample sizes were used in the power calculations. Calculations were performed using then framework defined in Sham and Purcell^[63].

Trait	African or African-American ($\times 10^{-6}$)	East Asian ($\times 10^{-6}$)	AIAN ($\times 10^{-6}$)	Native Hawaiian ($\times 10^{-6}$)	Hispanic and Latin American ($\times 10^{-6}$)
Basophil count	1.121	2.197	NA	NA	NA
BMI	2.096	2.197	2.073	2.093	2.072
CRP	2.097	2.085	2.072	2.100	2.073
Cholesterol	2.096	2.198	2.073	2.092	2.073
DBP	2.096	2.197	2.072	NA	2.073
EGFR	2.097	2.198	2.073	NA	2.073
Eosinophil count	2.121*	2.197	NA	NA	NA
HBA1C	2.096	2.198	2.073	2.093	2.072
HDL	2.097	2.198	2.073	2.093	2.073
Height	2.097	2.131	2.073	2.094	2.072
Hematocrit	2.121*	2.197	NA	NA	NA
Hemoglobin	2.121*	2.197	NA	NA	NA
LDL	2.096	2.198	2.073	2.093	2.073
Lymphocyte count	2.121*	2.197	NA	NA	NA
MCH	2.121*	2.197	NA	NA	NA
MCHC	2.096	2.197	2.877	NA	2.072
MCV	2.121*	2.197	NA	NA	NA
Monocyte count	2.121*	2.197	NA	NA	NA
Neutrophil count	2.121*	2.197	NA	NA	NA
PLC	2.097	2.197	2.072	NA	2.073
RBC	2.121*	2.197	NA	NA	NA
SBP	0.412	8.844	0.597	NA	5.692
Triglyceride	2.096	2.197	NA	2.072	2.073
Urate	2.121*	2.197	NA	NA	NA
WBC	2.092	2.197	2.072	NA	2.073

Table S16: Bonferroni p -value threshold corrected for number of gene-level association tests performed for each ancestry-trait pair. Thresholds are calculated as 0.05 divided by the number of SNPs tested in each ancestry-trait pair. The term "NA" indicates that there was no data for that ancestry-trait pair. The threshold for Bonferroni-corrected significance was the same for every trait in the European (p -value $< 2.092 \times 10^{-6}$) and South Asian (p -value $< 1.085 \times 10^{-6}$) cohorts from the UK Biobank. Traits for which the UK Biobank African cohort was used are denoted with a *; otherwise, the African-American cohort from the PAGE study data was used. See [Table S2](#) for expansion of trait codes.

Trait Name or Code	Initial gene-level associations	Pruned gene-level associations $r^2 > 0.25$	Number of replicated associations	Proportion of replicated associations
MCV	434	336	174	0.400
PLC	241	295	116	0.481
Height	192	327	119	0.620
BMI	347	482	93	0.268
DBP	215	717	63	0.293
SBP	524	375	53	0.101
WBC	167	279	49	0.293
RBC	233	476	77	0.330
Hemoglobin	175	525	79	0.451
Hematocrit	267	356	72	0.270
MCH	246	562	161	0.654
MCHC	205	388	106	0.517
Lymphocyte	38	52	23	0.605
Monocyte	179	122	71	0.397
Neutrophil	211	549	124	0.588
Eosinophil	87	482	56	0.644
Basophil	88	237	35	0.398
Urate	391	444	54	0.138
Triglyceride	285	346	136	0.477
Cholesterol	167	477	136	0.814
LDL	120	443	67	0.558
HDL	213	496	136	0.638
HBA1C	235	421	89	0.379
CRP	105	526	34	0.324
EGFR	294	181	77	0.262

Table S17: Number and proportion of gene- ϵ gene-level associations that are replicated under a more stringent pruning threshold. In our initial analysis of the European ancestry cohort we pruned all variants using an $r^2 > 0.5$ threshold. Here, we set the threshold as $r^2 > 0.25$ and recalculated the gene- ϵ gene-level association statistics for each trait (see). Replication of associated genes using different r^2 thresholds varies by trait, the inclusion of as many SNPs as computationally possible in the gene- ϵ framework is optimal in identifying trait associated genes.

Trait	PESCA EUR only and EUR GWA nominal significance	PESCA EAS only and EAS GWA nominal significance	PESCA both and EUR GWA nominal significance	PESCA both and EAS GWA nominal significance	PESCA both and GWA nominal significance in both
BMI	0	0	97	539	94
Cholesterol	2	13	14	54	11
HDL	5	8	29	74	27
LDL	0	6	16	43	13
MCH	3	14	39	180	39
MCV	1	11	44	215	44
Triglyceride	4	8	15	49	15

Table S18: Overlap between SNPs identified by PESCA and GWA analyses in the European ancestry cohort from the UK Biobank and the East Asian ancestry cohort from the Biobank Japan. For seven continuous traits, we compared SNP-level association p -values from our analysis to the posterior probabilities calculated in Shi et al. [64] using the PESCA framework. For each of the seven traits, there were SNPs that had a posterior probability > 0.8 of being causal in both ancestries and were also nominally significant (p -value $5 < 10^{-6}$) using the standard GWA SNP-level framework.

Trait Name or Code	Median Effect Size Correlation	Effect Sizes > 0.1 (Mean)	Median PIP Correlation	PIPs > 0.01 (Mean)
BMI	0.0143	0	0.073	67.3
Basophil	3.69×10^{-6}	0	0.002	211.8
CRP	0.096	0.7	0.159	142.6
Cholesterol	0.966	1	0.232	53.1
DBP	0.001	0.6	0.012	173.1
EGFR	4.71×10^{-6}	0	0.005	149
Eosinophil	0.0179	0.2	0.042	325.8
HBA1C	0.012	0.2	0.025	26.8
HDL	0.325	0.1	0.219	57.6
Height	9.20×10^{-5}	1.6	0.010	187.7
Hematocrit	-4.16×10^{-6}	0.5	0.015	40.3
Hemoglobin	-1.13×10^{-5}	0.6	0.014	45.8
LDL	0.949	1	0.331	60.9
Lymphocyte	-1.01×10^{-6}	1.5	0.001	1368.5
MCH	7.098×10^{-6}	0.6	0.007	60.9
MCHC	-2.00×10^{-6}	0.9	0.01	58.7
MCV	1.71×10^{-5}	0.6	0.01	70
Monocyte	0.002	0.1	0.017	349.4
Neutrophil	0.038	0.1	0.071	66.5
PLC	0.609	0.9	0.154	112.5
RBC	9.650×10^{-5}	0.9	0.028	49.7
SBP	0.001	0.6	0.019	166.8
Triglyceride	0.348	0.0	0.247	164.7
Urate	0.252	0.5	0.24	39.9
WBC	0.0002	0.1	0.01	347.8

Table S19: Replication of effect sizes and posterior inclusion probabilities (PIPs) among ten independent subsamples of the UK Biobank European ancestry cohort using SuSiE⁶⁵ for fine-mapping. The sample size of the ten independent, non-overlapping subsamples of the UK Biobank European ancestry cohort was set to 10,000. For the 1,895,051 SNPs that were analyzed in every European ancestry cohort subsample (Table S1) and the effect sizes and PIPs (columns 2 and 4, respectively) generated using the SuSiE method⁶⁵, we calculated the median correlation coefficient between all possible pairwise comparisons (10 choose 2) of the European ancestry cohort subsamples. Column 3 reports the mean number of SNPs with effect sizes greater than 0.1 across all ten European ancestry cohort subsamples for each trait. Column 5 reports the mean number of SNPs with a posterior inclusion probability greater than 0.01 across the ten European ancestry cohort subsamples for each trait.

Trait Name or Code	Number of Shared Effect Sizes > 0.1	Median Effect Size Correlation	African Effect Sizes > 0.1	European Effect Sizes > 0.1 (Mean)	Number of Shared PIPs > 0.01	Median PIP Correlation	African PIPs > 0.01	European PIPs > 0.01 (Mean)
BMI	0	5.12×10^{-5}	2	0	1	0.027	1206	8.9
Basophil	0	-3.01×10^{-5}	0	0	0	0.001	403	40.3
CRP	0	-3.68×10^{-6}	0	0.4	0	5.88×10^{-5}	95	33.6
Cholesterol	1	0.5	1	0.9	5	0.467	1144	8.4
DBP	0	1.58×10^{-5}	10	0.3	0	0.008	1249	20.3
EGFR	0	2.41×10^{-6}	1	0	0	0.001	984	24.7
Eosinophil	0	-1.97×10^{-5}	0	0	0	0.003	979	29.3
HBA1C	0	-1.15×10^{-6}	5	0.2	0	0.004	959	6.5
HDL	0	0.014	0	0.1	2	0.014	31	11.6
Height	0	-1.22×10^{-5}	19	0.7	0	0.003	208	33.7
Hematocrit	0	-1.14×10^{-5}	1	0	0	0.016	199	12.2
Hemoglobin	0	-6.31×10^{-6}	1	0	0	0.022	568	12.5
LDL	1	0.674	1	1	8	0.497	995	13.5
Lymphocyte	0	2.71×10^{-5}	0	0	1	0.001	60	115.5
MCH	0	1.14×10^{-5}	1	0.2	0	0.005	1332	11.8
MCHC	0	-1.56×10^{-6}	1	0.2	0	0.008	646	13.6
MCV	0	2.58×10^{-6}	1	0.2	0	0.005	917	11.8
Monocyte	0	-2.44×10^{-5}	0	0	2	0.002	2215	27.7
Neutrophil	0	-0.0001	1	0	0	0.001	2386	10.2
PLC	0	-0.017	1	0.6	3	0.035	2088	13.7
RBC	0	-6.35×10^{-6}	1	0.1	0	-0.002	3	12.7
SBP	0	4.31×10^{-5}	13	0.1	0	0.008	1133	20
Triglyceride	0	0.004	0	0.1	8	0.009	2231	25.6
Urate	1	0.01	2	0.3	3	0.051	334	9.8
WBC	0	-0.0001	1	0	5	0.0006	2862	48.3

Table S20: Replication of effect sizes and posterior inclusion probabilities (PIPs) between the UK Biobank African ancestry cohort and ten independent subsamples of the UK Biobank European ancestry cohort using SuSiE⁶⁵ for fine-mapping. Each of the ten independent, non-overlapping subsamples of the UK Biobank European ancestry cohort was set to be equal in size to the sample size of the African ancestry cohort ($N = 4,967$). **Table S1** Column headers containing “(mean)” indicate a mean is generated averaging over the ten independent European ancestry cohort subsamples. For the 496,997 SNPs that were analyzed in both the African ancestry cohort and every European ancestry cohort subsample, we compared the SuSiE⁶⁵ effect size estimates and PIPs. For both effect sizes and PIPs, the median correlation coefficient between the African ancestry cohort and the pairwise comparison to each European ancestry cohort subsample is reported in the third and seventh columns, respectively. Column 3 reports the total number of SNPs with effect sizes greater than 0.1 in the African cohort. Column four gives the mean number of effect sizes greater than 0.1 in the European ancestry cohort subsamples for each trait. We performed the same comparison for the PIPs using a threshold of 0.01. Column 2 reports the number of SNPs that surpassed an effect size of 0.1 in both the African ancestry cohort and at least one of the European ancestry cohort subsamples. Column 6 reports the number of SNPs that surpasses a PIP of 0.01 in the African ancestry cohort and at least one European ancestry cohort subsample.

Trait Name or Code	Number of Shared Effect Sizes > 0.1	Median Effect Size Correlation	South Asian Effect Sizes > 0.1	European Effect Sizes > 0.1 (Mean)	Number of Shared PIPs > 0.01	Median PIP Correlation	South Asian PIPs > 0.01	European PIPs > 0.01 (Mean)
BMI	0	7.07×10^{-5}	1	0	0	0.0173	180	18
Basophil	0	-1.10×10^{-5}	0	0	0	0.0008	210	78.4
CRP	0	0.0309	0	0.4	17	0.121	181	64.7
Cholesterol	0	0.004	0	0.9	2	0.0127	20	9
DBP	0	-2.12×10^{-5}	0	0.6	0	0.013	115	40
EGFR	0	-1.26×10^{-5}	0	0	0	5.12×10^{-5}	452	44.2
Eosinophil	0	2.16×10^{-5}	0	0	0	0.006	63	69.1
HBA1C	0	-3.33×10^{-5}	2	0.3	0	0.011	133	13.3
HDL	0	0.525	0	0.1	3	0.505	78	12.2
Height	0	-2.13×10^{-5}	12	1.1	1	0.001	754	66.8
Hematocrit	0	-4.78×10^{-6}	1	0.3	0	6.24×10^{-5}	24	17.4
Hemoglobin	0	-4.19×10^{-6}	1	0.3	0	0.011	19	16.1
LDL	0	0.491	1	1	14	0.386	44	15.6
Lymphocyte	0	-4.40×10^{-6}	0	1.1	0	0.0001	113	343.1
MCH	0	5.29×10^{-6}	2	0.5	0	0.008	78	22.3
MCHC	0	-5.77×10^{-6}	1	0.9	0	0.007	45	20.3
MCV	0	1.74×10^{-5}	3	0.5	0	0.005	81	26.3
Monocyte	0	-4.05×10^{-6}	0	0.1	0	0.001	156	76.8
Neutrophil	0	0.221	0	0	16	0.172	70	25.7
PLC	0	0.577	0	0.8	1	0.679	126	22.7
RBC	0	2.79×10^{-6}	0	0.3	0	-0.011	41	20.9
SBP	0	-0.0004	0	0.3	0	0.037	116	43.2
Triglyceride	0	0.158	0	0	53	0.173	189	46.4
Urate	0	0.137	1	0.4	6	0.150	52	15.8
WBC	0	0.001	0	0	18	0.008	52	93

Table S21: Replication of effect sizes and posterior inclusion probabilities (PIPs) between the UK Biobank South Asian ancestry cohort and ten independent subsamples of the UK Biobank European ancestry cohort using SuSiE⁶⁵ for fine-mapping. Each of the ten independent, non-overlapping subsamples of the UK Biobank European ancestry cohort was set to be equal in size to the sample size of the South Asian ancestry cohort ($N = 5,660$), **Table S1**. Column headers containing "(mean)" indicate a mean is generated averaging over the ten independent European ancestry cohort subsamples. For the 863,569 SNPs that were analyzed in both the South Asian ancestry cohort and every European ancestry cohort subsample, we compared the SuSiE⁶⁵ effect size estimates and PIPs. For both effect sizes and PIPs, the median correlation coefficient between the South Asian ancestry cohort and the pairwise comparison to each European ancestry cohort subsample is reported in the third and seventh columns, respectively. Column 3 reports the total number of SNPs with effect sizes greater than 0.1 in the South Asian cohort. Column four gives the mean number of effect sizes greater than 0.1 in the European ancestry cohort subsamples for each trait. We performed the same comparison for the PIPs using a threshold of 0.01. Column 2 reports the number of SNPs that surpassed an effect size of 0.1 in both the South Asian ancestry cohort and at least one of the European ancestry cohort subsamples. Column 6 reports the number of SNPs that surpasses a PIP of 0.01 in the South Asian ancestry cohort and at least one European ancestry cohort subsample.

Trait Name or Code	Cochran's Q among European subsamples (<i>p</i> -value)	Cochran's Q between African and European subsamples (<i>p</i> -value)	Cochran's Q between South Asian and European subsamples (<i>p</i> -value)
Height	641.91 (2.10e-132)	395.01 (1.09e-78)	4036.8(0.0)
BMI	316.69 (7.48e-63)	6,916.75 (0.0)	1076.76 (5.39e-225)
MCV	160.05 (7.25e-30)	11,489.97 (0.0)	155.06 (3.37e-28)
PLC	51.29 (6.15e-08)	13,141.96 (0.0)	386.07 (8.67e-77)
DBP	254.32 (1.22e-49)	9,725.02 (0.0)	241.54 (3.26e-46)
SBP	126.20 (7.16e-23)	1,0479.39 (0.0)	286.38 (1.17e-55)
WBC	1458.39 (1.87e-308)	20,351.80 (0.0)	374.37 (2.65e-74)
RBC	102.75 (4.36e-18)	29.34 (0.001)	153.12 (8.51e-28)
Hemoglobin	114.35 (1.91e-20)	5,022.47 (0.0)	76.74 (2.18e-12)
Hematocrit	149.67 (1.03e-27)	1,205.09 (1.15e-252)	93.03 (1.34e-15)
MCH	90.29 (1.42e-15)	14,366.33 (0.0)	158.25 (7.44e-29)
MCHC	260.58 (5.80e-51)	14,674.80 (0.0)	112.79 (1.46e-19)
Lymphocyte	3105.01 (0.0)	396.931 (4.23e-79)	1,062.61 (6.05e-222)
Monocyte	811.20 (8.26e-169)	9,186.25 (0.0)	433.65 (6.41e-87)
Neutrophil	95.72 (1.15e-16)	24,580.86 (0.0)	141.67 (1.92e-25)
Eosinophil	4,919.90 (0.0)	3,615.16 (0.0)	873.53 (3.16e-181)
Basophil	833.69 (1.18e-173)	1,879.65 (0.0)	541.10 (7.19e-110)
Urate	73.29 (3.44e-12)	93.37 (1.15e-15)	110.03 (5.26e-19)
HBA1C	100.17 (1.45e-17)	14,073.79 (0.0)	639.21 (6.93e-131)
EGFR	361.48 (2.23e-72)	11,478.25 (0.0)	3,012.83 (0.0)
CRP	288.30 (7.91e-57)	117.51 (1.62e-20)	509.40 (4.33e-103)
Triglyceride	138.42 (2.19e-25)	9,133.51 (0.0)	564.80 (6.09e-115)
HDL	175.95 (3.54e-33)	30.98 (0.00059)	292.39 (6.32e-57)
LDL	101.33 (8.45e-18)	3,935.88 (0.0)	86.14 (3.12e-14)
Cholesterol	158.82 (1.30e-29)	5,919.75 (0.0)	43.87 (3.47e-06)

Table S22: Cochran's Q Statistics and *p*-values for comparisons of SuSiE⁶⁵ for fine-mapping posterior inclusion probabilities among UKB ancestry cohorts. We calculated the Cochran's Q statistic for posterior inclusion probabilities > 0.01 for each pairwise comparison of European cohort subsamples. We reported the median value of these comparisons for each trait. We then calculated the median Cochran's Q when comparing the ten European subsamples to the African and South Asian ancestry cohorts in the UK Biobank.

False discovery rate					
gene- ϵ					
Structured Population			Unstructured Population		
Sparsity	0.01	0.1		0.01	0.1
$h^2 = 0.2$	0 (0)	0.010 (0.044)	$h^2 = 0.2$	0.418 (0.183)	0.618 (0.085)
$h^2 = 0.6$	0.020 (0.141)	0 (0)	$h^2 = 0.6$	0.097 (0.284)	0.327 (0.245)
GWAS					
Sparsity	0.01	0.1	Sparsity	0.01	0.1
$h^2 = 0.2$	0.447 (0.153)	0.636 (0.075)	$h^2 = 0.2$	0.01 (0.1)	0.001 (0.011)
$h^2 = 0.6$	0.127 (0.324)	0.38 (0.241)	$h^2 = 0.6$	0.057 (0.227)	0 (0)
Power					
gene- ϵ					
Structured Population			Unstructured Population		
Sparsity	0.01	0.1	Sparsity	0.01	0.1
$h^2 = 0.2$	0.023 (0.043)	0.045 (0.104)	$h^2 = 0.2$	0.002 (0.038)	0.392 (0.108)
$h^2 = 0.6$	0.0006 (0.0006)	0.0002 (0.002)	$h^2 = 0.6$	0.0006 (0.0006)	0.0004 (0.002)
GWAS					
Sparsity	0.01	0.1	Sparsity	0.01	0.1
$h^2 = 0.2$	0.154 (0.038)	0.397 (0.052)	$h^2 = 0.2$	0.010 (0.038)	0.001 (0.108)
$h^2 = 0.6$	0.0002 (0.0008)	0.005 (0.004)	$h^2 = 0.6$	0.057 (0.0006)	0 (0.002)

Table S23: Performance of the standard GWA framework and gene- ϵ in simulations of a small cohort with $N = 2,000$ individuals. Mean false discovery rate and power for 100 simulations of a population under each parameter set shown in [Figure S8](#). Standard errors are given in parentheses.

Gene	African-American	European	South Asian	East Asian	AIAN	Hispanic and Latin American
<i>RDH13</i>	4.14×10^{-10}	9.95×10^{-1}	8.80×10^{-2}	1.76×10^{-6}	1	7.88×10^{-1}
<i>AGPAT5</i>	1	1.30×10^{-6}	7.83×10^{-1}	5.00×10^{-1}	7.33×10^{-8}	1
<i>GP6</i>	7.20×10^{-10}	9.93×10^{-1}	1.47×10^{-1}	9.07×10^{-7}	1	6.92×10^{-1}
<i>ALDH2</i>	1	1.00×10^{-20}	1.13×10^{-2}	1.00×10^{-20}	1	1
<i>RAB8A</i>	9.57×10^{-1}	1.00×10^{-20}	1	5.76×10^{-6}	1	9.97×10^{-1}
<i>CUX2</i>	1	5.13×10^{-7}	1.16×10^{-1}	3.44×10^{-11}	1	1
<i>ACAD10</i>	1	1.47×10^{-10}	1.10×10^{-2}	2.00×10^{-10}	1	1

Table S24: Gene-level association p -values for seven genes associated with platelet count in at last two ancestry cohorts. Of the 65 genes that were associated with platelet count in at least two ancestry cohorts, these seven contained previously identified SNP-level associations in studies submitted to the GWAS Catalog. Previous associations in the GWAS Catalog are discussed in the Supplemental Information. Ancestry-specific Bonferroni corrected significance thresholds for gene-level association analysis of platelet count are shown in [Table S16](#)

Gene	African or African-American	European	East Asian	Hispanic
<i>ANGPTL4</i>	42	28	NA	28
<i>APOA1</i>	21	21	NA	21
<i>APOA4</i>	NA	22	NA	NA
<i>APOA5</i>	24	23 26	27	24
<i>APOB</i>	29	29	NA	29
<i>APOC1</i>	21	22	NA	21
<i>APOC2</i>	24	24	NA	24
<i>APOC3</i>	21	21 22	NA	21
<i>APOC4</i>	22	22	NA	22
<i>APOE</i>	22	22 24	NA	22
<i>CETP</i>	21	22	NA	21
<i>LMF1</i>	NA	22	NA	NA
<i>LPL</i>	21	22	27	21
<i>PCSK6</i>	42	22	NA	42
<i>PCSK7</i>	24	24	27	24
<i>PLTP</i>	21 24 28 29	21 22 28 31	NA	21 24 28 29

Table S25: Genes shown in Figure 3 as associated with triglyceride levels are supported by publications in the GWAS Catalog. Each of the genes listed is present in the significantly mutated subnetworks identified using Hierarchical HotNet⁵⁰ as enriched for associations with triglyceride levels in the European, East Asian, or Native Hawaiian ancestry cohorts. We mapped SNP-level associations from the GWAS Catalog to the 29 genes present in the significantly mutated subnetworks shown in Figure 3 (using the gene list provided by Gusev et al.⁶²) to generate the results for the 16 genes shown here.

Gene	African-American (PAGE)	European	South Asian	East Asian	Native Hawaiian	Hispanic and Latin American
<i>APOA1</i>	4.99×10^{-1}	1.00×10^{-20}	9.91×10^{-1}	1.00×10^{-20}	7.52×10^{-1}	4.99×10^{-1}
<i>APOA4</i>	4.99×10^{-1}	1.00×10^{-20}	2.51×10^{-5}	1.00×10^{-20}	9.15×10^{-1}	4.99×10^{-1}
<i>APOA5</i>	4.99×10^{-1}	1.42×10^{-11}	1.60×10^{-6}	9.95×10^{-1}	3.67×10^{-12}	4.99×10^{-1}
<i>APOC3</i>	4.99×10^{-1}	1.00×10^{-20}	9.82×10^{-1}	9.83×10^{-1}	3.05×10^{-15}	4.99×10^{-1}
<i>APOE</i>	4.99×10^{-1}	1.00×10^{-20}	8.65×10^{-1}	1.00×10^{-20}	1	1
<i>PLTP</i>	4.99×10^{-1}	4.29×10^{-9}	9.66×10^{-1}	6.66×10^{-15}	1.00×10^{-2}	4.99×10^{-1}
<i>LPL</i>	4.99×10^{-1}	4.08×10^{-13}	3.00×10^{-3}	1.00×10^{-20}	6.59×10^{-1}	4.99×10^{-1}
<i>ANGPTL3</i>	4.99×10^{-1}	8.86×10^{-8}	2.00×10^{-3}	1.00×10^{-20}	4.00×10^{-3}	1
<i>ANGPTL4</i>	4.99×10^{-1}	1.00×10^{-20}	9.78×10^{-1}	9.99×10^{-1}	9.89×10^{-1}	1
<i>APOC1</i>	4.99×10^{-1}	1.67×10^{-16}	4.99×10^{-1}	1.00×10^{-20}	9.81×10^{-1}	4.99×10^{-1}
<i>APOC2</i>	4.99×10^{-1}	3.57×10^{-13}	7.71×10^{-1}	1.11×10^{-1}	9.11×10^{-1}	4.99×10^{-1}
<i>APOC4</i>	4.99×10^{-1}	3.72×10^{-13}	7.36×10^{-1}	2.58×10^{-14}	9.73×10^{-1}	4.99×10^{-1}
<i>APOB</i>	4.99×10^{-1}	1.00×10^{-20}	9.99×10^{-1}	7.32×10^{-12}	1.00×10^{-3}	1
<i>LMF1</i>	9.98×10^{-1}	8.03×10^{-7}	1	3.21×10^{-2}	3.79×10^{-5}	9.98×10^{-1}
<i>APOL1</i>	4.99×10^{-1}	5.30×10^{-2}	6.40×10^{-2}	1	8.89×10^{-11}	4.99×10^{-1}
<i>HBA1</i>	4.99×10^{-1}	3.75×10^{-5}	9.99×10^{-1}	4.51×10^{-1}	2.46×10^{-10}	1
<i>HBA2</i>	4.99×10^{-1}	1.30×10^{-5}	9.99×10^{-1}	4.51×10^{-1}	3.93×10^{-10}	4.99×10^{-1}
<i>B4GALT3</i>	4.99×10^{-1}	6.80×10^{-2}	7.21×10^{-1}	4.99×10^{-1}	1.23×10^{-6}	1
<i>KLK8</i>	1	1	1.62×10^{-6}	9.89×10^{-1}	1.00×10^{-3}	1
<i>PNLIP</i>	4.99×10^{-1}	9.99×10^{-1}	9.26×10^{-1}	7.75×10^{-1}	1.00×10^{-3}	4.99×10^{-1}
<i>WNT4</i>	4.99×10^{-1}	9.61×10^{-1}	9.99×10^{-1}	4.99×10^{-1}	3.29×10^{-5}	4.99×10^{-1}
<i>BACE1</i>	4.99×10^{-1}	5.55×10^{-17}	2.20×10^{-2}	9.99×10^{-16}	6.69×10^{-1}	4.99×10^{-1}
<i>CETP</i>	4.99×10^{-1}	1.00×10^{-3}	9.99×10^{-1}	1.41×10^{-6}	9.99×10^{-1}	4.99×10^{-1}
<i>PCSK6</i>	4.99×10^{-1}	1	9.99×10^{-1}	1.83×10^{-5}	1.00×10^{-3}	4.99×10^{-1}
<i>PCSK7</i>	4.99×10^{-1}	1.66×10^{-8}	9.97×10^{-1}	1.00×10^{-20}	9.99×10^{-1}	4.99×10^{-1}
<i>LCAT</i>	4.99×10^{-1}	5.00×10^{-1}	1	6.24×10^{-3}	4.38×10^{-1}	4.99×10^{-1}
<i>APOF</i>	4.99×10^{-1}	5.78×10^{-1}	7.79×10^{-1}	4.10×10^{-3}	9.64×10^{-1}	4.99×10^{-1}
<i>TYRO3</i>	4.99×10^{-1}	9.28×10^{-1}	9.99×10^{-1}	1.20×10^{-2}	8.57×10^{-1}	4.99×10^{-1}

Table S26: Gene- ϵ p -values for the 28 genes present in the significantly mutated subnetworks associated with triglyceride level in the European, East Asian, and Native Hawaiian cohorts. Each of these genes is present in Figure 3 which depicts the overlapping significantly mutated subnetworks identified using Hierarchical HoNet⁵⁰ identified in an analysis of triglyceride levels in the European, East Asian, and Native Hawaiian cohorts. Known SNP-level associations identified within the bounds of these genes in previous studies submitted to the GWAS Catalog are discussed in the Supplemental Information. Ancestry-specific Bonferroni corrected significance thresholds for gene-level association analysis of triglyceride levels are shown in Table S16

Supplemental Subjects and Methods

UK Biobank Data

We downloaded individual genotype data using the UK Biobank's (UKB) `ukbgene` resource, <https://biobank.ctsu.ox.ac.uk/crystal/download.cgi>. European individuals from the UK Biobank data were selected using the self-identified ancestry (data field 21000) using values outlined at <https://biobank.ctsu.ox.ac.uk/crystal/field.cgi?id=21000>. Using the relatedness file provided by the UK Biobank, one individual from each related pair was then randomly removed. This process was repeated for individuals whose self-identified ancestry was South Asian.

We performed unsupervised genome-wide ancestry estimation using ADMIXTURE by setting $K = 3$ ⁶⁶ on the self-identified African ancestry cohort. We also included YRI and CEU individuals in the ADMIXTURE runs from the 1000 Genomes Project, to identify the ancestry components corresponding to African and European ancestry. We removed individuals containing less than 5% membership in the African ancestry component and more than 5% membership in the third component, which corresponds to American Indian/Alaskan Native (AIAN) ancestry (??). We downloaded imputed SNP data from the UK Biobank for all remaining individuals and removed SNPs with an information score below 0.8. Information scores for each SNP are provided by the UK Biobank (<http://biobank.ctsu.ox.ac.uk/crystal/refer.cgi?id=1967>). The remaining genotype and high-quality imputed SNPs were put through a stringent quality control pipeline in each ancestry cohort to obtain cohort-specific SNPs to be used for further analysis as detailed in the main text (detailed below).

We performed the following quality control filters in the European, South Asian, and African cohorts from the UK Biobank (Application number 22419). Genotype data for 488,377 individuals in the UK Biobank were downloaded using the UK Biobank's `ukbgene` (<https://biobank.ctsu.ox.ac.uk/crystal/download.cgi>) tool and converted using the provided `ukbconv` tool (<https://biobank.ctsu.ox.ac.uk/crystal/refer.cgi?id=149660>). Phenotype data was also downloaded for those same individuals using the `ukbgene` tool. Individuals identified by the UK Biobank to have high heterozygosity, excessive relatedness, or aneuploidy were removed (1,550 individuals). After then separating individuals into self-identified ancestral groups using data field 21000. Within these cohorts, unrelated individuals were then selected by randomly selecting an individual from each pair of related individuals. This resulted in 349,469 European individuals, 5,716 South Asian individuals, and 4,967 African individuals.

Genotype quality control was then performed on each cohort separately using the following steps. All structural variants were first removed, leaving only single nucleotide polymorphisms in the genotype data. Next, all AT/CG SNPs were removed to avoid possible confounding due to sequencing errors. Then, SNPs

183 with minor allele frequency less than 1% were removed using the plink2⁶⁷ `--maf 0.01`. We then removed
184 all SNPs found to be in Hardy-Weinberg equilibrium, using the plink `--hwe 0.000001` flag to remove all
185 SNPs with a Fisher’s exact test p -value $> 10^{-6}$. Finally, all SNPs with missingness greater than 1% were
186 removed using the plink `--mind 0.01` flag.

187 Finally, we note that the number of filtered SNPs in the African cohort is smaller than the number
188 of filtered SNPs in the European cohort. These results stand in contrast to expectation about number of
189 independent variants in these two populations. We believe this to be due to ascertainment bias on the
190 genotyping array.

191 **Biobank Japan Data**

192 We downloaded summary statistics for 25 quantitative traits from the Biobank Japan (BBJ) website (<http://jenger.riken.jp/en/result>)^{59,61,68}. The sample descriptions and number of SNPs included in our
193 analyses are given in [Table S5](#). The number of SNPs included in the analysis of each trait represent those
194 SNPs that: (i) contained an rsid number that could be mapped to the hg19 genome build, (ii) overlapped
195 with SNPs contained within the 1000 Genomes Project phase 3 genotype data, and (iii) had a minor allele
196 frequency greater than 0.01 in Japanese (JPT) individuals in the 1000 Genomes Project. We used the 1000
197 Genomes phase 3 data from 93 JPT individuals to estimate the linkage disequilibrium (LD) between SNPs
198 in BioBank Japan for which we had the summary statistic data; LD was estimated separately for each of
199 the 25 quantitative traits using the trait specific SNP arrays. LD estimates were used in the calculation of
200 regional association statistics.
201

202 **Population Architecture using Genomics and Epidemiology (PAGE) Study Data**

203 Summary statistics for genotyped and imputed SNPs in five admixed populations were downloaded from the
204 Population Architecture using Genomics and Epidemiology (PAGE)⁶⁹ with permission granted via approval
205 of manuscript proposal. We included summary statistics for up to 14 quantitative traits for African-American,
206 Hispanic and Latin American, Native Hawaiian, American Indian/Alaska Native, and Asian ancestry cohorts
207 when available. All AT/CG SNPs were omitted, and SNPs with an IMPUTE2 information score greater than
208 0.8 were included in this analysis. Number of individuals and SNPs varied across ancestry-trait combinations
209 and are given in [Table S5](#) - [Table S10](#)

210 Individuals from the 1000 Genomes Project phase 3⁷⁰ and the Human Genome Diversity Panel (HGDP)⁷¹
211 were used to obtain LD estimates between SNPs for each ancestry cohort. To construct the LD reference
212 panel for PAGE summary statistics from the African-American ancestry cohort, unrelated individuals from
213 the 1000 Genomes Americans of African Ancestry in SW USA (ASW) and African Caribbeans in Barbados

214 (ACB) were used. Only SNPs found in both the 1000 Genomes imputed data and PAGE summary statistics
215 files were used in gene-level association and heritability analyses. We used the same approach to compute
216 reference LD estimates between SNPs for the Hispanic and Latin American, AIAN, and Asian ancestry
217 cohorts, with the following 1000 Genomes reference population, respectively: Mexican Ancestry from Los
218 Angeles USA (MXL) and Puerto Ricans from Puerto Rico (PUR); Colombians from Medellin, Colombia
219 (CLM) and Peruvians from Lima, Peru (PEL); and the East Asian superpopulation (EAS). For the Native
220 Hawaiian individuals from the PAGE study, there were no appropriate reference populations in the 1000
221 Genomes data. In order to construct a reference LD matrix for the Native Hawaiian ancestry cohort, we
222 randomly sampled individuals from populations in the most recent release of the HGDP proportional to the
223 global ancestry of the Native Hawaiian cohort. The Native Hawaiian cohort's global ancestry proportions
224 were determined using ADMIXTURE runs to be 47.89% Oceanian, 25.16% East Asian, 25.51% European,
225 0.90% African, and 0.54% AIAN in a separate publication (Wojcik preprint - in prep.). We did not sample
226 from populations with less than 1% of the total ancestry in the admixture analysis referenced above. The
227 resulting sample from which LD was estimated included 39 individuals from the Papuan Sepik in New
228 Guinea and Melanesian in Bougainville, 14 individuals from the French in France, and 14 individuals from
229 the Yoruba in Nigeria.

230 **WHI study cohort description**

231 The Women's Health Initiative (WHI) is a long-term, prospective, multi-center cohort study investigating
232 post-menopausal women's health in the US. WHI was funded by the National Institutes of Health and the
233 National Heart, Lung, and Blood Institute to study strategies to prevent heart disease, breast 124 cancer,
234 colon cancer, and osteoporotic fractures in women 50-79 years of age. WHI involves 161,808 women recruited
235 between 1993 and 1998 at 40 centers across the US. The study consists of two parts: the WHI Clinical Trial
236 which was a randomized clinical trial of hormone therapy, dietary modification, and calcium/Vitamin D
237 supplementation, and the WHI Observational Study, which focused on many of the inequities in women's
238 health research and provided practical information about incidence, risk factors, and interventions related
239 to heart disease, cancer, and osteoporotic fractures. For this project, women who self identified as European
240 were excluded from the study sample (dbGaP study accession number: phs000227).

241 **HCHC/SOL study cohort description**

242 The Hispanic Community Health Study / Study of Latinos (HCHS/SOL) is a multi center study of His-
243 panic/Latino populations with the goal of determining the role of acculturation in the prevalence and devel-
244 opment of diseases, and to identify other traits that impact Hispanic/Latino health. The study is sponsored

245 by the National Heart, Lung, and Blood Institute (NHLBI) and other institutes, centers, and offices of the
246 National Institutes of Health (NIH). Recruitment began in 2006 with a target population of 16,000 persons
247 of Cuban, Puerto Rican, Dominican, Mexican or Central/South American origin. Household sampling was
248 employed as part of the study design. Participants were recruited through four sites affiliated with San Diego
249 State University, Northwestern University in Chicago, Albert Einstein College of Medicine in Bronx, New
250 York, and the University of Miami. Researchers from seven academic centers provided scientific and logistical
251 support. Study participants who were self-identified Hispanic/Latino and aged 18-74 years underwent ex-
252 tensive psycho-social and clinical assessments during 2008-2011. A re-examination of the HCHS/SOL cohort
253 is conducted during 2015-2017. Annual telephone follow-up interviews are ongoing since study inception to
254 determine health outcomes of interest. (dbGaP study accession number: phs000555).

255 **BioMe Biobank study cohort description**

256 The Charles Bronfman Institute for Personalized Medicine at Mount Sinai Medical Center (MSMC), BioMe™
257 54 BioBank (BioMe) is an EMR-linked bio-repository drawing from Mount Sinai Medical Center consented
258 patients which were drawn from a population of over 70,000 inpatients and 800,000 outpatients annually.
259 The MSMC serves diverse local communities of upper Manhattan, including Central Harlem (86% African
260 American), East Harlem (88% Hispanic/Latino), and Upper East Side (88% Caucasian/White) with broad
261 health disparities. BioMe™ 58 enrolled over 26,500 participants from September 2007 through August
262 2013, with 25% African American, 36% Hispanic/Latino (primarily of Caribbean origin), 30% Caucasian,
263 and 9% of Other ancestry. The BioMe™ 60 population reflects community-level disease burdens and health
264 disparities with broad public health impact. Biobank operations are fully integrated in clinical care pro-
265 cesses, including direct recruitment from clinical sites waiting areas and phlebotomy stations by dedicate
266 Biobank recruiters independent of clinical care providers, prior to or following a clinician standard of care
267 visit. Recruitment currently occurs at a broad spectrum of over 30 clinical care sites. Study participants
268 of self-reported European ancestry were not included in this analysis. (dbGaP study accession number:
269 phs000925).

270 **MEC study cohort description**

271 The Multiethnic Cohort (MEC) is a population-based prospective cohort study including approximately
272 215,000 men and women from Hawaii and California. All participants were 45-75 years of age at baseline, and
273 primarily of 5 ancestries: Japanese Americans, African Americans, European Americans, Hispanic/Latinos,
274 and Native Hawaiians. MEC was funded by the National Cancer Institute in 1993 to examine lifestyle risk
275 factors and genetic susceptibility to cancer. All eligible cohort members completed baseline and follow-up

276 questionnaires. Within the PAGE II investigation, MEC proposes to study: 1) diseases for which we have
277 DNA available for large numbers of cases and controls (breast, prostate, and colorectal cancer, diabetes,
278 and obesity); 2) common traits that are risk factors for these diseases (e.g., body mass index / weight,
279 waist-to-hip ratio, height), and 3) relevant disease-associated biomarkers (e.g., fasting insulin and lipids,
280 steroid hormones). The specific aims are: 1) to determine the population-based epidemiologic profile (al-
281 lele frequency, main effect, heterogeneity by disease characteristics) of putative causal SNPs in the five
282 racial/ethnic groups in MEC; 2) for SNPs displaying effect heterogeneity across ethnic/racial groups, we will
283 utilize differences in LD to identify a more complete spectrum of associated SNPs at these loci; 3) investi-
284 gate gene x gene and gene x environment interactions to identify modifiers; 4) examine the associations of
285 putative causal SNPs with already measured intermediate phenotypes (e.g., plasma insulin, lipids, steroid
286 hormones); and 5) for SNPs that do not fall within known genes, start to investigate their relationships with
287 gene expression and epigenetic patterns in small genomic studies. For this project, MEC contributed African
288 American, Japanese American, and Native Hawaiian samples.(dbGaP study accession number: phs000220).

289 **Fine-mapping analyses**

290 **Methods: Protocol for implementation of SuSiE and PESCA**

291 To perform SNP-level fine mapping analyses on a given quantitative trait, we applied Sum of Single Effects
292 (SuSiE) variable selection software⁶⁵. SuSiE implements a Bayesian linear regression model on individual
293 level data where sparse prior distributions are placed on the effect size of SNP and posterior inclusion
294 probabilities (PIPs) are used to summarize their statistical relevance to the trait of interest. The software
295 for SuSiE requires an input ℓ which fixes the maximum number of causal SNPs to include in the model. In
296 this work, we consider results when this parameter is chosen conservatively ($\ell = 3000$). We used the three
297 cohorts for which we had genotype data from the UK Biobank (African, European, and South Asian) to
298 test whether there was effect size heterogeneity among ancestries in the 25 traits analyzed in this study. We
299 first selected ten independent, non-overlapping subsamples of 10,000 individuals from the European ancestry
300 cohort and filtered out any SNPs that had a minor allele frequency of less than 0.01. For each subsample, we
301 then applied SuSiE to each of the 25 traits and compared the effect sizes and posterior inclusion probabilities.
302 The average number of SNPs with an effect size greater than 0.01 and average number of SNPs with a PIP
303 greater than 0.01 for each trait across the ten cohorts are reported in [Table S19](#) [Table S19](#) also reports the
304 median correlation coefficient of effect sizes and PIPs among the 45 pairwise comparisons between the 10
305 subsample cohorts.

306 We then applied SuSiE to the African and South Asian ancestry cohorts and compared their resulting

307 effect sizes and PIPs to ten independent, non-overlapping subsamples of the European ancestry cohort. The
308 number of SNPs with an effect size greater than 0.1 and PIPs greater than 0.01 in both the focal cohort
309 (either African or South Asian) and at least one of the ten European ancestry subsamples of the same size
310 are reported in [Table S20](#) and [Table S21](#). Also reported in these tables, are the mean number of effect sizes
311 greater than 0.01 and PIPs greater than 0.01 across the European ancestry subsamples for each trait and the
312 number of unique effect sizes greater than 0.01 and PIPs greater than 0.01 that were only identified in the
313 African or South Asian ancestry cohorts. Finally, [Table S20](#) and [Table S21](#) report the median correlation
314 coefficient of the African or South Asian ancestry cohort effect sizes and PIPs with the ten European ancestry
315 subsample cohorts of the same size.

316 We report the median Cochran’s Q statistic calculated among all pairs of European subsamples for
317 posterior inclusion probabilities (PIPs) [Table S22](#). Additionally, we report the median Cochran’s Q for
318 both PIPs and effect sizes between the ten European ancestry subsamples and the South Asian and African
319 ancestry cohorts from the UK Biobank.

320 We compared the results of two fine-mapping methods, SuSie⁶⁵ and PESCA⁷², when applied to SNP-level
321 summary statistics in the European (UKB) and East Asian (BBJ) cohorts. SuSie is an iterative Bayesian
322 stepwise selection method that identifies a credible set of SNPs that contribute to a phenotype of interest⁶⁵.
323 Using the effect sizes and standard errors generated from the standard GWA framework for each trait in each
324 ancestry, we applied SuSiE in order to identify probable sets of causal SNPs. We then found the correlation
325 between the posterior inclusion probabilities of each SNP in the European and East Asian cohorts.

326 Unlike SuSiE, the PESCA framework is explicitly designed for identifying shared SNP-level association
327 signals between multiple ancestry cohorts versus ancestry-specific associations⁷². In addition to GWA sum-
328 mary statistics, PESCA uses information about the correlation structure between SNPs (i.e., LD) to identify
329 SNPs that are likely to be causal in two cohorts of interest. Shi et al.⁷² analyzed seven continuous traits in
330 the European (UKB) and East Asian (BBJ) cohorts using PESCA and produced posterior probabilities that
331 individual SNPs were: (i) associated with a phenotype in both the both cohorts, (ii) associated with the
332 trait of interest only in the European cohort, or (iii) associated with the trait of interest only in the East
333 Asian cohort. For each trait, we calculated the number of SNPs that were nominally significant (p -value
334 $< 10^{-5}$, as in the original PESCA analysis) in the standard GWA framework in both the European and
335 East Asian cohorts and had a PESCA posterior probability of being associated in both ancestries > 0.8 (see
336 [Table S18](#)). We also found the number of SNPs that had a PESCA posterior probability of being associated
337 in both ancestries > 0.8 that were only identified as significant in one ancestry using the GWA framework.

338 Finally, we explored the recent proposition of Mathieson⁷³ that the direction of effect for SNP-level
339 summary statistics might be conserved among ancestry cohorts even if those variants are not genome-wide

340 significant in either cohort. To that end, for each of the 25 traits that we analyzed, we compared the direction
341 of SNP effect sizes between the European and East Asian ancestry cohorts. We were only able to carry this
342 analysis out for variants that were genotyped in both cohorts (Table S18). For each remaining nominally
343 significant variant, we stored the direction of the effect size and checked the direction of effect size in the
344 other ancestry. When zero was included within the range of the effect size plus or minus one standard
345 deviation, we assumed the SNP did not have the same direction in both cohorts. We note that this test
346 may be confounded by the precision of effect size estimation and warrants further exploration, including an
347 analysis of local false sign discovery rates (see 7475).

348 **Results: Fine-mapping methods have variable efficacy in identification of SNP level associa-** 349 **tions among ancestry cohorts**

350 Often, replication of GWA results across cohorts is tested using genomic regions centered on a SNP. Scans
351 across the region surrounding the SNP of interest are usually defined arbitrarily — using physical windows
352 (or “clumps”) to smooth over ascertainment bias and varying LD across cohorts or ancestries instead of
353 using regions that are biologically annotated such as genes or transcriptional elements. While clumping
354 presents an easy way to scan for regional replication of a given GWA finding, the corresponding results are
355 not readily interpretable when prioritizing GWA results for downstream validation. We performed clumping
356 using windows of size 1Mb centered around significant SNP-level associations (see Materials and Methods).
357 Height had the largest proportion of windows that contain a SNP-level association that replicated in at least
358 two ancestries (Figure S5B and Figure S5E). In the three traits with the greatest proportion of windows
359 containing SNP-level replications — height (77.09% of clumps), urate (65.89%), and low density lipoprotein
360 (54.40%) — we then recorded the number of genes and transcriptional elements within the window that
361 contained GWA significant SNP-level associations. We found that for all three traits, the vast majority of
362 1Mb windows that were used to clump SNP-level associations contained multiple genes and transcriptional
363 elements with significantly associated SNPs: height (94.04% of significant variants are within 1 Mb of two
364 or more genes, 17.93 genes in clump (mean) \pm 15.71 (standard deviation)), urate (97.47%, 18.44 ± 13.72),
365 and low density lipoprotein (99.12%, 14.85 ± 12.89). Thus, we find window-based clumping does not easily
366 produce biologically interpretable hypotheses for downstream validation.

367 Recent analyses of multi-ancestry GWA cohorts have also tested for effect size heterogeneity 64 65 69 76 77.
368 We applied the fine-mapping method SuSiE 65 to identify signals of effect size heterogeneity in the three
369 ancestry cohorts for which we had access to raw genotype data (UK Biobank European ancestry, African
370 ancestry, and South Asian ancestry individuals; see Table S1). We find little evidence of correlated SuSiE
371 effect size estimates among ancestry cohorts, including among independent subsamples of the UK Biobank

372 European ancestry individuals [Table S19](#) - [Table S21](#). In addition, we applied PESCA (a method developed
373 by Shi et al. [64](#)) to the results of our SNP-level analysis to understand how the modeling of LD affected the
374 power to identify probably causal SNPs shared in the European and East Asian ancestry cohorts. PESCA
375 improves upon standard clumping approaches by modeling the LD in a region to identify SNPs that are
376 likely to be causal for the same trait in multiple ancestries. In a comparison with the results from seven
377 continuous traits analyzed in the original study [64](#), we found that the vast majority of SNPs identified by
378 PESCA as causal (posterior probability > 0.8) in both ancestries were also nominally significant in our SNP-
379 level association results (see [Table S18](#)). Both SuSiE [65](#) and PESCA [64](#) demonstrate the utility of modeling
380 variation in LD structure among ancestries when conducting multi-ancestry GWA studies.

381 Recently, Mathieson [73](#) proposed the hypothesis that the direction of effect sizes is the same among
382 ancestries, even when the effects are not genome-wide significant. To test this, we compared the direction
383 of effect in SNPs that were significant in either the European or East Asian ancestry cohort to the direction
384 of the effect in the other ancestry where the SNP was tested using the standard GWA framework. We limit
385 the comparison to the European and East Asian cohorts due to their large sample sizes which increases the
386 precision of effect size estimates. [Table S18](#) shows the number of variants that were significantly associated
387 with each trait in at least one of the European and East Asian ancestry cohorts, and also displays the number
388 of those variants that have the same direction of effect as the significant variant in the other ancestry. In the 25
389 traits that we analyzed, the direction of effect was conserved in both the European and East Asian ancestry
390 cohorts (between effect direction concordance from 55.87% and 76.56% of SNPs across 25 traits). The
391 remaining SNPs where the direction of the effect size was not conserved represent those SNPs that: (i) had
392 different direction of effect size, (ii) were not tested in both ancestry cohorts, or (iii) had effect size estimates
393 within one standard error of zero ([Table S18](#)). The observed conservation of effect size direction in multiple
394 ancestry cohorts, even when SNPs are non-significant in one or more cohorts, is a primary assumption
395 of regional enrichment methods and supports Mathieson [73](#)'s hypothesis and findings. This suggests that
396 regional enrichment methods, which are sensitive to shared patterns of effect size direction among cohorts,
397 are a natural approach to apply to GWA summary statistics even in the absence of replication SNP-level
398 GWA signals among cohorts. We ultimately acknowledge that a more in depth analysis of fine-mapping
399 application to multi-ancestry genetic data is needed to make any conclusions. This precursory analysis using
400 the SuSiE [54](#) and PESCA [64](#) highlights that there is widespread heterogeneity in direction of effect.

401 **S0.2 Description of the gene- ε framework**

402 A unique feature of gene- ε is that it treats SNPs with spuriously associated nonzero effects as non-associated.
403 gene- ε assumes a reformulated null distribution of SNP-level effects $\tilde{\beta}_j \sim \mathcal{N}(0, \sigma_\varepsilon^2)$, where σ_ε^2 is the SNP-

404 level null threshold and represents the maximum proportion of phenotypic variance explained (PVE) by a
405 spurious or non-associated SNP. This leads to the reformulated SNP-level null hypothesis $H_0: \mathbb{E}[\beta_j^2] \leq \sigma_\varepsilon^2$.
406 To infer an appropriate σ_ε^2 , gene- ε fits a K -mixture of normal distributions over the regularized effect sizes
407 with successively smaller variances (i.e., $\sigma_1^2 > \dots > \sigma_K^2 = 0$). In this study as in Cheng et al.^[53], we
408 assume that associated SNPs will appear in the first set, while spurious and non-associated SNPs appear
409 in the latter sets. As a final step, gene- ε computes its gene-level association test statistic for the g -th gene
410 by conformably partitioning the regularized GWA effect size estimates and computing the quadratic form
411 $\tilde{Q}_g = \tilde{\beta}_g^\top \tilde{\beta}_g$. Corresponding p -values are then derived using Imhof’s method. This assumes the common gene-
412 level null $H_0: Q_g = 0$, where the null distribution of Q_g is dependent upon the eigenvalues from the scaled
413 LD matrix $\sigma_\varepsilon^2 \Sigma$. For details on implementation, validation and performance comparison with simulations,
414 and empirical application to UK Biobank white British individuals in six traits, see Cheng et al.^[53].

415 **S0.3 Regression with Summary Statistics (RSS) Enrichment.**

Consider a GWA study with N individuals typed on P SNPs. For the j -th SNP, assume that we are given
corresponding effect sizes $\hat{\beta}_j$ and standard error \hat{s}_j via a single-SNP linear model fit using OLS. RSS then
implements the following likelihood to model the GWA summary statistics^[54]

$$\hat{\beta} \sim \mathcal{N}(\hat{\mathbf{S}}\Sigma\hat{\mathbf{S}}^{-1}\beta, \hat{\mathbf{S}}\Sigma\hat{\mathbf{S}}) \quad (1)$$

where $\hat{\mathbf{S}} = \text{diag}(\hat{\mathbf{s}})$ is a $J \times J$ diagonal matrix of standard errors, Σ is again used to represent some empirical
estimate of the LD matrix (i.e., using some external reference panel with ancestry matching the cohort of
interest), and β are the true (unobserved) SNP-level effect sizes. To model gene-level enrichment, RSS
assumes the following hierarchical prior structure on the true effect sizes

$$\beta_j \sim \pi_j \mathcal{N}(0, \sigma_\beta^2) + (1 - \pi_j) \delta_0, \quad (2)$$

$$\sigma_\beta^2 = h^2 \left(\sum_{j=1}^J \pi_j N^{-1} \hat{s}_j^{-2} \right)^{-1}, \quad (3)$$

$$\pi_j = \left(1 + 10^{-(\theta_0 + a_j \theta)} \right)^{-1}, \quad (4)$$

where δ_0 is point mass centered at zero, h^2 denotes the narrow-sense heritability of the trait, a_j is an indicator
detailing whether the j -th SNP is inside a particular gene, θ_0 is the background proportion of trait-associated
SNPs, and θ reflects the increase in probability (on the \log_{10} -odds scale) when a SNP within a gene has
non-zero effect. Here, the authors follow earlier works^[78] and place independent uniform grid priors on the

hyper-parameters $\{h^2, \theta_0, \theta\}$. Note that, unlike other methods, RSS does not calculate a P -value for assessing gene-level association. Instead, RSS produces a posterior enrichment probability that at least one SNP in a given gene boundary is associated with the trait

$$P_g := 1 - \Pr[\beta_j = 0, \forall j \in \mathcal{J}_g | \mathbf{D}] \quad (5)$$

416 where \mathbf{D} represents all of the input data including the GWA summary statistics $\{\hat{\boldsymbol{\beta}}, \hat{\mathbf{s}}\}$, the estimated LD
 417 matrix $\boldsymbol{\Sigma}$, and any applicable SNP annotations or weights $\mathbf{a} = (a_1, \dots, a_J)$. See [5479](#) for more details on
 418 preferred hyper-parameter settings. As noted in the main text, RSS relies on a Markov chain Monte Carlo
 419 (MCMC) scheme for sampling posterior distributions and estimating model parameters. As a result, its
 420 algorithm can be subject to convergence issues if these (or the random seed) are not chosen properly.

421 **S0.4 SNP-set (Sequence) Kernel Association Test (SKAT).**

The implementation of SKAT required access to raw phenotype \mathbf{y} and genotype \mathbf{X} information for N individuals typed on J SNPs. To assess enrichment of the $|\mathcal{J}_g|$ variants within gene g , consider the linear model with sub-matrix \mathbf{X}_g

$$\mathbf{y} = \beta_0 + \mathbf{X}_g \boldsymbol{\beta}_g + \mathbf{e}, \quad \mathbf{e} \sim \mathcal{N}(\mathbf{0}, \tau^2 \mathbf{I}) \quad (6)$$

where β_0 is an intercept term, $\boldsymbol{\beta}_g = (\beta_1, \dots, \beta_{|\mathcal{J}_g|})$ is a vector of regression coefficients for the SNPs within the gene of interest, and \mathbf{e} is a normally distributed error term with mean zero and scaled variance τ^2 . For model flexibility, gene-specific SNP effects β_j are assumed to follow an arbitrary distribution with mean zero and marginal variances $a_j \sigma_\beta^2$, where σ_β^2 is a variance component and a_j is a pre-specified weight for the j -th SNP. To this end, SKAT uses a variance component scoring approach and tests the null hypothesis $H_0: \boldsymbol{\beta} = \mathbf{0}$, or equivalently $H_0: \sigma_\beta^2 = 0$. The corresponding gene-level test statistic \hat{Q}_g then takes on the familiar quadratic form

$$\hat{Q}_g = (\mathbf{y} - \hat{\boldsymbol{\beta}}_0)^\top \mathbf{K}_g (\mathbf{y} - \hat{\boldsymbol{\beta}}_0) \quad (7)$$

where $\hat{\boldsymbol{\beta}}_0$ is the predicted mean of trait under the null hypothesis, and is computed by projecting \mathbf{y} onto the column space of the intercept (i.e., a vector of ones). The term $\mathbf{K}_g = \mathbf{X}_g \mathbf{A}_g \mathbf{A}_g \mathbf{X}_g^\top$ is commonly referred to as an $N \times N$ kernel matrix, where $\mathbf{A}_g = \text{diag}(a_1, \dots, a_{|\mathcal{J}_g|})$ is used to denote a diagonal weight matrix that

changes for each gene g . Each element of \mathbf{K}_g is computed via the linear kernel function

$$k(\mathbf{x}_i, \mathbf{x}_{i'}) = \sum_{j=1}^{|\mathcal{J}_g|} a_j x_{ij} x_{i'j}. \quad (8)$$

422 While implementing SKAT in this work, we follow previous works and set each weight to be $\sqrt{a_j} =$
423 $\text{Beta}(\text{MAF}_j, 1, 25)$ — the beta distribution density function with pre-specified parameters evaluated at the
424 sample minor allele frequency (MAF) for the j -th SNP in the gene region. For more details, see [55](#)[80](#)[82](#).

425 **Clustering traits sharing a core set of associated genes using the WINGS algorithm**

426 We used the WINGS algorithm^{[83](#)} to identify clusters of traits sharing a core set of genes enriched for
427 associated mutations. WINGS takes as input a gene (M) by trait (N) matrix and uses the Ward distance
428 metric to find the distance among vectors of gene scores for different phenotypes; in this study, we used
429 gene- ε gene-level association statistics as the input to WINGS. The more significantly associated genes that
430 two traits share, the closer they will be in the gene-dimensional space. Applying WINGS to a matrix of
431 gene scores for each ancestry separately, we examined whether the same traits clustered together, separately
432 in each ancestry. We constructed matrices of gene- ε gene-level association statistics for the UK Biobank
433 European, African, South Asian (from the UK Biobank) and East Asian (Biobank Japan) ancestry cohorts.
434 Each of these matrices contained gene-level association statistics for all 25 quantitative traits of interest.
435 The total number of genes and regulatory regions included were: European (23,603), African (23,575),
436 South Asian(23,671), and East Asian (21,435). For the East Asian ancestry cohort, we limited the genes
437 to the intersection of genes with gene- ε gene-level association statistics across all 25 traits. The number of
438 gene scores calculated for each trait in the East Asian ancestry cohort varies due to the heterogeneity in
439 imputed and genotype SNP arrays in the Biobank Japan studies ([Table S5](#) and [Table S16](#)). [Figure S21](#) shows
440 the resulting dendrograms displaying prioritized phenotypes identified using the WINGS algorithm on each
441 cohort’s gene score matrix. The WINGS algorithm is designed to run on 25 phenotypes or more (see McGuirl
442 et al.^{[83](#)} for details), and we therefore did not apply the WINGS algorithm to the AIAN, Native Hawaiian,
443 or Hispanic and Latin American cohorts as there was not data for enough phenotypes ([Table S6](#) [Table S10](#)).

444 **Analysis of GWAS Catalog Metadata and Previous GWA Publications**

445 We cross-referenced our results from association testing at multiple genomic scales against previously pub-
446 lished results in the GWAS catalog (<https://www.ebi.ac.uk/gwas/>) and in PubMed using the following
447 processes.

448 In order to collect PubMed IDs (PMIDs) for publications associated with the UK Biobank, a two-part

449 data collection process was used. The first process was to directly search for publications with variations
450 of the term “UK Biobank” (e.g., U.K. Biobank, United Kingdom Biobank) from PubMed using the Entrez
451 Programming Utilities (E-Utilities) API. The E-Utilities API is the public API to the NCBI Entrez sys-
452 tem and allows direct access to all Entrez databases including PubMed. Search queries were formulated by
453 narrowing publications using year published and then further narrowing to those publications with varia-
454 tions of the search term “UK Biobank” in either the title or abstract. The open-source Python package
455 Entrez (<https://biopython.org/DIST/docs/api/Bio.Entrez-module.html>) from the Biopython Project
456 was used to facilitate interaction with the E-Utilities API.

457 The second data collection process was to gather information from publications listed directly on the UK
458 Biobank website (<https://www.ukbiobank.ac.uk/>). Since the majority of publications on the website did
459 not have an easily accessible PMID, identifying information including publication title and year was scraped
460 and used to retrieve a publication’s corresponding PMID (again using the E-Utilities API). The HTML/XML
461 document parsing Python library BeautifulSoup ([https://www.crummy.com/software/BeautifulSoup/
462 bs4/doc/](https://www.crummy.com/software/BeautifulSoup/bs4/doc/)) was used to parse the HTML of the various UK Biobank webpages, and the Python Requests
463 library (<https://requests.readthedocs.io/en/master/>) was used to programatically send HTTP calls
464 to the server hosting the website. PMIDs were retrieved directly from the XML output of the E-Utilities
465 API calls.

466 The PMIDs retrieved from both processes were aggregated into a single set of unique PMIDs, as some
467 publications were identified by both processes. Publications that could not get associated PMIDs from the
468 second data collection process were flagged for manual processing. The PMIDs that were retrieved from
469 PubMed directly but could not be found based on the publication information provided on the UK Biobank
470 website were noted. Conversely, the PMIDs that could be retrieved from publication information found on
471 the UK Biobank website but not directly from PubMed were also noted.

472 Using the compiled list of PMIDs, analyses of the UK Biobank data set reported in the GWAS cat-
473 alog association data were compiled. Previous genotype-to-phenotype association data and sample an-
474 cestry descriptions were downloaded from <https://www.ebi.ac.uk/gwas/docs/file-downloads>. Unique
475 genotype-to-phenotype associations were parsed using a set of custom python scripts. All scripts used
476 in the curation of PMIDs, parsing of GWAS catalog summary data, and determination of previously
477 published genotype-to-phenotype associations from UK Biobank studies are available on GitHub ([https:
478 //github.com/ramachandran-lab/redefining_replication](https://github.com/ramachandran-lab/redefining_replication)).

479 **Simulation design to test the power and false discovery rate of GWA and gene-level association**
480 **analyses**

481 **Simulations of a single population**

482 In our simulation studies, we used the following general simulation scheme to generate quantitative traits
483 using real genotype data on chromosome 1 from N randomly sampled individuals of European ancestry in
484 the UK Biobank. This pipeline follows from previous studies^{53,84}. We will use \mathbf{X} to denote the $N \times J$
485 genotype matrix, with J denoting the number of single nucleotide polymorphisms (SNPs) encoded as 0, 1, 2
486 copies of a reference allele at each locus and \mathbf{x}_j representing the genotypic vector for the j -th SNP. Following
487 quality control procedures detailed in the Supplemental Information, our simulations included $J = 36,518$
488 SNPs distributed across genome. We used the NCBI’s RefSeq database in the UCSC Genome Browser to
489 assign SNPs to genes which resulted in $G = 1,408$ genes in the simulation studies.

490 After the annotation step, we simulated phenotypes by first assuming that the total phenotypic variance
491 $\mathbb{V}[\mathbf{y}] = 1$, and that all observed genetic effects explained a fixed proportion of this value (i.e., narrow-sense
492 heritability, h^2). Next, we randomly selected a certain percentage of genes to be enriched for associations
493 and denoted the sets of SNPs that they contained as \mathcal{C} . Within \mathcal{C} , we selected causal SNPs in a way such
494 that each associated gene at least contains one SNP with non-zero effect size. Quantitative continuous traits
495 were then generated under the following two general linear models:

496 • Standard Model: $\mathbf{y} = \sum_{c \in \mathcal{C}} \mathbf{x}_c \beta_c + \mathbf{e}$

497 • Population Structure Model: $\mathbf{y} = \mathbf{W}\mathbf{b} + \sum_{c \in \mathcal{C}} \mathbf{x}_c \beta_c + \mathbf{e}$

498 where \mathbf{y} is an N -dimensional vector containing all the phenotype states; \mathbf{x}_c is the genotype for the c -th
499 causal SNP; β_c is the additive effect size for the c -th SNP; and $\mathbf{e} \sim \mathcal{N}(0, \tau^2 \mathbf{I})$ is an N -dimensional vector
500 of normally distributed environmental noise. Additionally, in the model with population structure, \mathbf{W} is an
501 $N \times M$ matrix of the top $M = 10$ principal components (PCs) from the genotype matrix and represents
502 additional population structure with corresponding fixed effects \mathbf{b} . The effect sizes of SNPs in genes enriched
503 for associations are randomly drawn from standard normal distributions and then rescaled so they explain
504 a fixed proportion of the narrow-sense heritability $\mathbb{V}[\sum \mathbf{x}_c \beta_c] = h^2$. The coefficients for the genotype PCs
505 are also drawn from standard normal distributions and rescaled such that $\mathbb{V}[\mathbf{W}\mathbf{b}] = 10\%$ of the total
506 phenotypic variance, with the variance of all non-genetic effects contributing $\mathbb{V}[\mathbf{W}\mathbf{b}] + \mathbb{V}[\mathbf{e}] = (1 - h^2)$. For
507 any simulations conducted under the population structure model, genotype PCs are not included in any of
508 the model fitting procedures, and no other preprocessing normalizations were carried out to account for the
509 additional population structure. More specifically, GWA summary statistics are then computed by fitting a

single-SNP univariate linear model via ordinary least squares (OLS):

$$\hat{\beta}_j = (\mathbf{x}_j^T \mathbf{x}_j)^{-1} \mathbf{x}_j^T \mathbf{y}_j; \quad (9)$$

for every SNP in the data $j = 1, \dots, J$. These OLS effect size estimates, along with an empirically LD matrix Σ computed directly from the full $N \times J$ genotype matrix \mathbf{X} , are given to gene- ε . We also retain standard errors and p -values for the implementation of competing methods: RSS⁵⁴, SKAT⁵⁵, and the standard GWA SNP-level association test. Given the simulation procedure above, we simulate a wide range of scenarios for comparing the performance of gene-level association approaches by varying the following parameters:

- Number of individuals: $N = 5,000$ and $10,000$;
- Narrow-sense heritability: $h^2 = 0.2$ and 0.6 ;
- Percentage of enriched genes: 1% (sparse) and 10% (polygenic);

Furthermore, we set the number of causal SNPs with non-zero effects to be some fixed percentage of all SNPs located within the designated genes enriched for associations. We set this percentage to be 0.125% in the 1% associated SNP-set case, and 3% in the 10% associated SNP-set case. All performance comparisons are based on 100 different simulated runs for each parameter combination. Lastly, for each simulated dataset, we also selected some number of intergenic SNPs (i.e., SNPs not mapped to any gene) to have non-zero effect sizes. This was done to mimic genetic associations in unannotated regulatory elements. Specifically, five randomly selected intergenic SNPs were given non-zero contributions to the trait heritability in the 1% enriched genes case, and 30 intergenic SNPs were selected in the 10% enriched genes case.

All performance comparisons are based on 100 different simulated runs for each parameter combination. We computed gene-level p -values for gene- ε , SKAT, and the single-SNP GWAS. For evaluating the performance of RSS, we compute posterior enrichment probabilities. For all approaches, we assessed the power and false discovery rates when identifying enriched genes at either a Bonferroni-corrected threshold ($p = 0.05/1,408$ genes = 3.55×10^{-5}) or according to the median probability model (posterior enrichment probability > 0.5)⁸⁵. [Figure S6](#) and [Figure S7](#) show the mean performances (and standard errors) across all simulated replicates. [Figure S8](#) illustrates that both GWAS and gene- ε are limited by the sample size of the cohort of interest. Specifically, when the sample size is set to 2,000 individuals power is low and false discovery rates are high for both the standard GWA framework and gene- ε .

536 Simulations of genetic trait architecture in two populations

537 We used the African (UKB) cohort and a subset of the European cohort and simulation studies to test the
538 ability of GWAS and gene- ϵ to detect shared causal SNPs (in the case of gene- ϵ , genes containing causal
539 SNPs) in a multi-ancestry study. Using the same simulation protocol as that described for testing power of
540 different enrichment analysis methods, described in *Simulations in a single population*, we labeled all genes
541 containing at least one causal SNP as "causal". We first determined the power of gene- ϵ to identify SNPs or
542 genes that are causal in each cohort under a variety of genomic architectures. The total amount of variance
543 explained in the phenotype by the causal SNPs (i.e. the narrow-sense heritability) to be equal to 0.2 or
544 0.6. In each of these contexts, the sparsity of causal variants as a function of the total number of variants
545 was set to either 0.1 or 0.5. These values of causal SNP sparsity were selected in order to ensure that an
546 ample number of SNPs were associated with the phenotype in both cohorts. Finally, the overlap in causal
547 SNPs between the two cohorts was tested at proportions equal to 0 (no overlap in causal between SNPs
548 cohorts) 0.25, 0.5, and 1 (complete overlap in causal SNPs between cohorts). For each of these parameter
549 sets, 50 replicate simulations were performed of two cohorts derived from 10,000 European individuals and
550 4,967 African individuals, respectively. We summarize the performance of the standard GWA framework
551 and gene- ϵ across the parameter space. Generally, gene- ϵ performs better on the European cohort than it
552 does in the African cohort, but is better powered in the African cohort when the causal SNPs are the same
553 in both cohorts (Figure S9 and Figure S10). Additionally, gene- ϵ performs better when identifying causal
554 genes that are shared between the two cohorts - particularly when traits have high heritability (Figure S11 -
555 Figure S12).

556 References

- 557 [1] Terhi Kettunen, Carita Eklund, Mika Kähönen, Antti Jula, Hannu Päivä, Leo-Pekka Lyytikäinen, Mikko
558 Hurme, and Terho Lehtimäki. Polymorphism in the c-reactive protein (crp) gene affects crp levels in
559 plasma and one early marker of atherosclerosis in men: The health 2000 survey. Scandinavian journal
560 of clinical and laboratory investigation, 71(5):353–361, 2011.
- 561 [2] Amy Z Fan, Ajay Yesupriya, Man-huei Chang, Meaghan House, Jing Fang, Renée Ned, Donald Hayes,
562 Nicole F Dowling, and Ali H Mokdad. Gene polymorphisms in association with emerging cardiovascular
563 risk markers in adult women. BMC medical genetics, 11(1):6, 2010.
- 564 [3] E Komurcu-Bayrak, N Erginel-Unaltuna, A Onat, B Ozsait, C Eklund, M Hurme, N Mononen, R Laak-

- 565 sonen, G Hergenc, and T Lehtimäki. Association of c-reactive protein (crp) gene allelic variants with
566 serum crp levels and hypertension in turkish adults. Atherosclerosis, 206(2):474–479, 2009.
- 567 [4] AJ Szalai, J Wu, EM Lange, MA McCrory, CD Langefeld, A Williams, SO Zakharkin, Varghese George,
568 DB Allison, GS Cooper, et al. Single-nucleotide polymorphisms in the c-reactive protein (crp) gene
569 promoter that affect transcription factor binding, alter transcriptional activity, and associate with dif-
570 ferences in baseline serum crp level. Journal of Molecular Medicine, 83(6):440–447, 2005.
- 571 [5] Shi-Chao Zhang, Ming-Yu Wang, Jun-Rui Feng, Yue Chang, Shang-Rong Ji, and Yi Wu. Reversible
572 promoter methylation determines fluctuating expression of acute phase proteins. Elife, 9:e51317, 2020.
- 573 [6] S-N Chang, C-T Tsai, C-K Wu, J-K Lee, L-P Lai, S-W Huang, L-Y Huang, C-D Tseng, J-L Lin, F-T
574 Chiang, et al. A functional variant in the promoter region regulates the c-reactive protein gene and is a
575 potential candidate for increased risk of atrial fibrillation. Journal of internal medicine, 272(3):305–315,
576 2012.
- 577 [7] Hyoun-Ah Kim, Hye-Young Chun, Seung-Hyun Kim, Hae-Sim Park, and Chang-Hee Suh. C-reactive
578 protein gene polymorphisms in disease susceptibility and clinical manifestations of korean systemic lupus
579 erythematosus. The Journal of rheumatology, 36(10):2238–2243, 2009.
- 580 [8] Abbas Dehghan, Josée Dupuis, Maja Barbalić, Joshua C Bis, Gudny Eiriksdottir, Chen Lu, Niina
581 Pellikka, Henri Wallaschofski, Johannes Kettunen, Peter Henneman, et al. Meta-analysis of genome-wide
582 association studies in 80 000 subjects identifies multiple loci for c-reactive protein levels. Circulation,
583 123(7):731–738, 2011.
- 584 [9] Paul M Ridker, Guillaume Pare, Alex Parker, Robert YL Zee, Jacqueline S Danik, Julie E Buring, David
585 Kwiakowski, Nancy R Cook, Joseph P Miletich, and Daniel I Chasman. Loci related to metabolic-
586 syndrome pathways including lepr, hnf1a, il6r, and gckr associate with plasma c-reactive protein: the
587 women’s genome health study. The American Journal of Human Genetics, 82(5):1185–1192, 2008.
- 588 [10] Symen Ligthart, Ahmad Vaez, Urmo Võsa, Maria G Stathopoulou, Paul S De Vries, Bram P Prins,
589 Peter J Van der Most, Toshiko Tanaka, Elnaz Naderi, Lynda M Rose, et al. Genome analyses of 200,000
590 individuals identify 58 loci for chronic inflammation and highlight pathways that link inflammation and
591 complex disorders. The American Journal of Human Genetics, 103(5):691–706, 2018.
- 592 [11] Alex P Reiner, Sandra Beleza, Nora Franceschini, Paul L Auer, Jennifer G Robinson, Charles Kooper-
593 berg, Ulrike Peters, and Hua Tang. Genome-wide association and population genetic analysis of c-

- 594 reactive protein in african american and hispanic american women. The American Journal of Human
595 Genetics, 91(3):502–512, 2012.
- 596 [12] Paul Elliott, John C Chambers, Weihua Zhang, Robert Clarke, Jemma C Hopewell, John F Peden,
597 Jeanette Erdmann, Peter Braund, James C Engert, Derrick Bennett, et al. Genetic loci associated with
598 c-reactive protein levels and risk of coronary heart disease. Jama, 302(1):37–48, 2009.
- 599 [13] Deog Kyeom Kim, Michael H Cho, Craig P Hersh, David A Lomas, Bruce E Miller, Xiangyang Kong,
600 Per Bakke, Amund Gulsvik, Alvar Agustí, Emiel Wouters, et al. Genome-wide association analysis of
601 blood biomarkers in chronic obstructive pulmonary disease. American journal of respiratory and critical
602 care medicine, 186(12):1238–1247, 2012.
- 603 [14] William J Astle, Heather Elding, Tao Jiang, Dave Allen, Dace Ruklisa, Alice L Mann, Daniel Mead,
604 Heleen Bouman, Fernando Riveros-Mckay, Myrto A Kostadima, et al. The allelic landscape of human
605 blood cell trait variation and links to common complex disease. Cell, 167(5):1415–1429, 2016.
- 606 [15] Juraj Sokol, Kamil Biringer, Maria Skerenova, Miroslav Hasko, Lenka Bartosova, Jan Stasko, Jan
607 Danko, and Peter Kubisz. Platelet aggregation abnormalities in patients with fetal losses: the gp6 gene
608 polymorphism. Fertility and sterility, 98(5):1170–1174, 2012.
- 609 [16] Andrew D Johnson, Lisa R Yanek, Ming-Huei Chen, Nauder Faraday, Martin G Larson, Geoffrey Tofler,
610 Shio J Lin, Aldi T Kraja, Michael A Province, Qiong Yang, et al. Genome-wide meta-analyses identifies
611 seven loci associated with platelet aggregation in response to agonists. Nature genetics, 42(7):608–613,
612 2010.
- 613 [17] Takao Shimizu. Lipid mediators in health and disease: enzymes and receptors as therapeutic targets
614 for the regulation of immunity and inflammation. Annual review of pharmacology and toxicology, 49:
615 123–150, 2009.
- 616 [18] Yuji Shimizu, Kazuhiko Arima, Yuko Noguchi, Shin-Ya Kawashiri, Hirotomo Yamanashi, Mami Tamai,
617 Yasuhiro Nagata, and Takahiro Maeda. Potential mechanisms underlying the association between sin-
618 gle nucleotide polymorphism (brap and aldh2) and hypertension among elderly japanese population.
619 Scientific Reports, 10(1):1–9, 2020.
- 620 [19] John D Eicher, Nathalie Chami, Tim Kacprowski, Akihiro Nomura, Ming-Huei Chen, Lisa R Yanek,
621 Salman M Tajuddin, Ursula M Schick, Andrew J Slater, Nathan Pankratz, et al. Platelet-related
622 variants identified by exomechip meta-analysis in 157,293 individuals. The American Journal of Human
623 Genetics, 99(1):40–55, 2016.

- 624 [20] Rehan Qayyum, Beverly M Snively, Elad Ziv, Michael A Nalls, Yongmei Liu, Weihong Tang, Lisa R
625 Yanek, Leslie Lange, Michele K Evans, Santhi Ganesh, et al. A meta-analysis and genome-wide associa-
626 tion study of platelet count and mean platelet volume in african americans. PLoS Genet, 8(3):e1002491,
627 2012.
- 628 [21] Raymond Noordam, Maxime M Bos, Heming Wang, Thomas W Winkler, Amy R Bentley, Tuomas O
629 Kilpeläinen, Paul S de Vries, Yun Ju Sung, Karen Schwander, Brian E Cade, et al. Multi-ancestry
630 sleep-by-snp interaction analysis in 126,926 individuals reveals lipid loci stratified by sleep duration.
631 Nature communications, 10(1):1–13, 2019.
- 632 [22] Tom G Richardson, Eleanor Sanderson, Tom M Palmer, Mika Ala-Korpela, Brian A Ference, George
633 Davey Smith, and Michael V Holmes. Evaluating the relationship between circulating lipoprotein lipids
634 and apolipoproteins with risk of coronary heart disease: A multivariable mendelian randomisation
635 analysis. PLoS medicine, 17(3):e1003062, 2020.
- 636 [23] Alexander M Kulminski, Jian Huang, Yury Loika, Konstantin G Arbeev, Olivia Bagley, Arseniy Yashkin,
637 Matt Duan, and Irina Culminkaya. Strong impact of natural-selection-free heterogeneity in genetics
638 of age-related phenotypes. Aging (Albany NY), 10(3):492, 2018.
- 639 [24] Thomas J Hoffmann, Elizabeth Theusch, Tanushree Haldar, Dilrini K Ranatunga, Eric Jorgenson,
640 Marisa W Medina, Mark N Kvale, Pui-Yan Kwok, Catherine Schaefer, Ronald M Krauss, et al. A large
641 electronic-health-record-based genome-wide study of serum lipids. Nature genetics, 50(3):401–413, 2018.
- 642 [25] Aldi T Kraja, Dhananjay Vaidya, James S Pankow, Mark O Goodarzi, Themistocles L Assimes,
643 Iftikhar J Kullo, Ulla Sovio, Rasika A Mathias, Yan V Sun, Nora Franceschini, et al. A bivariate
644 genome-wide approach to metabolic syndrome: Stampeed consortium. Diabetes, 60(4):1329–1339, 2011.
- 645 [26] Cassandra N Spracklen, Peng Chen, Young Jin Kim, Xu Wang, Hui Cai, Shengxu Li, Jirong Long, Ying
646 Wu, Ya Xing Wang, Fumihiko Takeuchi, et al. Association analyses of east asian individuals and trans-
647 ancestry analyses with european individuals reveal new loci associated with cholesterol and triglyceride
648 levels. Human molecular genetics, 26(9):1770–1784, 2017.
- 649 [27] Makoto Kurano, Kazuhisa Tsukamoto, Shigeo Kamitsuji, Naoyuki Kamatani, Masumi Hara, Toshio
650 Ishikawa, Bong-Jo Kim, Sanghoon Moon, Young Jin Kim, and Tamio Teramoto. Genome-wide asso-
651 ciation study of serum lipids confirms previously reported associations as well as new associations of
652 common snps within pcsk7 gene with triglyceride. Journal of human genetics, 61(5):427–433, 2016.

- 653 [28] Paul S De Vries, Michael R Brown, Amy R Bentley, Yun J Sung, Thomas W Winkler, Ioanna Ntalla,
654 Karen Schwander, Aldi T Kraja, Xiuqing Guo, Nora Franceschini, et al. Multiancestry genome-wide as-
655 sociation study of lipid levels incorporating gene-alcohol interactions. American journal of epidemiology,
656 188(6):1033–1054, 2019.
- 657 [29] Amy R Bentley, Yun J Sung, Michael R Brown, Thomas W Winkler, Aldi T Kraja, Ioanna Ntalla,
658 Karen Schwander, Daniel I Chasman, Elise Lim, Xuan Deng, et al. Multi-ancestry genome-wide gene-
659 smoking interaction study of 387,272 individuals identifies new loci associated with serum lipids. Nature
660 genetics, 51(4):636–648, 2019.
- 661 [30] Ida Surakka, Momoko Horikoshi, Reedik Mägi, Antti-Pekka Sarin, Anubha Mahajan, Vasiliki Lagou,
662 Letizia Marullo, Teresa Ferreira, Benjamin Miraglio, Sanna Timonen, et al. The impact of low-frequency
663 and rare variants on lipid levels. Nature genetics, 47(6):589–597, 2015.
- 664 [31] Tanya M Teslovich, Kiran Musunuru, Albert V Smith, Andrew C Edmondson, Ioannis M Stylianou,
665 Masahiro Koseki, James P Pirruccello, Samuli Ripatti, Daniel I Chasman, Cristen J Willer, et al.
666 Biological, clinical and population relevance of 95 loci for blood lipids. Nature, 466(7307):707–713,
667 2010.
- 668 [32] Cristen J Willer, Ellen M Schmidt, Sebanti Sengupta, Gina M Peloso, Stefan Gustafsson, Stavroula
669 Kanoni, Andrea Ganna, Jin Chen, Martin L Buchkovich, Samia Mora, et al. Discovery and refinement
670 of loci associated with lipid levels. Nature genetics, 45(11):1274, 2013.
- 671 [33] Rita PS Middelberg, Manuel AR Ferreira, Anjali K Henders, Andrew C Heath, Pamela AF Madden,
672 Grant W Montgomery, Nicholas G Martin, and John B Whitfield. Genetic variants in lpl, oasl and
673 tomm40/apoe-c1-c2-c4 genes are associated with multiple cardiovascular-related traits. BMC medical
674 genetics, 12(1):123, 2011.
- 675 [34] Sekar Kathiresan, Olle Melander, Candace Guiducci, Aarti Surti, Noël P Burt, Mark J Rieder, Gre-
676 gory M Cooper, Charlotta Roos, Benjamin F Voight, Aki S Havulinna, et al. Six new loci associated
677 with blood low-density lipoprotein cholesterol, high-density lipoprotein cholesterol or triglycerides in
678 humans. Nature genetics, 40(2):189–197, 2008.
- 679 [35] Jaspal S Kooner, John C Chambers, Carlos A Aguilar-Salinas, David A Hinds, Craig L Hyde, Gregory R
680 Warnes, Francisco J Gómez Pérez, Kelly A Frazer, Paul Elliott, James Scott, et al. Genome-wide scan
681 identifies variation in mxipl associated with plasma triglycerides. Nature genetics, 40(2):149, 2008.

- 682 [36] Sekar Kathiresan, Cristen J Willer, Gina M Peloso, Serkalem Demissie, Kiran Musunuru, Eric E Schadt,
683 Lee Kaplan, Derrick Bennett, Yun Li, Toshiko Tanaka, et al. Common variants at 30 loci contribute to
684 polygenic dyslipidemia. Nature genetics, 41(1):56–65, 2009.
- 685 [37] Maria Keller, Dorit Schleinitz, Julia Förster, Anke Tönjes, Yvonne Böttcher, Antje Fischer-Rosinsky,
686 Jana Breitfeld, Kerstin Weidle, Nigel W Rayner, Ralph Burkhardt, et al. Thoc5: a novel gene involved
687 in hdl-cholesterol metabolism. Journal of lipid research, 54(11):3170–3176, 2013.
- 688 [38] Richa Saxena, Benjamin F Voight, Valeriya Lyssenko, Noël P Burt, Paul IW de Bakker, Hong Chen,
689 Jeffrey J Roix, Sekar Kathiresan, Joel N Hirschhorn, Mark J Daly, et al. Genome-wide association
690 analysis identifies loci for type 2 diabetes and triglyceride levels. Science, 316(5829):1331–1336, 2007.
- 691 [39] Yurii S Aulchenko, Samuli Ripatti, Ida Lindqvist, Dorret Boomsma, Iris M Heid, Peter P Pramstaller,
692 Brenda WJH Penninx, A Cecile JW Janssens, James F Wilson, Tim Spector, et al. Loci influencing
693 lipid levels and coronary heart disease risk in 16 european population cohorts. Nature genetics, 41(1):
694 47, 2009.
- 695 [40] Rubina Tabassum, Joel T Rämö, Pietari Ripatti, Jukka T Koskela, Mitja Kurki, Juha Karjalainen, Priit
696 Palta, Shabbeer Hassan, Javier Nunez-Fontarnau, Tuomo TJ Kiiskinen, et al. Genetic architecture of
697 human plasma lipidome and its link to cardiovascular disease. Nature communications, 10(1):1–14,
698 2019.
- 699 [41] Liang He, Yelena Kernogitski, Irina Kulminskaya, Yury Loika, Konstantin G Arbeev, Elena Loiko,
700 Olivia Bagley, Matt Duan, Arseniy Yashkin, Svetlana V Ukraintseva, et al. Pleiotropic meta-analyses
701 of longitudinal studies discover novel genetic variants associated with age-related diseases. Frontiers in
702 genetics, 7:179, 2016.
- 703 [42] Derek Klarin, Scott M Damrauer, Kelly Cho, Yan V Sun, Tanya M Teslovich, Jacqueline Honerlaw,
704 David R Gagnon, Scott L DuVall, Jin Li, Gina M Peloso, et al. Genetics of blood lipids among ~ 300,000
705 multi-ethnic participants of the million veteran program. Nature genetics, 50(11):1514–1523, 2018.
- 706 [43] Dawn M Waterworth, Sally L Ricketts, Kijoung Song, Li Chen, Jing Hua Zhao, Samuli Ripatti, Yurii S
707 Aulchenko, Weihua Zhang, Xin Yuan, Noha Lim, et al. Genetic variants influencing circulating lipid
708 levels and risk of coronary artery disease. Arteriosclerosis, thrombosis, and vascular biology, 30(11):
709 2264–2276, 2010.
- 710 [44] Gina M Peloso, Paul L Auer, Joshua C Bis, Arend Voorman, Alanna C Morrison, Nathan O Stitzel,
711 Jennifer A Brody, Sumeet A Khetarpal, Jacy R Crosby, Myriam Fornage, et al. Association of low-

712 frequency and rare coding-sequence variants with blood lipids and coronary heart disease in 56,000
713 whites and blacks. The American Journal of Human Genetics, 94(2):223–232, 2014.

714 [45] Tuomas O Kilpeläinen, Amy R Bentley, Raymond Noordam, Yun Ju Sung, Karen Schwander,
715 Thomas W Winkler, Hermina Jakupović, Daniel I Chasman, Alisa Manning, Ioanna Ntalla, et al.
716 Multi-ancestry study of blood lipid levels identifies four loci interacting with physical activity. Nature
717 communications, 10(1):1–11, 2019.

718 [46] Yoichiro Kamatani, Koichi Matsuda, Yukinori Okada, Michiaki Kubo, Naoya Hosono, Yataro Daigo,
719 Yusuke Nakamura, and Naoyuki Kamatani. Genome-wide association study of hematological and bio-
720 chemical traits in a japanese population. Nature genetics, 42(3):210, 2010.

721 [47] Marc A Coram, Qing Duan, Thomas J Hoffmann, Timothy Thornton, Joshua W Knowles, Nicholas A
722 Johnson, Heather M Ochs-Balcom, Timothy A Donlon, Lisa W Martin, Charles B Eaton, et al. Genome-
723 wide characterization of shared and distinct genetic components that influence blood lipid levels in
724 ethnically diverse human populations. The American Journal of Human Genetics, 92(6):904–916, 2013.

725 [48] Deepti Gurdasani, Tommy Carstensen, Segun Fatumo, Guanjie Chen, Chris S Franklin, Javier Prado-
726 Martinez, Heleen Bouman, Federico Abascal, Marc Haber, Ioanna Tachmazidou, et al. Uganda genome
727 resource enables insights into population history and genomic discovery in africa. Cell, 179(4):984–1002,
728 2019.

729 [49] Elisabeth M van Leeuwen, Aniko Sabo, Joshua C Bis, Jennifer E Huffman, Ani Manichaikul, Albert V
730 Smith, Mary F Feitosa, Serkalem Demissie, Peter K Joshi, Qing Duan, et al. Meta-analysis of 49
731 549 individuals imputed with the 1000 genomes project reveals an exonic damaging variant in angptl4
732 determining fasting tg levels. Journal of medical genetics, 53(7):441–449, 2016.

733 [50] Matthew A Reyna, Mark DM Leiserson, and Benjamin J Raphael. Hierarchical hotnet: identifying
734 hierarchies of altered subnetworks. Bioinformatics, 34(17):i972–i980, 2018.

735 [51] Christoph Heiring, Björn Dahlbäck, and Yves A Muller. Ligand recognition and homophilic interactions
736 in tyro3 structural insights into the axl/tyro3 receptor tyrosine kinase family. Journal of Biological
737 Chemistry, 279(8):6952–6958, 2004.

738 [52] Alice B Popejoy and Stephanie M Fullerton. Genomics is failing on diversity. Nature News, 538(7624):
739 161, 2016.

- 740 [53] Wei Cheng, Sohini Ramachandran, and Lorin Crawford. Estimation of non-null snp effect size distribu-
741 tions enables the detection of enriched genes underlying complex traits. PLoS genetics, 16(6):e1008855,
742 2020.
- 743 [54] Xiang Zhu and Matthew Stephens. Bayesian large-scale multiple regression with summary statistics
744 from genome-wide association studies. The annals of applied statistics, 11(3):1561, 2017.
- 745 [55] Michael C Wu, Seunggeun Lee, Tianxi Cai, Yun Li, Michael Boehnke, and Xihong Lin. Rare-variant
746 association testing for sequencing data with the sequence kernel association test. The American Journal
747 of Human Genetics, 89(1):82–93, 2011.
- 748 [56] Jake R Conway, Alexander Lex, and Nils Gehlenborg. Upsetr: an r package for the visualization of
749 intersecting sets and their properties. Bioinformatics, 33(18):2938–2940, 2017.
- 750 [57] Antonio Fabregat, Konstantinos Sidiropoulos, Phani Garapati, Marc Gillespie, Kerstin Hausmann,
751 Robin Haw, Bijay Jassal, Steven Jupe, Florian Korninger, Sheldon McKay, et al. The reactome pathway
752 knowledgebase. Nucleic acids research, 44(D1):D481–D487, 2016.
- 753 [58] Sabry Razick, George Magklaras, and Ian M Donaldson. irefindex: a consolidated protein interaction
754 database with provenance. BMC bioinformatics, 9(1):405, 2008.
- 755 [59] Masahiro Kanai, Masato Akiyama, Atsushi Takahashi, Nana Matoba, Yukihide Momozawa, Masashi
756 Ikeda, Nakao Iwata, Shiro Ikegawa, Makoto Hirata, Koichi Matsuda, et al. Genetic analysis of quanti-
757 tative traits in the japanese population links cell types to complex human diseases. Nature genetics, 50
758 (3):390–400, 2018.
- 759 [60] Masato Akiyama, Yukinori Okada, Masahiro Kanai, Atsushi Takahashi, Yukihide Momozawa, Masashi
760 Ikeda, Nakao Iwata, Shiro Ikegawa, Makoto Hirata, Koichi Matsuda, et al. Genome-wide association
761 study identifies 112 new loci for body mass index in the japanese population. Nature genetics, 49(10):
762 1458, 2017.
- 763 [61] Masato Akiyama, Kazuyoshi Ishigaki, Saori Sakaue, Yukihide Momozawa, Momoko Horikoshi, Makoto
764 Hirata, Koichi Matsuda, Shiro Ikegawa, Atsushi Takahashi, Masahiro Kanai, et al. Characterizing rare
765 and low-frequency height-associated variants in the japanese population. Nature communications, 10
766 (1):1–11, 2019.
- 767 [62] Alexander Gusev, Arthur Ko, Huwenbo Shi, Gaurav Bhatia, Wonil Chung, Brenda WJH Penninx, Rick
768 Jansen, Eco JC De Geus, Dorret I Boomsma, Fred A Wright, et al. Integrative approaches for large-scale
769 transcriptome-wide association studies. Nature genetics, 48(3):245, 2016.

- 770 [63] Pak C Sham and Shaun M Purcell. Statistical power and significance testing in large-scale genetic
771 studies. Nature Reviews Genetics, 15(5):335–346, 2014.
- 772 [64] Huwenbo Shi, Kathryn S Burch, Ruth Johnson, Malika K Freund, Gleb Kichaev, Nicholas Mancuso,
773 Astrid M Manuel, Natalie Dong, and Bogdan Pasaniuc. Localizing components of shared transethnic
774 genetic architecture of complex traits from gwas summary data. The American Journal of Human
775 Genetics, 106(6):805–817, 2020.
- 776 [65] Gao Wang, Abhishek Sarkar, Peter Carbonetto, and Matthew Stephens. A simple new approach to
777 variable selection in regression, with application to genetic fine mapping. Journal of the Royal Statistical
778 Society: Series B (Statistical Methodology), 82(5):1273–1300, 2020.
- 779 [66] David H Alexander, John Novembre, and Kenneth Lange. Fast model-based estimation of ancestry in
780 unrelated individuals. Genome research, 19(9):1655–1664, 2009.
- 781 [67] Christopher C Chang, Carson C Chow, Laurent CAM Tellier, Shashaank Vattikuti, Shaun M Pur-
782 cell, and James J Lee. Second-generation plink: rising to the challenge of larger and richer datasets.
783 Gigascience, 4(1):s13742–015, 2015.
- 784 [68] Akiko Nagai, Makoto Hirata, Yoichiro Kamatani, Kaori Muto, Koichi Matsuda, Yutaka Kiyohara,
785 Toshiharu Ninomiya, Akiko Tamakoshi, Zentaro Yamagata, Taisei Mushiroda, et al. Overview of the
786 biobank japan project: study design and profile. Journal of epidemiology, 27(Supplement.III):S2–S8,
787 2017.
- 788 [69] Genevieve L Wojcik, Mariaelisa Graff, Katherine K Nishimura, Ran Tao, Jeffrey Haessler, Christopher R
789 Gignoux, Heather M Highland, Yesha M Patel, Elena P Sorokin, Christy L Avery, et al. Genetic analyses
790 of diverse populations improves discovery for complex traits. Nature, 570(7762):514–518, 2019.
- 791 [70] Peter H Sudmant, Tobias Rausch, Eugene J Gardner, Robert E Handsaker, Alexej Abyzov, John Hud-
792 dleston, Yan Zhang, Kai Ye, Goo Jun, Markus Hsi-Yang Fritz, et al. An integrated map of structural
793 variation in 2,504 human genomes. Nature, 526(7571):75–81, 2015.
- 794 [71] Anders Bergström, Shane A McCarthy, Ruoyun Hui, Mohamed A Almarri, Qasim Ayub, Petr Danecek,
795 Yuan Chen, Sabine Felkel, Pille Hallast, Jack Kamm, et al. Insights into human genetic variation and
796 population history from 929 diverse genomes. Science, 367(6484), 2020.
- 797 [72] Huwenbo Shi, Steven Gazal, Masahiro Kanai, Evan M Koch, Armin P Schoech, Katherine M Siewert,
798 Samuel S Kim, Yang Luo, Tiffany Amariuta, Hailiang Huang, et al. Population-specific causal disease

- 799 effect sizes in functionally important regions impacted by selection. Nature Communications, 12(1):
800 1–15, 2021.
- 801 [73] Iain Mathieson. The omnigenic model and polygenic prediction of complex traits. The American Journal
802 of Human Genetics, 2021.
- 803 [74] Matthew Stephens. False discovery rates: a new deal. Biostatistics, 18(2):275–294, 2017.
- 804 [75] Sarah M Uebachs, Gao Wang, Peter Carbonetto, and Matthew Stephens. Flexible statistical methods
805 for estimating and testing effects in genomic studies with multiple conditions. Nature genetics, 51(1):
806 187–195, 2019.
- 807 [76] Farhad Hormozdizadeh, Emrah Kostem, Eun Yong Kang, Bogdan Pasaniuc, and Eleazar Eskin. Identifying
808 causal variants at loci with multiple signals of association. Genetics, 198(2):497–508, 2014.
- 809 [77] Alicia R Martin, Meng Lin, Julie M Granka, Justin W Myrick, Xiaomin Liu, Alexandra Sockell, Eliza-
810 beth G Atkinson, Cedric J Werely, Marlo Möller, Manjinder S Sandhu, et al. An unexpectedly complex
811 architecture for skin pigmentation in africans. Cell, 171(6):1340–1353, 2017.
- 812 [78] Peter Carbonetto and Matthew Stephens. Integrated enrichment analysis of variants and pathways in
813 genome-wide association studies indicates central role for il-2 signaling genes in type 1 diabetes, and
814 cytokine signaling genes in crohn’s disease. PLoS genetics, 9(10):e1003770, 2013.
- 815 [79] Xiang Zhu and Matthew Stephens. Large-scale genome-wide enrichment analyses identify new trait-
816 associated genes and pathways across 31 human phenotypes. Nature communications, 9(1):1–14, 2018.
- 817 [80] Michael C Wu, Peter Kraft, Michael P Epstein, Deanne M Taylor, Stephen J Chanock, David J Hunter,
818 and Xihong Lin. Powerful snp-set analysis for case-control genome-wide association studies. The
819 American Journal of Human Genetics, 86(6):929–942, 2010.
- 820 [81] Seunggeun Lee, Mary J Emond, Michael J Bamshad, Kathleen C Barnes, Mark J Rieder, Deborah A
821 Nickerson, ESP Lung Project Team, David C Christiani, Mark M Wurfel, Xihong Lin, et al. Optimal
822 unified approach for rare-variant association testing with application to small-sample case-control whole-
823 exome sequencing studies. The American Journal of Human Genetics, 91(2):224–237, 2012.
- 824 [82] Iuliana Ionita-Laza, Seunggeun Lee, Vlad Makarov, Joseph D Buxbaum, and Xihong Lin. Sequence
825 kernel association tests for the combined effect of rare and common variants. The American Journal of
826 Human Genetics, 92(6):841–853, 2013.

- 827 [83] Melissa R McGuirl, Samuel Pattillo Smith, Björn Sandstede, and Sohini Ramachandran. Detecting
828 shared genetic architecture among multiple phenotypes by hierarchical clustering of gene-level associa-
829 tion statistics. Genetics, 2020.
- 830 [84] Lorin Crawford, Ping Zeng, Sayan Mukherjee, and Xiang Zhou. Detecting epistasis with the marginal
831 epistasis test in genetic mapping studies of quantitative traits. PLoS genetics, 13(7):e1006869, 2017.
- 832 [85] Maria Maddalena Barbieri, James O Berger, et al. Optimal predictive model selection. The annals of
833 statistics, 32(3):870–897, 2004.